



Universitat Autònoma de Barcelona

ADVERTIMENT. L'accés als continguts d'aquesta tesi queda condicionat a l'acceptació de les condicions d'ús establertes per la següent llicència Creative Commons:  http://cat.creativecommons.org/?page_id=184

ADVERTENCIA. El acceso a los contenidos de esta tesis queda condicionado a la aceptación de las condiciones de uso establecidas por la siguiente licencia Creative Commons:  <http://es.creativecommons.org/blog/licencias/>

WARNING. The access to the contents of this doctoral thesis it is limited to the acceptance of the use conditions set by the following Creative Commons license:  <https://creativecommons.org/licenses/?lang=en>

Universitat Autònoma de Barcelona

Facultat de Ciències

Departament de Biologia cel·lular, Fisiologia i Immunologia

PhD in Advanced Immunology

**Cell base assays to investigate
the functional relevance of HLH
genetic variants**

Immunology Division

Hospital Universitari Vall d'Hebron

Barcelona 2019

Laura Viñas Giménez

2016-2019

Universitat Autònoma de Barcelona

Facultat de Ciències

Departament de Biologia cel·lular, Fisiologia i Immunologia

**Cell base assays to investigate
the functional relevance of HLH
genetic variants**

PhD in Advanced Immunology

Laura Viñas Giménez

Directors:

Dra. Mónica Martínez Gallo

Dr. Joan Sayós Ortega

Tutor:

Dr. Ricard Pujol Borrell

Dra. Mónica Martínez Gallo principal investigator in Immunology Department, at Vall d'Hebron Research Institute (VHIR), and Associate professors at Cell Biology, Physiology and Immunology Department in Universitat Autònoma de Barcelona (UAB) and Dr. Joan Sayós Ortega principal investigator in Immune Regulation and Immunotherapy Group at VHIR.

Certify that:

This thesis, titled "CELL BASE ASSAYS TO INVESTIGATE THE FUNCTIONAL RELEVANCE OF HLH GENETIC VARIANTS" has been done under their supervision by Laura Viñas Giménez and is approved to be presented and defended to qualify for the degree of Doctor in Immunology by the Universitat Autònoma de Barcelona.

Directors:

Dra. Mónica Martínez Gallo

Dr. Joan Sayós Ortega

Tutor:

Dr. Ricard Pujol Borrell

ACKNOWLEDGMENTS

Vull agrair la col·laboració de totes aquelles persones i institucions que han fet possible la realització d'aquesta tesi.

En primer lloc als directors de la tesi, a la Dra. Mónica Martínez Gallo per confiar en mi des de l'inici per tal de dur a terme aquest treball i al Dr. Joan Sayós Ortega per introduir-me en el món de la recerca bàsica. També li he d'agrair el seu suport i interès al tutor de la tesi, al Dr. Ricard Pujol Borrell per ajudar a posar en ordre les idees i també per la seus valuosos comentaris i revisions.

Als companys del laboratori d'Immuno.

A la família

INDEX

ACKNOWLEDGMENTS	i
LIST OF ABBREVIATIONS.....	11
ABSTRACT	16
I. INTRODUCTION	19
1. The immune system	21
2. Homeostasis in the immune system	22
2.1. The intrinsic pathway (mitochondria-mediated)	23
2.2. The extrinsic pathway (receptor-mediated)	23
2.3. Perforin/Granzyme Apoptosis Pathway	24
3. Granule exocytosis pathway.....	25
3.1. Biogenesis of cytotoxic granules.....	25
3.2. Polarization and docking.....	25
3.3. Priming and fusion	26
4. Role of granule-dependent exocytosis pathways in immune homeostasis	28
5. What is Hemophagocytic syndrome (HLH)?.....	30
6. Epidemiology	30
7. Classification	31
7.1. Familial Hemophagocytic Lymphohistiocytosis type 2-5	31
7.2. Primary immunodeficiency syndromes associated with HLH	34
7.3. Primary HLH due to macrophagic hyperactivation.....	36
7.4. Secondary HLH	39
7.5. Monoallelic HLH	39
8. Clinical Presentation of HLH	39
9. Laboratory findings	40
9.1. Cytopenia(s)	40
9.2. Bone Marrow Aspirate	40
9.3. Ferritin	40
9.4. sCD25	40
9.5. NK cytotoxicity assay	40
9.6. Intracellular staining	41
9.7. NK and CTL degranulation assay	41

9.8.	High triglyceride levels.....	42
9.9.	Hypofibrinogenemia	42
9.10.	Cytokines.....	42
10.	Pathogenesis.....	42
10.1.	Pathogenesis in the cytolytic pathway.....	43
10.2.	Pathogenesis in the macrophagic hyperactivation	43
10.3.	Pathogenesis due to monoallelic variants	44
10.4.	Pathogenesis in the secondary HLH	45
II.	HYPOTHESIS AND OBJECTIVE	47
1.	GENERAL HYPOTHESIS	49
2.	GENERAL OBJECTIVES	50
3.	CONCRETE OBJECTIVES	50
III.	MATERIALS AND METHODS.....	52
1.	Cells culture	54
3.	Other cells	55
4.	Healthy controls.....	55
5.	Plasmid dna constructs.....	55
5.1.	Generation of electrocompetent bacteria	57
5.2.	Bacterial transformation and plasmid amplification.....	57
6.	TRANSFECTIONS AND TRANSDUCTIONS	57
6.1.	Transient transfection of plasmid DNA in COS-7 mammal cell line 58	
6.2.	Stable transfection of plasmid DNA in RBL-2H3 cell line.....	58
6.3.	Stable transduction of shRNA in THP-1 cell line.....	58
7.	Protein immunoblotting by Western Blot.....	59
8.	Immunoprecipitation	59
9.	Flow cytometry.....	60
9.1.	Extracellular and intracellular staining.....	60
9.2.	NK cell Cytotoxicity.....	61
9.3.	NK cell Degranulation	61
10.	β -hexosaminidase release of RBL-H3.....	62
11.	THP-1 differentiation assay	63
12.	LUMINEX Cytokine detection	63

V.	RESULTS	66
	CHAPTER 1: KINETICS OF PHYTOHEMAGGLUTININ (PHA) AND K562 INDUCED DEGRANULATION BASED ON CD107a EXPRESSION IN PEDIATRIC POPULATION	68
	1.1. PHA degranulation showed and increased % of NK cells expressing CD107a	68
	1.2. Cytotoxic functions of activated NK cells in both adults and children display inter-individual variation.....	69
	1.3. Measurement of CD107a upregulation in activated NK cells after PHA STIMULATION has a high diagnostic accuracy for detecting HLH patients.	70
	1.4. Application in clinical practice	71
	CHAPTER 2: ANALYSIS OF THE NOVEL MUTATION L243R FOUND IN A PATIENT WITH FHL5: FUNCTIONAL AND MOLECULAR CHARACTERIZATION	73
	2.1. CLINICAL CASE PRESENTATION: EBV-induced HLH.	73
	2.2. NORMAL PERCENTATGE OF nk CELLS EXPRESSING CD107a BUT ABERRANT degranulation PATTERN.	74
	2.3. STXBP2 ^{L243R} missense mutation results in a lost of MUNC18-2 AND SYNTAXIN-11 expression in both transfected cells and patient's PBMCs..	75
	CHAPTER 3: FUNCTIONAL AND MOLECULAR CHARACTERIZATION OF NOVEL AND REPORTED MUTATIONS FOUND IN PATIENTS DIAGNOSED WITH AN ATYPICAL FORM OF HLH.	79
	4.1. Case reports: UNSUAL HLH Clinical presentation	79
	4.2. degranulation AND Cytotoxicity REACHED NORMAL LEVELS after HLH acute phase.....	81
	4.3. Genetic analysis revealed monoallelic variants in hlh related genes	83
	CHAPTER 4: GENERATE STABLE STXBPD2 KNOCKDOWN CELL LINES TO STUDY THE ROLE OF STXBP2 IN CELL TRAFICKING.	94
	5.1. STXBP2 IS INVOLVED IN THE Endosomal trafficking	95
	5.2. STXBP2-KD Ramos cells express less CD107a.....	95
	CHAPTER 5. COMPREHENSIVE REPOSITORY OF HLH MUTATION DATA FOR MEDICAL RESEARCH AND GENETIC DIAGNOSIS OF HLH.	97
VI.	DISCUSSION	106
VII.	CONCLUSIONS	120
VIII.	BIBLIOGRAPHY.....	126
IX.	ANNEX.....	148

LIST OF ABBREVIATIONS

A

APC: antigen presenting cell

B

BIRC4: gene that encodes for X-linked inhibitory of apoptosis (XIAP)

C

CD: clusters of differentiation

cDMEM: Complete Dulbecco's Modified Eagle's Medium

CHS: Chédiak-Higashi syndrome

cRPMI: Complete Roswell Park Memorial Institute Medium

cSMAC: central supramolecular activation cluster

CTLs: cytotoxic T lymphocytes

E

EBV: Epstein-Barr

F

FHL: familial form of HLH

FHL: Familial hemophagocytic lymphohistiocytosis

FHL-2: FHL type 2

FHL-3: FHL type 3

FHL-4: FHL type 4

FHL-5: FHL type 5

G

GS-2: Griscelli síndrome type 2

H

HLH: Hemophagocytic lymphohistiocytosis
HLH: Hemophagocytic lymphohistiocytosis syndromes
HPSII: Hermansky-Pudlak syndrome type II

I

IFN- γ : interferon-gamma
IS: Immune system

K

K.D: knock down

L

LAMP1(CD107a): lysosome associated membrane protein
LB: lysis buffer
LB-Agar: Luria Broth Base, Invitrogen, plus Agar
LYST: Lysosomal trafficking regulator

M

MACPF: N-terminal membrane attack complex/perforin
mRNA: messenger RNA
MTOC: microtubule organizing center
Munc13-4: Protein unc-13 homolog D
Munc18-2 (STXBP2): Syntaxin-binding protein 2

N

NK: natural killer
NLRC4: cytoplasmic NOD (NOD-like) receptor

O

O/N: overnight

OD: optical density

P

PBMCs: Peripheral blood mononuclear cells

PBS: Phosphate-buffered saline

PEI: Polyethyleneimine reagent

PHA: phytohemagglutinin

PID: primary immunodeficiency

PMA: Phorbol 12-myristate 13-acetate

pSMAC: peripheral SMAC

PVDF: polyvinylidene fluoride

R

RAB11: Ras-related protein Rab-11

RAB27a: Ras-related protein Rab-27A

S

SAP: signaling lymphocyte activation molecule (SLAM)-associated protein

sCD25: Soluble CD25 or sIL2r

SH2D1: encodes for signaling lymphocyte activation molecule (SLAM)-associated protein (SAP)

sHLH: secondary HLH

shRNA: Short hairpin or small hairpin RNA

sIL2r: Soluble interleukin-2 receptor

siRNA: Small interfering RNA

SLAM: signaling lymphocyte activation molecule

Slp: synaptotagmin-like

SNAP23: synaptosomal-associated protein of 23 kDa

STX11: syntaxin 11

STXBP2: Munc18-2

T

TCR: T cell receptor

TNF: tumor necrosis factor

TPH: transplantation of hematopoietic progenitors

t-SNARE: target membrane soluble N-ethylmaleimide-sensitive factor accessory protein receptor

V

vSNARE: vesicle membrane soluble N-ethylmaleimide-sensitive factor accessory protein receptor

W

WB: western blot

X

XIAP: X-linked inhibitory of apoptosis

XLP: X-linked lymphoproliferative syndrome

XLP-1: X-linked proliferative disorder type 1

XLP2: X-linked lymphoproliferative syndrome type 2

ABSTRACT

Hemophagocytic lymphohistiocytosis (HLH) is a life-threatening hyperinflammatory disorder caused by an uncontrolled and dysfunctional immune response. Biallelic mutations in involved genes leads to the familial form of HLH (FHL) which is potentially lethal in the first weeks of life. HLH can also develop in the context of infections, malignancies, autoinflammatory or metabolic diseases but without mutations. This is the so called secondary HLH (sHLH). Nevertheless, there is an increasing evidence that typical FHL cases with biallelic mutations and sHLH without genetic and immunological defects represent only the extremes of the wide spectrum of HLH. To deepen the understanding in the genetics of HLH we analyzed the molecular and functional impact of previously unidentified biallelic and monoallelic mutations in patients diagnosed with HLH. In this study we diagnosed 12 patients with HLH, of which 75% (n=9) presented biallelic mutations and 25% (n=3) monoallelic mutations. The diagnosis of these patients allowed the novel description of 4 mutations not previously identified. Among those, we describe one mutation in perforin (p. Pro477X in homozygosity), two mutations in *STXBP2* (L243R as compound heterozygous with other mutation and R190C as monoallelic) and three in *UNC13D* (P271S, R928C and R1075Q as monoallelic). Moreover, we also included into the characterization eleven mutations in *STXBP2* reported in the literature as monoallelic but not yet characterized.

Here, we describe that the novel biallelic mutation L243R is found in an evolutionarily highly preserved site acting as the center of a rich network of interactions important for stabilizing domains 2 and 3 of the *STXBP2* protein.

Moreover, on the study of monoallelic mutation we assessed protein structural destabilization and expression levels by transfecting different constructs containing monoallelic mutations on *STXBP2* and *UNC13D*. *STXBP2* mutations showed an hypomorphic effect while *UNC13D* protein expression was not affected by any of the studied mutations. As so, we evaluated the effect of these mutations into protein-to-protein interactions and found that interaction capacity was maintained within the studied partners.

For mutations with no effects on the expression levels and protein-to-protein interaction, we addressed their effect as dominant negative by a degranulation assay. We show that mutant *STXBP2*R190C acts as a dominant negative, producing a decrease in degranulation compared to the controls.

Finally, we studied whether the described mutations that involve genes in the cytotoxic pathway had functional impact on macrophages and B lymphocytes. For that, we analyzed the role of STXBP2 in the cellular traffic process. Our data demonstrate that in the absence of STXBP2 there is an accumulation of CD103 on the surface of LPS + IFN γ activated cells compared to controls, demonstrating an active disruption of endosomal trafficking. Moreover, we also show reduction of CD107a dependent degranulation when using KD cells. Thus, mutations in STXBP2, which is involved in the cytotoxic pathway, appear to have a functional impact on macrophages and B lymphocytes at endosomal trafficking level.

Overall, this work describes several previously unidentified mutations related to FHL and SHLH and unveils their effects at a protein level. Moreover, these results represent a primary approach in the understanding of STXBP2 role in macrophages and B lymphocytes.

I. INTRODUCTION

1. THE IMMUNE SYSTEM

The immune system (IS) consists of multiple cell types and molecular components that interact in a coordinated manner in space and time to protect the organism from external aggressions, mainly of infectious agents, but also of own cells with neoplastic potential(Nicholson 2016). The human IS is divided into two main arms: Innate immunity and adaptive immunity. The innate immune system is rapid and gives a non-specific immune response, while the adaptive immune system rises highly specific response to a given antigen.

The innate immune system recognizes conserved patterns in nature such as LPS, peptidoglycan or double stranded RNA(Marshall et al. 2018). These patterns are recognized by pattern recognition receptors (PRR) located on the cells surface and activate intracellular signaling pathways. Different cell types comprise the innate immune system including Dendritic Cells (DC), macrophage a natural killer cells as well as several soluble factors such as complement components, defensins, mannose binding lectins, interferons, cytokines and chemokines.

In contrast to innate immunity, adaptive immune response recognizes and reacts to a large number of microbial and nonmicrobial substances. The defining characteristics of adaptive immunity are the ability to distinguish different substances being more specific, and the ability to respond more vigorously to repeated exposures to the same antigen, known as memory. Antigens that induce the adaptative response, are recognized by B, T lymphocytes and antibodies(Bonilla and Oettgen 2010).

Recently, intrinsic immunity has been recognized as a potent anti-viral defense mechanism. It can be considered a third branch of the IS and comprises a cell-mediated or anti-viral defense mechanism(Perera and Saksena 2012). This immunity is initiated because of proteins genetically encoded and unlike adaptive and innate immunity, the effectors are expressed at a constant level allowing viral infections to resolve quickly(Yan and Chen 2012).

Immune responses (IR) include the mechanisms necessary to react to an external aggression and resolve it favorably. To be effective, these responses must be fast, effective and proportionate, but it is also important not to be extended in time(Payne and Payne 2017). Thus, mechanisms of regulation and coordination of the response are essential for an adequate development of the Immune response. In some cases,

alterations in these mechanisms lead to a decreased or exacerbated IR leading to immunodeficiency, autoimmune disorders or auto inflammatory disorders(Nicholson 2016).

Primary immunodeficiencies (PIDs) are a heterogeneous group of disorders with a partial or total decrease in the functionality of one or more elements of the immune system(Picard et al. 2015). Most PIDs are caused by defects in genes that are crucial for the maturation of the immune system or cause defects in functional pathways on the IS. The clinical and genetic studies of patients with these immunodeficiencies have allowed the scientific community to expand the knowledge about the affected mechanisms. However, it is increasingly common to complement the study of patients with molecular studies or with animal models for a better understanding of the mechanisms beneath.

2. HOMEOSTASIS IN THE IMMUNE SYSTEM

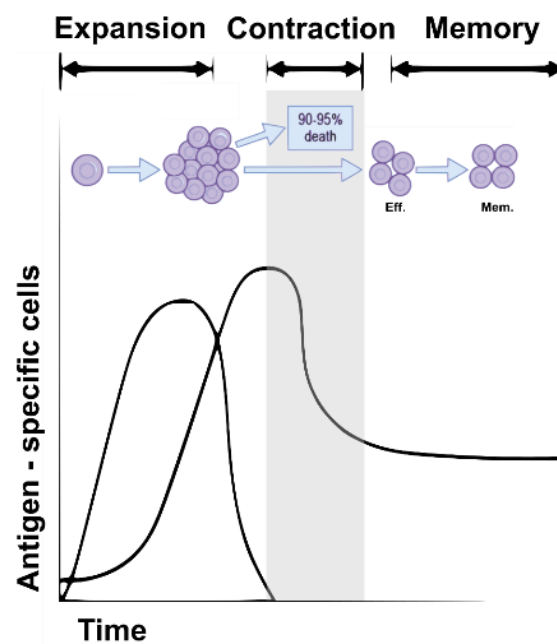


Figure 1. Schematic representation of expansion contraction and memory phases of adaptive immunity and memory cell subsets. T-cell responses undergo expansion after antigen stimulation evolving from naïve to effector (Eff.) cells. In the contraction phase approximately 95% of effector cells die by a process termed activation-induced cell death in order to prevent a long-activated state. Macrophages are the responsible to clear the apoptotic cells. Finally, memory effector (Mem.) cells gradually convert to central memory cells

Several regulatory mechanisms terminate the responses against foreign antigens, returning to a basal state after the antigen clearance (Sun et al. 2008). This process is known as homeostasis and allows the immune system to respond and contract efficiently to antigens (Figure 1). Homeostasis control, before and after antigen exposition, is important to maintain an appropriate pool of mature lymphocytes and necessary for the contract phase, respectively (Abbas 1998). In order to do so, it is necessary to maintain a balance between cell proliferation and cell death by apoptosis. There are several pathways that lead to apoptosis (Figure 2).

2.1. The intrinsic pathway (mitochondria-mediated)

A range of exogenous and endogenous stimuli, such as DNA damage, ischemia, and oxidative stress, activate the intrinsic apoptosis pathway. Thus, this pathway plays an important function in the development and in the elimination of damaged cells. The functional consequence of these stimuli is mitochondrial membrane perturbation and release of cytochrome c in the cytoplasm, where it forms a complex with apoptotic protease activating factor 1 (APAF1) and the inactive form of caspase 9. This complex hydrolyzes adenosine triphosphate to cleave and activate caspase 9. Finally, caspase-9 cleaves and activates the executioner caspases-3/6/7, resulting in cell apoptosis (Jourdan, D. V. J., and Klein 2000; Veis, S. C., and SJ. 1993; Hotchkiss et al. 1999).

2.2. The extrinsic pathway (receptor-mediated)

The extrinsic pathway is stimulated by the death receptors including Fas receptors, tumor necrosis factor (TNF) receptors, and TNF-related apoptosis-inducing ligand (TRAIL) receptors. Death receptors interact with death ligands (FasL, TNF- α , TRAIL...) to induce the recruitment of adaptor proteins such as Fas-associated protein with death domain (FADD) and Tumor necrosis factor receptor type 1-associated DEATH domain protein (TRADD). Eventually, all ligand binding will lead to recruitment of downstream factors, including caspase-8 and caspase-10 that initiate apoptosis by cleaving and activating executioner caspase-3/6/7 (Siegel, C. F., and MJ. 2000).

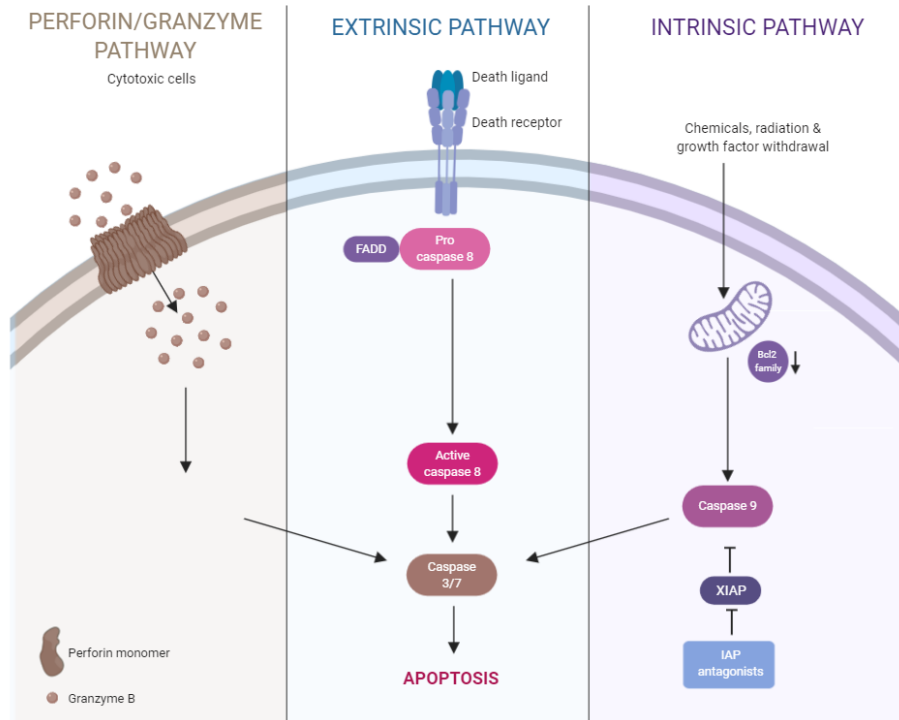


Figure 2. Schematic representation of perforin/granzyme, extrinsic and intrinsic pathways leading to a common cell death apoptosis. In order to start the apoptosis cascade is necessary a specific trigger which is different for each pathway (infection, death ligand or chemicals). Initiator caspases are caspase 8, 9 and 10 which will activate the executioner caspase 3/7 leading to cell shrinkage, chromatin condensation, formation of cytoplasmic blebs and apoptotic bodies. Finally, macrophages are the responsible to phagocyte the apoptotic bodies. This proteolytic cascade is useful since amplifies the apoptotic signaling leading to rapid cell death.

2.3. Perforin/Granzyme Apoptosis Pathway

The secretion of cytotoxic granules containing perforin and granzyme by cytotoxic cells is crucial for either both of the the caspase dependent or independent cell death (de Saint Basile and G. M.a.A. F. 2010). We can find granzyme A, B, H, K, and M in humans, being Granzyme A and granzyme B the most studied. Granzyme A induces loss of mitochondrial inner membrane potential and the release of reactive oxygen species (ROS). Granzyme B mainly triggers caspase activation by activating pro-apoptotic members of the BCL-2 family leading to cytochrome c release into the cytosol. Granzyme B can also mediate apoptosis by activating caspase-8 and caspase-3 (Bots and Medema 2006).

3. GRANULE EXOCYTOSIS PATHWAY

The immune system can fight against intracellular and extracellular pathogens combining both innate and adaptative mechanisms. In particular, cytotoxic T lymphocytes (CTLs), natural killer (NK) and NKT detect virus infected and transformed cells through different receptors, eliminating them by cytotoxicity (Bendelac, R. M., and JH. 1997). CTLs are activated by professional antigen-presenting cells which can both present intracellular peptides or cross-present extracellular peptides from endocytosed proteins into HLA class I molecules. In contrast, NK activation is triggered by recognizing altered HLA class I expression through the balance of activating and inhibitory signals (Orange 2008). NK cells have constitutively primed cytotoxic granules, whereas CTL must synthesize the cytotoxic machinery *de novo* after antigen recognition. Cytotoxicity is an effective and coordinate process divided in the following steps: Activation, biogenesis of cytotoxic granules and degranulation, which consists in polarization, docking, priming and fusion of the granules in the immunological synapsis(de Saint Basile, Ménasché, and Fischer 2010).

3.1. Biogenesis of cytotoxic granules

Cytolytic granules contain lysosomal hydrolases, including acid phosphatase, α -glucosidase, arylsulphatase, β -glucuronidase, cathepsins B and D, cathepsin A-like protective protein (CAPP; which possesses serine carboxypeptidase and deamidase activities), and lysosomal membrane proteins, Lamp-1, Lamp-2, and CD63(Smyth et al. 2001). These cytotoxic proteins are delivered from the *trans*-Golgi network (TGN) to lysosomes via early endosomes (EE), recycling endosomes (RE) and late endosomes/multivesicular bodies (LE/MVB)(Luzio et al. 2014). The process of sorting from TGN network to early endosomes is orchestrated by mannose-6- phosphate receptor (M6PR) followed by the action of AP3-complex which transport the proteins from early endosomes to lysosomes(Eskelinen 2006). Lysosomal trafficking regulator (LYST) regulates the following lysosome fusion and the terminal maturation of the cytotoxic granules(Fernando E. Sepulveda et al. 2015).

3.2. Polarization and docking

After cytotoxic cells activation, the microtubule organizing center (MTOC) undergoes reorganization allowing retrograde dynein/kinesin-dependent transport of cytotoxic granules to the immunological synapse(Yenan T. Bryceson 2012). The CTL synapse is formed by a central TCR cluster named central supramolecular activation cluster

(cSMAC) which is surrounded by a ring of adhesion molecules known as the peripheral SMAC (pSMAC), which mediates the stabilization of cell-cell interaction to enhance the cytotoxic activity (Beal 2008). The strength of TCR signalling modifies polarization speed. Following granule polarization at the synapse, the action of a new complex compounded by the proteins Rab27a, synaptotagmin-like (Slp3) and Kinesin allows the transport of lytic granules away from MTOC and toward the plasma membrane. Slp proteins have two N-terminal C2 domains allowing the association with membrane phospholipids, suggesting that these proteins not only are adaptor molecules but also have a key role in the vesicle membrane-docking. (Mathieu Kurowska N.G. and Ménasché 2012)

3.3. Priming and fusion

Priming step regulates the number of vesicles that are going to be released. The main protein involved in this step is Munc13-4 which is encoded by UNC13D gene. Munc13-4 is ubiquitously expressed in many cell types (brain, heart, skeletal muscle, kidney, lung, liver, pancreas, and prostate) however, is highly expressed in cells of the immune system (Feldmann et al. 2003). Munc13-4 is a multivalent protein with two calcium (C2) domains at both C- and N-terminal sites required for a proper function of the protein and a central tandem repeat of Munc13 homology domains (Koch, Hofmann, and Brose 2000) crucial for the priming step (Ren et al. 2010). In addition to serving as a priming factor at the immunological synapse, Munc13-4 is also required in the formation of a pool of endosomal vesicles that coalesce with cytotoxic granules before their exocytosis (Ménager et al. 2007).

The proteins required for the membrane fusion step are Munc18-2 encoded by STXBP2 gene and syntaxin11 encoded by STX11 gene (de Saint Basile, Ménasché, and Fischer 2010). Munc18-2 mediates the activation of syntaxin-11 by conformational change (Spessott et al. 2017). Syntaxin-11 is member of t-SNARE proteins family (target membrane soluble N-ethylmaleimide-sensitive factor accessory protein receptor) that interacts with SNAP23 (synaptosomal-associated protein of 23 kDa) and all together interact with vSNARE proteins (VAMP7 or VAMP8) forming the SNARE complex. This complex is essential to allow Munc18-2 protein interaction and consequent granule fusion with plasma membrane (Valdez, C. J., and Roche 1999; Hong 2005; Loo et al. 2009). Once perforin is released from the cytotoxic granules it binds to the target membrane and through the C-terminal C2 domain mediates the membrane binding in a calcium dependent manner which is the first key step in cytotoxic activity (Voskoboinik, Smyth, and Trapani 2006). Subsequently, monomers polymerize into a ring between residues in adjacent N-terminal membrane attack complex/perforin (MACPF) domains

and finally two clusters of α -helices inside MACPF domain rearrange into anti-parallel β -strands that puncture and span the membrane and create the pore (Law et al. 2010; Liu, Walsh, and Young 1995).

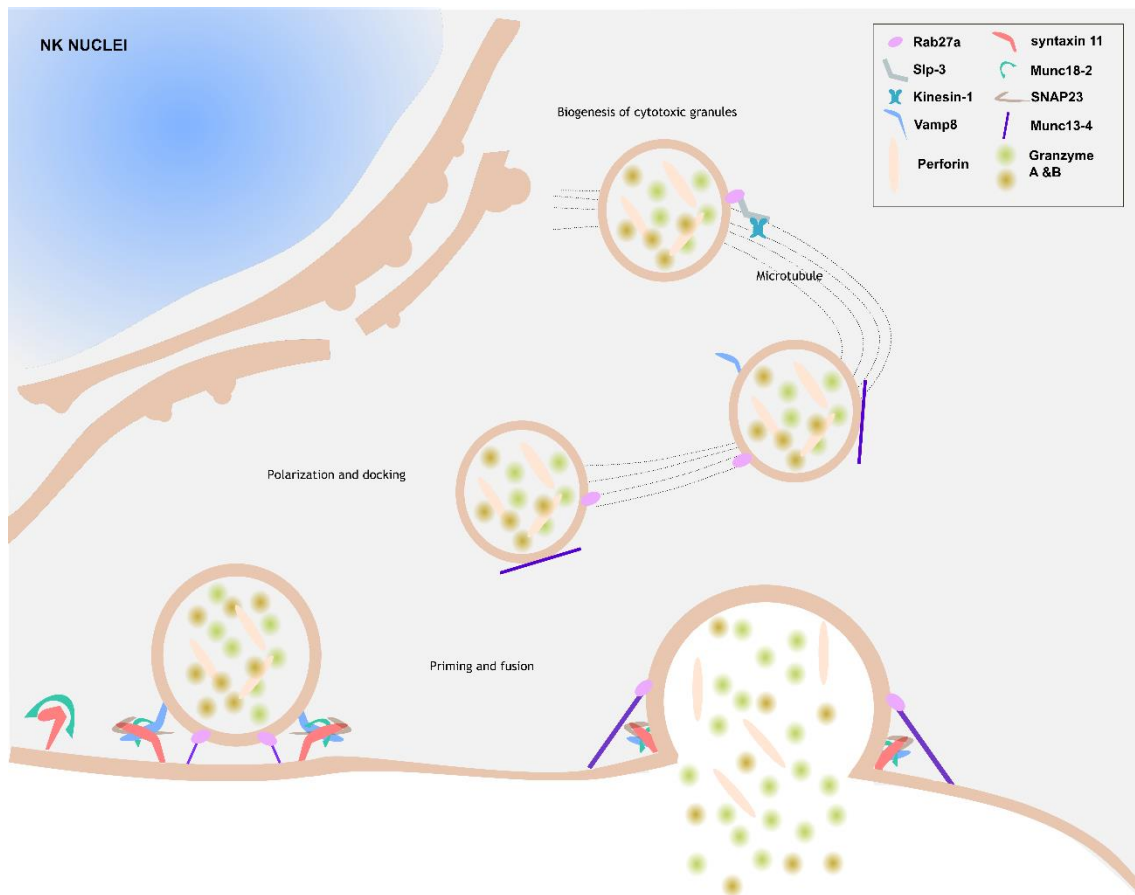


Figure 3. Fusion and exocytosis of lytic granules during NK cell-mediated cytotoxicity.

Release of lytic granules is a multi-step process: (1) *Biogenesis of cytotoxic granules*: Granzymes, perforins and other soluble proteins, including lysosomal hydrolases, are sorted from the trans-Golgi network to early endosomes by the mannose-6-phosphate receptor (M6PR). (2) *Polarization*: Cytotoxic granules are rapidly clustered around the MTOC and transported by kinesin-Rab27a-Slp3 protein complex. (3) *Docking step*: Rab27a located on the cytotoxic granules interact with munc13-4 allowing the facing between the cytotoxic granule and the plasma membrane. (4) *Priming and fusion*: docked vesicles are primed by Munc13-4 leading to the formation of the SNARE complex between the cytotoxic granule membrane and plasma membrane. Protein VAMP8 located on the cytotoxic granule membrane, interacts with syntaxin 11 and SNAP23 located on the plasma membrane. Finally, Munc18-2 clasps across the zippering four-helix SNARE complex bundle to promote the cytotoxic granule fusion.

4. ROLE OF GRANULE-DEPENDENT EXOCYTOSIS PATHWAYS IN IMMUNE HOMEOSTASIS

The granule-dependent cytotoxic pathway is a major immune effector mechanism in the resistance to viral and intracellular bacterial infections and in the prevention of tumor development(de Saint Basile et al. 2015b). However, another supported role of the granule exocytosis pathway is its participation in preventing an uncontrolled expansion of T cells during acute immune response(Smyth et al. 2001). Several reports have pointed out that deficiency of perforin leads to an exacerbation of lymphocytes expansion which can evolve into a persistent, antibody-mediated response and a potential humoral autoimmunity(Kägi, Odermatt, and Mak 1999; Stepp 1999; J et al. Feldmann 2005). Therefore, lymphocyte cytotoxic activity in humans is crucial in the resolution of inflammation and an illustration of the break of this balance the occurrence of excessive, uncontrolled, and fatal antigen-specific T-cell expansion, known as the Hemophagocytic lymphohistiocytosis syndromes (HLH) which are the focus of the thesis.

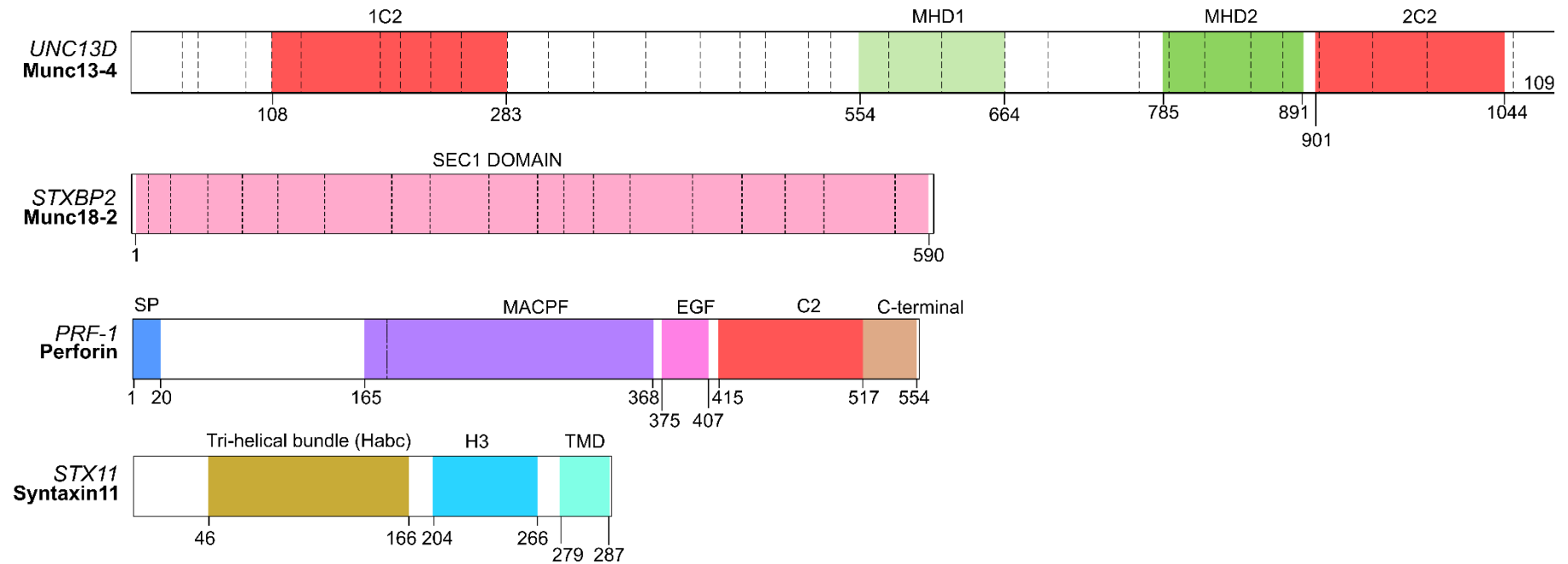


Figure 4. Schematic representation and domain structure the proteins involved in HLH. Munc13-4 is encoded by UNC13D gene comprised with 53 exons. Munc13-4 has two calcium (1C2 and 2C2) domains at both C- and N-terminal and a central tandem repeat of Munc13 homology domains domain (MHD1 and MHD2). STXBP2 gene (19 exons) codified the protein Munc18-2 with a functional domain Sec1 which is important for the assembly and disassembly of the SNARE complex and consequently to control of membrane fusion. Perforin is codified by exons 2 and 3 of PRF-1 gene. Perforin has a terminal C2 domain by which mediates the membrane binding in a calcium dependent manner. The N-terminal membrane attack complex/perforin (MACPF) is essential to produce the monomers polymerization into a ring. Exon 2 of STX11 gene codifies by syntaxin 11 protein which contains an amino-terminal helical domain called Habc, a carboxy-terminal helical region called H3 (SNARE core motif) and a transmembrane anchor domain (TMD). Dotted lines indicated exons.

5. WHAT IS HEMOPHAGOCYTIC SYNDROME (HLH)?

Hemophagocytic syndrome (HLH) is a primary immunodeficiency (PID) belonging to the group of the Disorders of immune dysregulation (Picard et al. 2015). This group is characterized because of the presence of dysfunctional lymphocytes that cause the development of excessive autoreactivity, which in turn leads to a potential autoimmune disease and/or other symptoms of immune dysregulation (McCusker, Upton, and Warrington 2018). The term HLH was coined by the "International Histiocyte Society" in 1998 (J. I. Henter et al. 1998) to explain the familial form of the disease described for the first time in 1939 as a disorder with proliferating histiocytes in the lymphoreticular system and they called it "histiocytic medullary reticulosis" or HMR (Scott R 1939). In 1952, this familial form was described more accurately in two siblings with HLH (Farquhar and Claireaux 1952). In particular, HLH represents a spectrum of hyperinflammatory disorders associated with activation of cytotoxic T, NK cells, and macrophages. Subsequently, it was described that HLH could occur in a hereditary way due to genetic alterations (primary form or familial HLH, FHL) or association to infections, malignant or autoimmune diseases (secondary form, sHLH). In any of the forms, the treatment must be implemented early with the main objective of suppressing the potentially deadly inflammatory process (Lehmberg et al. 2015). However, the treatment of choice will be different according to the identified form. The only cure for the primary forms of HLH is a transfer from a healthy donor hematopoietic stem cells (HSC), while in the secondary form an immunosuppression strategy is applied and the treatment must be focused on resolving the triggering factor (Jordan et al. 2011). However, because primary HLH and secondary HLH are not easy to discriminate, the treatment is sometimes delayed leading to an impact on patient survival (Jordan et al. 2011).

6. EPIDEMIOLOGY

The true epidemiology of primary HLH has not been properly addressed and it is even less known for acquired HLH cases (George 2014). First reviews reported an incidence of 1.2 children per million per year (J. I. Henter et al. 1991) or 1 in 100,000 children (Niece et al. 2010). Latest reviews estimated that approximately 1 child in 3000 admitted to a tertiary care pediatric hospital will have HLH (Jordan et al. 2011). Although HLH is primarily a pediatric disease, it is diagnosed in adult patients as well (Ramos-Casals et al. 2014). The average age of debut for primary HLH is before 2 years of age, but recent reports have described the late-onset primary HLH as not as rare as previously thought (Wang et al. 2014). On the other hand, secondary forms tend to occur in patients

with delayed onset (Machaczka 2013) and are more frequently associated with an infectious episode, especially with Epstein-Barr virus (EBV)(Ishii 2016).

7. CLASSIFICATION

Hemophagocytic lymphohistiocytosis is classically divided into primary (hereditary cases or FHL) and into secondary (acquired cases or sHLH). FHL comprises several genetically heterogeneous conditions, including FLH type 2, type 3, type 4 and type 5, Griscelli syndrome type II, Chédiak-Higashi syndrome, Hermansky-Pudlak syndrome type II and the X-linked lymphoproliferative syndromes, among others. Primary HLH predominantly occurs during childhood and may be triggered by an infection(Morimoto, Nakazawa, and Ishii 2016). Secondary HLH can occur under a variety of circumstances, however, the most frequent trigger is infection, specially Epstein-Barr virus (EBV) and cytomegalovirus (CMV). Other triggers include malignancies, and autoimmune or autoinflammatory conditions. There is an overlap between primary and acquired HLH in terms of clinical manifestation and laboratory findings, thus this distinction may not be as clear as it may seem. There is increasing evidence(Cetica et al. 2016) that typical FHL cases with biallelic mutations and secondary HLH with neither genetic nor immunological defects represent only the extremes of the HLH wide spectrum (*Figure 5*).

7.1.Familial Hemophagocytic Lymphohistiocytosis type 2-5

Familial hemophagocytic lymphohistiocytosis (FHL) is characterized by proliferation and infiltration of hyperactivated macrophages and T-lymphocytes manifesting as acute illness with prolonged fever, cytopenias, and hepatosplenomegaly. Onset is typically within the first months or years of life although later childhood or adult onset is also seen. HLH is diagnosed using clinical criteria developed by the HLH Study Group of the Histiocyte Society (Table 1)(J.-I. Henter et al. 2007). Other findings included liver dysfunction, neurologic abnormalities and bone marrow hemophagocytosis. Impaired NK and CTL cells cytotoxic activity is a major feature of FHL as well as absent or reduced degranulation in FHL3 to 5.

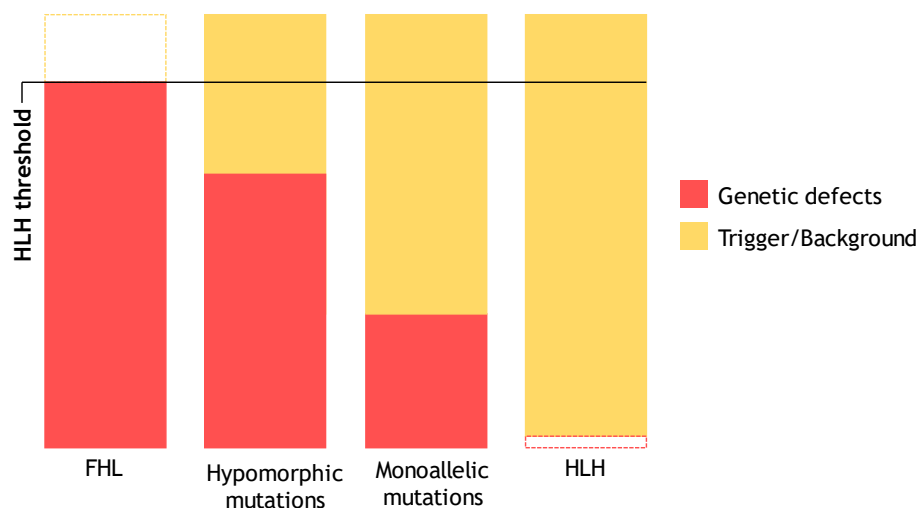


Figure 5. Risk of developing HLH base on triggers, genetic and/or inflammatory background, and confirmed mutations in HLH-known-genes. *Patients with mutations in HLH-related genes (PRF1, UNC13D, STX11, STXBP2, RAB27A, LYST, SH2D1A, XIAP, and AP3B1) are represented in the first column, thus the genetic defect by itself is enough to cause HLH, having an infectious trigger is optional (yellow dotted line). Patients with hypomorphic mutations of harboring monoallelic variants need a trigger (infectious and/or inflammation) to overcome the HLH threshold. Finally, patients without genetic defects may develop HLH under the presence of a strong trigger. Adapted from (Strippoli, Caiello, and De Benedetti 2013)*

Table 1. Hemophagocytic lymphohistiocytosis (HLH) 2004 diagnostic criteria. Adapted from (J.-I. Henter et al. 2007)

Fever
Splenomegaly
Cytopenias (≥ 2 cell lines)
Hemoglobin <90 g/L
Platelets $<100 \times 10^9/L$
Neutrophils $<1.0 \times 10^9/L$
Hyperferritinemia $>500\mu g/mL$
Hypertriglyceridemia >3.0 mmol/L or Hypofibrinogenemia <1.5 g/L
Hemophagocytosis in bone marrow, spleen, or lymph nodes
Low or absent NK-cell activity
sIL-2R >2400 UI/mL

The gene involved FHL-1 has not been reported yet only the chromosome region 9q21.3-22. It was reported to be linkage in two Pakistani consanguineous (Ohadi et al. 1999).

FHL-2 is caused by mutations in *PRF1* gene which is coding for the granule effector protein perforin. *PRF1* has 3 exons, 2 of which (exons 2 and 3) contain coding sequences. Perforin is a pore forming multi-domain protein that oligomerizes to form circular pores on target cell membrane. Once perforin is released from the cytotoxic granules it binds to the target membrane and through the C-terminal C2 domain mediates the membrane binding and pore forming in a calcium dependent manner leading to the cytotoxic activity (Voskoboinik, Smyth, and Trapani 2006). Defects in perforin were the first to be causally linked to primary HLH (Stepp 1999) and nowadays within 30–40% of molecularly diagnosed patients possesses a mutation in *PRF1*, (Cetica et al. 2016). Genotype–phenotype studies show that there is a strong correlation between the genetic defect and the function of perforin (Horne et al. 2008). Pathogenic mutations lead to an absent or reduced perforin activity. Perforin deficiency can be easily assessed by intracellularly staining in NK cells using a conjugated monoclonal antibody (Chiang, Bleesing, and Marsh 2019).

FHL-3 is caused by mutations in *UNC13D* gene. This gene contains 32 exons and encodes a 123-kDa protein named Munc13-4 (Jérôme Feldmann et al. 2003). Most of the *UNC13D* mutations found in reported patients are missense, deletion, splice-site, or nonsense mutations predicted to be damaging. Moreover, deep intronic mutations (Qian et al. 2014) in this gene have been also reported as pathogenic. Cytotoxic defect can be assessed by the detection of CD107a with a conjugated monoclonal antibody on the cell surface of NK or CTL after specific stimulation.

FHL-4 is caused by mutations in *STX11* that consists of 2 exons and encodes for syntaxin11 protein. This protein regulates granule membrane fusion through Munc18-2 and SNARE proteins contacts. Most of the mutations in *STX11* so far reported are null mutations and most of them were identified in patients of Turkish origin, who account for approximately 20% of FHL patients (Stadt et al. 2006). The defective cytotoxic activity clearly detected using the same technique as for FHL-3.

Finally, FHL-5 is caused by mutations in *STXBP2* that consist in 19 exons and encodes for Munc18-2 protein. This protein interacts with syntaxin11 facilitating formation of the SNARE complex. Clinical presentation of FHL-5 differs from that of other FHL subtypes being more notorious patients with later onset with splenomegaly and unexplained fever or a COVID-like picture (Pagel, et al. 2012). Exists a high prevalence of the exon 15 splice site mutation c.1247-1G>C, which is associated with this a milder clinical phenotype and a later onset of the disease (Göransdotter Ericson et al. 2001).

In the remaining 8–10% of FHL cases (diagnosed based on familial history, consanguinity, or confirmed immunological deficiencies) the underlying molecular defects are not yet determined (Cetica et al. 2016; de Saint Basile et al. 2015a). In this subgroup are included patients with FHL-1.

7.2. Primary immunodeficiency syndromes associated with HLH

There is a well-defined group of patients in whom the HLH syndrome has been reported in a variety of PIDs. The clinical presentation of some of these cases are summarized below. Different pathophysiology and a common phenotypic endpoint

7.2.1. Primary failure of biogenesis, function and trafficking of secretory lysosomes

This group encompasses patients with partial oculo-cutaneous albinism and immunodeficiency, including Chediak–Higashi (CHS), Griscelli type 2 (GS2), Hermansky–Pudlak type 2 (HPS2), MAPBPIP-deficiency Syndrome and HPS-like syndrome, known as HSP-9. However, only CHS, GS2 and HPS2 have been associated with HLH. These are recessive syndromes clinically characterized by hypopigmentation of skin, hair and eyes, associated with recurrent infections. While some clinical skin and ocular manifestations are similar within syndromes, the hematologic symptoms can be extremely heterogeneous. Susceptibility to viral and bacterial infections is high in all syndromes. Defective cytotoxicity of both NK and CTL is observed in all patients being more severe in CHS and GS2 patients (Dotta et al. 2013).

Chediak–Higashi syndrome is caused by defect in the lysosomal trafficking regulator (LYST/CHS1) gene, located on chromosome 1q42.1-q42.2 (Nagle et al. 1996). Mutations in *LYST* gene trigger an enlargement of lysosomes and lysosome-related organelles as melanosomes, platelet-dense bodies and cytolytic granules. HLH develops in 50–85% of patients (Lozano et al. 2014; Nagai et al. 2013) and is fatal if not treated.

Griscelli type 2 syndrome is caused by mutation in the *RAB27A* gene that encodes for a small GTPase important for vesicular fusion, trafficking and docking at the plasma membrane. *RAB27A* is also affected by *Munc13-4*; hence patients with mutations in either of these genes share many immunological features. *Rab27a*-deficient NK cells

and CTLs exhibit impaired exocytosis of cytotoxic granules, although polarization is preserved (Ménasché et al. 2000). The decisive factor in order to discriminate this disorder from FLH or CHS is that GS-2 patients have silvery hair and lack of giant inclusive bodies (M Meeths et al. 2010).

Hermansky–Pudlak type 2 syndrome is caused by mutations in the AP3B1 gene that encodes for a subunit of the adaptor protein AP-3 complex (Enders et al. 2006). The AP-3 complex directs the cytotoxic proteins trafficking from TGN to the lysosome (Eskelinen 2006). AP-3 also plays an important role in loading of peptides on to MHC class II in antigen presenting cells (Sugita et al. 2002). Despite being linked to HLH, only few patients with Hermansky–Pudlak type 2 syndrome have been associated with HLH (B. Jessen et al. 2013).

7.2.2. Inherited T cell defects

Other defects that have been linked to HLH are associated with inherited T cell defects. For example, X-linked lymphoproliferative syndrome (XLP) but which does not present defects in NK or CTL cytotoxic function due to the fact that the defective proteins are not involved in granule-mediated cytotoxicity (Yenan T Bryceson et al. 2012; Usmani, Woda, and Newburger 2013). Instead, XLP is a congenital x-linked disease associated with EBV infection, usually leading at first encounter into a HLH (Janka and Lehmborg 2014). XLP-type I is due to mutations in SH2D1 gene, which encodes for signaling lymphocyte activation molecule (SLAM)-associated protein (SAP). SAP interacts with activating receptor 2B4 on NK cells, stimulating cytotoxicity and with costimulatory SLAM molecules in T and B cells promoting their effector function (Brisse, Wouters, and Matthys 2016). XLP-type II was described in patients with mutations in BIRC4 gene, which encodes for X-linked inhibitory of apoptosis (XIAP) (Rigaud et al. 2006). XIAP inhibits the activity of different caspases, cells of XIAP-deficient patients show higher apoptosis rates in vitro, however, the cytotoxic functions of NK and CTL is conserved (Marsh et al. 2010).

Another inherited T cell condition, IL2-inducible T cell kinase (ITK) deficiency causes severe immune dysregulation and B cell proliferation disease following EBV infection (Huck et al. 2009). This gene has been reported to be involved in the differentiation of naive CD4⁺ cells into Th2 cells. It is not known how ITK deficiency contribute to HLH, but it is suggested that the PID together with other triggers such as malignancy and/or the viral infection could contribute to the development of HLH (Faitelson and Grunebaum 2014). For this syndrome, only few patients have been

described with its subsequent lack of knowledge regarding the outcomes of the disease (Zheng et al. 2016).

Another protein involved in the B-, T- and NK-cell functions, survival and differentiation is the co-stimulatory CD27 molecule. When CD27 binds to its partner CD70 leads to activation of transcription factors. Patients with CD27 deficiency have normal NK cell numbers but mildly to moderately reduced NK cell function. Clinical manifestations vary from asymptomatic memory B-cell deficiency to EBV-associated HLH and malignant lymphoma. The role of this finding in the development of HLH is yet not clear (Zheng et al. 2016).

Of note, ITK and CD27 deficiency are characterized by a poor control of EBV infection, but as in XIAP deficiency, the molecular mechanisms predisposing to HLH so far remain elusive. Importantly, NK T-cell development, which may also be relevant for control of EBV infection, is impaired in all four diseases (Bode et al. 2012).

7.3. Primary HLH due to macrophagic hyperactivation

Affecting one of the main cells of the innate immune system, macrophages, systemic Juvenile Idiopathic Arthritis (sJIA) is characterized by arthritis, acute fever, characteristic skin rash, hepatosplenomegaly, lymphadenopathy and polyserositis. sJIA is defined as arthritis that begins before the age of 16 with high frequency in children of 1 to 3 years. Estimated prevalence of sJIA vary between 16 to 400 cases per 100,000 children. (Grom and Mellins 2010). Within 10-30% of patients with JIAs will develop a clinical MAS (macrophage activation syndrome) while the other 30-50% of patients will develop a subclinical MAS. In both cases, this potential complication represents the highest cause of mortality (mortality rates of 20-40%) associated with sJIA (Moradinejad and Ziaee 2011).

The exact mechanism of predisposition to MAS in sJIA has not yet been defined but could be independent of the underlying sJIA activity and similar to secondary HLH associated with infection. Although the genetic basis of MAS in patients with JIAs remains unclear, higher frequencies of polymorphisms have been observed in the PRF1 and UNC13D genes in patients with JIAs with a higher risk of MAS, which relates primary defects (FHL) with MAS in AIJs (Vastert et al. 2010). Recent studies by mass exome sequencing in patients with secondary HLH AIJs / MAS have shown that up to one third are carriers of infrequent hypomorphic variants that alter proteins in genes associated

with FHL. The appearance of other genetic variants in genes encoding proteins involved in reorganization and transport of vesicles has also taken relevance (Kaufman et al. 2014).

The presence of intronic or non-coding variants in AIJs / MAS has not been extensively explored, but variants that involve the first intron of the *UNC13D* gene have been identified as a key regulatory region in patients with FHLH. It has been shown that the variant, c.118-308C> T, disrupts the binding of the transcription factor to a cytotoxic specific lymphocyte promoter (Qian et al. 2014). In the same way, the c.117 + 143A> G variant, described in a patient with AIJs / MAS, disrupts an *NFKB1* binding site reducing *UNC13D* transcription levels, which potentially results in both such as decreased expression of *UNC13D* and NK cell degranulation (Schulert et al 2018).

In 2014, two independent groups identified a new gene, *NLRC4*, involved in development of HLH. *NLRC4* codes for a cytoplasmic NOD (NOD-like) receptor whose stimulation recruits and proteolytically activates caspase-1 within the multiprotein complex of the inflammasome. Functional data demonstrated that the monocytes and macrophages of these patients presented a gain-of-function of the *NLRC4* protein leading to an overproduction of IL-1 β and IL-18 and increased pyroptosis. However, the patients do not present with cytotoxic defect, thus providing a new paradigm for the pathogenesis (Canna et al. 2014; Romberg et al. 2014).

Table 2. Clinical and laboratory features of HLH patients.

	Gene	Protein	Protein function	Distinct Clinical findings	Main laboratory findings
Familial HLH type 1-5					
FHL1	<i>9q21.3-3.22</i>	Unknown	Unknown	Early onset with severe clinical manifestations	-----
FHL2	<i>PRF-1</i>	Perforin	Pore forming, involved in target cell cytotoxicity	Early onset with severe clinical manifestations	Perforin expression low or absent, normal NK degranulation.
FHL3	<i>UNC13D</i>	Munc13-4	Vesicle priming and exocytosis/secretion of lysosomes	Increased incidence of central nervous system (CNS) symptoms	Defective NK degranulation
FHL4	<i>STX11</i>	Syntaxin 11	Vesicle intracellular trafficking/membrane fusion	Usually mild recurrent HLH	Defective NK degranulation
FHL5	<i>STXBP2</i>	Munc18-2	Co-localization with syntaxin-11, stability of both proteins	Colitis and hypogammaglobulinemia	Defective NK degranulation
Immunodeficiency syndromes associated with HLH					
CH	<i>LYST</i>	Lysosomal trafficking regulator	Sorting of endosomal proteins into late endosomes, lysosomal fission	Partial albinism Giant lysosomes in leukocytes on blood smear Primary neurological disease	Defective NK degranulation
HP-III	<i>AP3B1</i>	β -subunit of adaptor protein AP3	Cytolytic lysosomal movement, sorting of granule proteins	Partial albinism Characteristic eye findings Increased bleeding Neutropenia	Defective NK degranulation
GS-II	<i>RAB27a</i>	Rab27a	Tethering/docking of secretory granules	Partial albinism Hair exhibit bigger and irregular melanin granules, distributed mainly near the medulla	Defective NK degranulation
XLP-I	<i>SH2D1</i>	SLAM associated Protein/SAP	Signal transduction in NK and CTL/vesicle trafficking	Hypogammaglobulinemia Lymphoma	SAP expression low or absent. Reduced number of NKT cells
XLP-II	<i>BIRC4</i>	X-linked inhibitor of apoptosis/ XIAP	Inhibition of caspases, the effectors of apoptosis	Colitis	XIAP expression low or absent. Reduced number of NKT cells
HLH due to macrophagic hyperactivation					
NLRC4	<i>NLRC4</i>	NOD-Like Receptor NLRC4	Activation of caspase-1 within the inflammasome	-----	-----

7.4. Secondary HLH

HLH can also develop in the absence of family recurrence or biallelic mutations but appears clinically identical to primary HLH. Secondary HLH arise when there is an imbalance into the immune system (Atteritano et al. 2012; Ramos-Casals et al. 2014). Mainly, following infections, malignancies, autoinflammation/autoimmunity disorders, in acquired immunodeficiencies, following chemotherapy, immunosuppression, and in rare cases as in inborn metabolic disorders. Infection-associated HLH accounts for approximately half of all adult HLH cases (Ramos-Casals et al. 2014). Malignancy-associated HLH accounts for 15–50% of adult HLH cases. Nonetheless, cases may be observed in children and adolescents. The most common underlying cancers are lymphomas, mostly T/NK cell, but also B cell lymphomas, and leukaemia. In the context of autoimmunity, HLH is most frequently reported in systemic juvenile idiopathic arthritis (sJIA). It is also seen in systemic lupus erythematosus, adult-onset Still's disease, Kawasaki disease and, sporadically, in rheumatoid arthritis, dermatomyositis, sarcoidosis, systemic sclerosis, polyarteritis nodosa and inflammatory bowel disease (Brisse, Wouters, and Matthys 2016).

7.5. Monoallelic HLH

Until very recently all these entities were considered as recessive, so it was necessary to have the two mutated alleles of the gene to manifest the disease. But recently a couple of cases of patients carrying monoallelic mutations in STXBP2 (Spessott et al. 2015) (Spessott et al 2015) and RAB27A (M. Zhang et al. 2016) have been described with a dominant negative effect, which expands the type of inheritance of the disease. Remarkably, in about 10% of patients with FHL, the genetic basis of the disease remains unresolved (Cetica et al. 2016)

8. CLINICAL PRESENTATION OF HLH

The onset of disease is below 1 year of age in 70–80 % of the cases but late-onset cases have been described in adolescence and in adulthood (Allen et al. 2001). Clinical manifestations include prolonged high-grade fever, progressive cytopenias, hepatosplenomegaly with liver dysfunction, skin rash, coagulopathy, and variable neurologic symptoms. It is important to highlight that cytopenias and hemophagocytosis in bone marrow aspirate may not be present in the initial stage of the disease and may evolve subsequently (Madkaikar, Shabrish, and Desai 2016). The disease is often triggered by infections, most commonly viral and the most common viral pathogens are

Epstein–Barr virus (EBV), cytomegalovirus and parvovirus (J. I. Henter et al. 1993). It has been reported that patients with FHL4 usually have milder clinical phenotypes than the other forms of FHL. In patients with FHL5 and XLP2, manifestations like colitis and/or hypogammaglobulinemia have been observed (Table 2).

9. LABORATORY FINDINGS

9.1. Cytopenia(s)

At diagnosis, cytopenias are fulfilled in 100% of FHL cases and in 80% of the sHLH (George 2014a). Cytopenias can be explained by high concentrations of cytokines as TNF- α and IFN- γ and because of direct hemophagocytosis.

9.2. Bone Marrow Aspirate

Hemophagocytosis is very unspecific and low sensitive evidence since it is not possible to exclude the diagnosis of HLH when is not detected and it can be detected because many other conditions. However, bone marrow aspirate is mandatory rule out the possibility that HLH has been triggered by a leukemia.

9.3. Ferritin

High ferritin levels have been reported as a useful finding, especially in children, with high sensitivity and specificity (Trottestam et al. 2011). However, it is important to highlight that low ferritin (<500 ng/mL) does not exclude the diagnosis of HLH and high levels only suggest HLH diagnosis without differencing primary versus secondary cases. Elevated ferritin >10,000 μ g/L has been demonstrated to be 90% sensitive and 96% specific for HLH

9.4. sCD25

Measurement of sCD25 (sIL2r) is useful in diagnosis, in follow-up and in assessing response to therapy. These high concentrations of sCD25 seen in HLH patients are produced by activated T lymphocyte. Thus, this biomarker reflects the degree of T cell activation.

9.5. NK cytotoxicity assay

Quantifying the amount of target cells (K562) killed by NK cells is measured through the incubation with K562 and NK cells at different ratios together with a fluorescent intercalating DNA agent used to stain dead cells. Reduced NK cytotoxicity was considered a standard component of HLH diagnostic criteria but in the recent years has been reported low sensitivity, specificity, and poor positive predictive value (Hines and Nichols 2017). On the other hand, low NK cytotoxicity has been an excellent negative predictive value.

9.6. Intracellular staining

Intercellular staining of Perforin, SAP or XIAP in cytotoxic lymphocytes is quick and these are reliable markers not affected by HLH treatment (Johnson et al. 2011). However, these markers are only valid to detect gene mutations seen in FHL2, XLP-1 or XLP-2. However, it is important to highlight that a positive detection of these proteins does not rule out an alteration in them.

9.7. NK and CTL degranulation assay

Since the first degranulation defects were published, degranulation assays quantifying surface expression of CD107a in NK and CTL cells have been applied for the diagnosis of different forms of primary HLH (Marcenaro et al. 2006; Y. T. Bryceson et al. 2007). Specifically, NK cell degranulation assay has been shown to be useful in diagnosis of FHL associated with defect in the granule release mechanism (FHL3–5, CHS, GS2). Therefore, in FHL2 patients in which the affected protein is perforin, this assay is expected to be normal. Interestingly, a reversible restoration of degranulation after IL-2 stimulation of NK cells was observed in FHL4 and FHL5 patients (Y. T. Bryceson et al. 2007; Saltzman et al. 2011). This could explain the less severe disease progression observed in these compared with FHL2 and FHL3 patients.

Hence, to validate the usefulness of this assay and to establish standardized easy-to-use and robust protocols, four European laboratories conducted the evaluation of NK cells and CTL degranulation on a large group of unselected patients (Bryceson 2012).

Based on these publications, it was strongly recommended to perform the degranulation test in patients with HLH and suspected primary defect. Moreover, it has been reported to exhibit good sensitivity and specificity (93.8% and 72%, respectively) for FLH (Hines and Nichols 2017). However, this assay is not yet included in the HLH diagnosis criteria. Rubin et al, suggest that perforin and degranulation assays should be preferentially performed to screen patients for primary HLH diseases.

9.8. High triglyceride levels

High triglyceride may be due to liver dysfunction and at diagnosis is fulfilled in 70 % of cases (George 2014b). High triglycerides are secondary to decreased lipoprotein lipase activity initiated by increased TNF- α levels.

9.9. Hypofibrinogenemia

Low fibrinogen (<1.5 g/L) is consequence of the highly activated macrophages which secrete plasminogen activators accelerating the conversion of plasminogen to plasmin. Thus, degrading fibrinogen.

9.10. Cytokines

Due to the persistent activation of macrophages, NK cells, and CTLs in patients with HLH, a cytokine storm is released leading to high mortality. Several inflammatory cytokines have been reported to be increased in this syndrome: interferon gamma (IFN gamma); tumor necrosis factor alpha (TNF alpha); interleukins (IL) such as IL-6, IL-10, and IL-12; and the soluble IL-2 receptor (CD25). These can be used as a biological markers of disease active state.

Other laboratory parameters include hepatic enzyme abnormalities, conjugated hyperbilirubinemia, hypoproteinemia, hyponatremia, elevated D-dimers, elevated VLDL (very low-density lipoprotein) and low HDL (high density lipoprotein). These parameters are not listed in the diagnostic criteria but can be helpful in some patients who do not fulfill the criteria (Madkaikar, Shabrish, and Desai 2016).

10. PATHOGENESIS

HLH is a syndrome of excessive inflammation and tissue destruction due to abnormal immune activation. However, this dysregulation can be caused by different pathways that at some point overlap but are distinctly clustered in origin (Figure 6).

Table 3. Summary of the causative effects of HLH findings

HLH sign	Cause
Fever	IL-1, IL-6, THF- α
Cytopenias	THF- α , INF- γ , hemophagocytosis
High triglycerids	Lipoprotein lipase action
Low fibrinogen	PAF secreted by M \emptyset that stimulate plasmin leading to hyperfibrinolysis
High ferritin	Released by activated M \emptyset
High levels of sCD25	Secreted by T lymphocytes
Hepatosplenomegaly	Organ infiltration by activated M \emptyset

10.1. Pathogenesis in the cytolytic pathway

One of the most studied pathophysiological mechanisms is the dysfunction of the cytotoxic capacity of CD8 + T cells and NK cells. The integrity of the cytotoxic function is essential to maintain the homeostasis of the IS(Brisse, Wouters, and Matthys 2016). Defects in this pathway lead to an uncontrolled expansion and persistent activation of CD8 + and NK T cells, as well as an excessive production of cytokines in which excessive production of IFN- γ by hyperactivated CTLs has been designated as a major underlying disease mechanism(X.-J. Xu et al. 2012). These induce the activation of macrophages, tissue infiltration and the production of pro-inflammatory interleukins (IL-6, IL-2, IL-1 β , IL-8, IL-10, IL-12, IL-18), responsible of tissue damage and clinical manifestations already mentioned.

10.2. Pathogenesis in the macrophagic hyperactivation

The discovery of the association within HLH and NLCR4 added a new way to explain the pathogenesis of HLH. NLCR4 gene encodes for cytoplasmic NOD-like receptors (NLRs) whose stimulation recruits and proteolytically activates caspase-1 within the inflammasome, a multiprotein complex(Canna et al. 2014). Caspase-1 mediates the production of interleukin-1 family cytokines (IL1FCs), leading to fever and inflammatory cell death (pyroptosis). So far, the mutations are found to produce a constitutively activation of these pathways leading to a pro-inflammatory state thus the HLH picture.

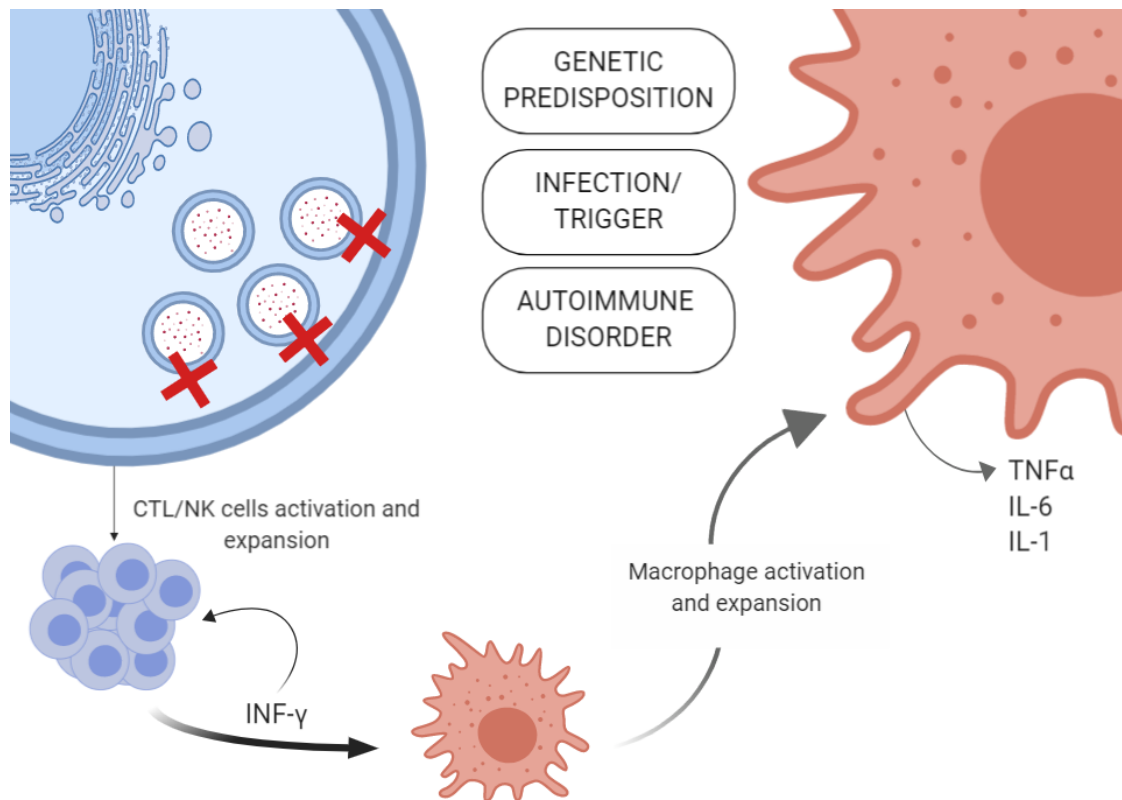


Figure 6. Proposed pathophysiology of HLH. The origin of HLH development may be mainly due to impairment of two pathways (degranulation and macrophage activation), which are not mutually exclusive. On the one hand in some patients with HLH, NK cells and CTLs fail to lyse the infected cells (primary or secondary causes). Thus, CTL / NK proliferate and produce a great quantity of IFN- γ which stimulates the macrophage. On the other hand, HLH can be trigger directly by an uncontrolled activation of the macrophages (primary or secondary causes) secreting high levels of IL-1, IL-6, IL-10, IL-18, and TNF α . At the end, the two pathways converge in an hypercytokinemia and accumulation of lymphohistiocytic infiltrates into organs and organ damage.

10.3. Pathogenesis due to monoallelic variants

HLH can also be explained by synergistic defects of several monoallelic hypomorphic mutations in the cytotoxic pathway (K. Zhang et al. 2014b; Gao et al. 2015). Some HLH patients have been found to have mutations in two different genes simultaneously, provoking an earlier onset of HLH compared to single-mutated patients (Fernando E Sepulveda et al. 2016). Moreover, in the recent years simple monoallelic mutations related with HLH have been found and are more common than previously thought. However, only in two monoallelic mutations the pathogenic effect has been proven. The patient with the heterozygous mutation in RAB27a (M. Zhang et al. 2016) showed a

delayed cytotoxicity because of less protein produced. Thus, leading to a prolonged interaction between the cytotoxic cell and APC so a deeper proinflammatory cytokine storm triggering HLH. Another clear dominant-negative mutation was reported in *STXBP2* gene (Spessott et al. 2015). In this case, the patient showed an impaired cytotoxicity and degranulation due to the mutant (*STXBP2*^{R65Q}) bind improperly to SNARE complex impairing complete membrane fusion.

10.4. Pathogenesis in the secondary HLH

Pathogenesis of secondary or acquired HLH is even less clear since all the misclassified HLH patterns are listed inside sHLH. In this thesis we considered sHLH when there was no proof of patient's genetic background. In this sense, in order to develop HLH the patient must have underwent to a viral infection, rheumatology condition, malignancy or activating immunotherapy. Overall, all of them lead to HLH because cause defective immune regulation, thus activating T cells and macrophages (Jordan et al. 2019).

In summary, patients with HLH who are found to have biallelic mutations in typical genes are immediately diagnosed as "primary HLH" and, therefore, placed on the HSCT protocol. In contrast, in patients with monoallelic variants the diagnosis and so on the treatment is challenging due to these variants have not been considered as a cause of the disease. Demonstrating the pathogenicity of monoallelic variants in typical genes and demonstrating their effect will be of great help for the accurate diagnosis and clinical management of these patients.

II. HIPOTHESIS AND OBJECTIVE

1. GENERAL HYPOTHESIS

In patients with primary HLH, the biallelic mutations in certain genes are responsible for the onset of the disease in the absence of other factors. However, in secondary HLH genetic defects predispose to the disease but an additional trigger stimulus -such as viral infections, inflammation or cancer- is required for the development of the disease. There are a range of different genotype-phenotype associations between primary and secondary HLH. In this regard, our **first hypothesis is that the molecular and functional study of HLH-related-genes mutations found in HLH patients will allow us to postulate a more accurate genetic basis for HLH cases.**

The development of the disease can be both through defects in the cytolytic pathway of NK and T CD8 lymphocytes as in mutations in genes that predispose to the activation of macrophages. In both cases, the end point is a cascade of proinflammatory cytokines that produce the activation and expansion of T lymphocytes and macrophages with hemophagocytic activity. Therefore, **our second hypothesis is that, mutations in the well-known genes of the cytotoxic pathway could have a functional impact on macrophages at endosomal trafficking level.**

Overlapping symptoms with chronic variable immunodeficiency such as hypogammaglobulinemia have already been described in patients with FHL5. The gene responsible for FHL-5 is STXBP2. Consequently, **our third hypothesis is that B lymphocytes might be affected by STXBP2 defects.**

2. GENERAL OBJECTIVES

Analyze in depth the genetic basis of HLH by studying novel mutations at molecular and functional level.

3. CONCRETE OBJECTIVES

- 3.1.** Establish reference ranges and thresholds for the cytotoxicity activity and for the NK cell degranulation assays in adult and pediatric population.
- 3.2.** Evaluation of HLH patients using functional techniques of cytotoxicity and degranulation
- 3.3.** To perform functional and molecular characterization of novel mutations found in patients diagnosed with FHL.
- 3.4.** Conduct functional and molecular characterization of novel and reported mutations found in patients diagnosed with an atypical form of HLH.
- 3.5.** To assess functional impact of the STXBP2 silencing in macrophages and B lymphocytes cell lines.
- 3.6.** To build a free access comprehensive repository of HLH mutation data for medical research and genetic diagnosis of HLH.

III. MATERIALS AND METHODS

1. CELLS CULTURE

Complete Dulbecco's Modified Eagle's Medium (cDMEM): Incomplete DMEM supplemented with 10% heat-inactivated fetal bovine serum (FBS), 2mM L-glutamine, 1mM sodium pyruvate, 100 U/ml penicillin and 100 µg/ml streptomycin antibiotics.

Complete Roswell Park Memorial Institute Medium (cRPMI): Incomplete RPMI (variety 1640) supplemented with 10% heat inactivated FBS, 1mM sodium Pyruvate, 100 U/ml penicillin, 25mM Hepes Buffer and 100 µg/ml streptomycin antibiotics.

2. CELL LINES

THP-1 (ATCC TIB-202) is an immortalized cell line of monocytes derived from acute monocytic leukemia. This is commonly used in the study of the mechanisms, signaling pathways and functions of monocytes and macrophages(Tsuchiya et al. 1980).

K562 (ATCC CCL-243) is a line of undifferentiated cells with lymphoblastic morphology derived from chronic myeloid leukemia originating in a 53-year-old adult. These cells lack MHC-I expression and are commonly used as a target cells in in vitro assays to evaluate cytotoxic activity(Andersson and N. K. 1979).

RBL-H3 (ATCC® CRL-2256) RBL-2H3 is a rat basophilic leukemia cell line widely used as a convenient model system to study the degranulation. They can be activated to secrete histamine and other mediators by aggregation of the high affinity IgE receptors or with calcium ionophores(Huang et al. 2016).

COS-7 (ATCC CRL-1651) are fibroblast-like cell lines derived from monkey kidney tissue obtained by immortalizing CV-1 cells. These cells are often transfected to produce recombinant proteins for molecular biology, biochemistry, and cell biology experiments(Aruffo 2002)

All the cells were maintained at 37°C with 5% CO₂ atmosphere.

Table 4. Characteristics of used cell lines

Cell line	Origin	Morphology	Growth properties	Growth medium
COS-7	Monkey Kidney SV40 transformed	Fibroblast-like	Adherent	cDEMEM
RBL-H3	Rat Basophilic Leukemia	Fibroblast-like	Adherent	cDEMEM
THP-1	Human acute monocytic leukemia	Fibroblast-like	Suspension	cRPMI+0.05mM β -mercaptoethanol
Ramos (RA 1)	Human Burkitt's lymphoma	Lymphoblast	Suspension	cRPMI

3. OTHER CELLS

Peripheral blood mononuclear cells (PBMCs) were isolated from whole blood from human donors, provided by the Banc de Sang i Teixits (Barcelona, Spain). In order to isolate PBMCs by density gradient we used Ficoll-Hypaque and centrifugation at 931xg without break for 20 min. After centrifugation, PBMCs layer was recovered and washed 2 times with PBS (1X). Finally, PBMCs were seeded at proper density in cRPMI medium.

4. HEALTHY CONTROLS

Blood was collected in vacutainer tubes containing ethylene-diamine-tetra-acetic acid (EDTA) as anticoagulant (BD-Plymouth, PL6 7BP, UK) and processed the same day. In total we obtained 60 adult healthy donors and 39 healthy pediatric donors (aged 1 month to 11 years). Samples were obtained in Hospital Universitari Vall d'Hebron, (Barcelona, Spain), with approval of the hospital ethics committee. All participants were registered anonymously. All participants or parents/legal guardians of the children were appropriately informed, and consent was obtained. Children with a history of immune system disorders, receiving immunosuppressive therapy, or blood-derivative transfusion in the previous year were excluded from the study

5. PLASMID DNA CONSTRUCTS

Constructs were obtained by GenScript and amplified in the laboratory by PCR-amplify. Detailed characteristics are listed in Table 5.

Table 5. Characteristics of DNA plasmids DNA.

Gene	Protein	Mutation	Vector(s)
STX11	STX11	Wild Type	pCDNA3/EGFP
STXBP2	Munc18-2	Wild Type	pCDNA3-HA, pCDNA3.1-eGFP
STXBP2	Munc18-2	R190C	pCDNA3-HA, pCDNA3.1-eGFP
STXBP2	Munc18-2	P477L*	pCDNA3-HA, pCDNA3.1-eGFP
STXBP2	Munc18-2	L243R	pCDNA3-HA
STXBP2	Munc18-2	N62D	pCDNA3-HA, pCDNA3.1-eGFP
STXBP2	Munc18-2	R192H	pCDNA3-HA
STXBP2	Munc18-2	L201F	pCDNA3-HA
STXBP2	Munc18-2	V205I	pCDNA3-HA
STXBP2	Munc18-2	R235G	pCDNA3-HA
STXBP2	Munc18-2	L256P	pCDNA3-HA
STXBP2	Munc18-2	T345M	pCDNA3-HA
STXBP2	Munc18-2	R405G	pCDNA3-HA
STXBP2	Munc18-2	A433V	pCDNA3-HA
STXBP2	Munc18-2	S454L	pCDNA3-HA
STXBP2	Munc18-2	V482I	pCDNA3-HA
STXBP2	Munc18-2	R529P	pCDNA3-HA, pCDNA3.1-eGFP
STXBP2	Munc18-2	R555G	pCDNA3-HA
STXBP2	Munc18-2	W561R	pCDNA3-HA
UNC13D	Munc13-4	Wild Type	pCDNA3-DYK, pCDNA3.1-eGFP
UNC13D	Munc13-4	R1075Q	pCDNA3-DYK, pCDNA3.1-eGFP
UNC13D	Munc13-4	R928C	pCDNA3-DYK, pCDNA3.1-eGFP
UNC13D	Munc13-4	P271S	pCDNA3-DYK, pCDNA3.1-eGFP
Rab27a	Rab27a	Wild Type	pCDNA3-DYK

*Mutation *STXBP2*^{P477L} was used as negative expression control since lead to a loss of protein expression (Côte et al. 2009).

5.1. Generation of electrocompetent bacteria

Using the standard method of transformation of *Escherichia coli* were made competent for DNA uptake by electroporation. Bacteria cells were seeded on a medium LB-Agar (Luria Broth Base, Invitrogen, plus Agar) plate O/N at 37°C. Next day a single fresh colony was expanded into 5 ml of LB medium O/N at 37°C. To obtain high transformation efficiency, it is crucial that cell growth be in the mid-log phase at the time of harvest (OD within 0.4 and 0.9). The harvested cells were washed with ice-cold deionized water several times by repeated pelleting and resuspension to remove salts and other components that may interfere with electroporation. Finally, cells were resuspended in 10% glycerol for storage at -80°C.

5.2. Bacterial transformation and plasmid amplification

For bacterial transformation, 50 µl of competent bacteria were mixed with 1 µg of plasmid DNA, transferred into 0.1 cm cuvettes and electroporated at field strength of >15 kV/cm. Following electroporation, transformed cells were cultured in antibiotic-free liquid medium for 1 hour and plated on LB agar with appropriate antibiotic. LB plates were incubated O/N at 37°C in an inverted position. Growth colonies were screened for the presence of the desired plasmid prior to proceed to plasmid DNA extraction by using NucleoBond Xtra Midi Plus kit (Macherey-Nagel) as manufactures instructions.

6. TRANSFECTIONS AND TRANSDUCTIONS

Transfection is a process that forces the delivery of nucleic acids into a eukaryotic cell. Different methods can be used in order to achieve the delivery of the nucleic acids. Here, we have used polyethyleneimine reagent (PEI) and Lipofectamine 2000. PEI is a polymer that condenses DNA into positively charged particles, allowing the binding with cell surface residues and entering inside the cell via endocytosis. Lipofectamine 2000 contains lipid subunits that form liposomes in an aqueous environment engloving the DNA plasmids. These DNA-containing liposomes are positively charged thus can fuse with the negatively charged plasma membrane of living cells and deliver the nuclei acid inside the cell. Transfections can be transient or stable in the cell, depending on the method and protocol of the transfection.

Transduction is a process by which nucleic acids are introduced into a cell by a virus or viral vector. We used Polybrene which is a polymer that neutralize the charge repulsion between virions and sialic acid on the cell surface. Polybrene improve transduction although is very toxic so it is necessary to be remove early.

6.1. TRANSIENT TRANSFECTION OF PLASMID DNA IN COS-7 MAMMAL CELL LINE

COS-7 cells were seeded at 2.5×10^5 cells in 6-well plate 24 hours prior to transfection. Nex day, for each transfection sample, we prepared the following mix: 400uL of incomplete DMEM, 3ug of plasmidic DNA and 9uL of PEI. We added each mix into the appropriate well plate. Sixteen hours later, we replaced medium with fresh cDMEM. The expression of the transfected DNAs was checked by WB of their lysates 48 hours post-transfection.

6.2. STABLE TRANSFECTION OF PLASMID DNA IN RBL-2H3 CELL LINE

To stable transfect RBL-2H3 cell line, we plated 5×10^5 cells in 6 well-plates in 2000 μ l of growth medium without antibiotics so that cells will be 90-95% confluent at the time of transfection one day before transfection. For each transfection sample, we prepared complexes by gently mixing: Solution A (4ug of DNA in 150 of incomplete DMEM medium) and Solution B (9uL of Lipofectamine™ 2000 diluted with 141uL of incomplete DMEM medium). After 10-minute incubation, we added the 300 μ l of complexes to each well containing cells and medium. Six hours pots-transfection we added 2000 μ g/ml of Neomycin (Sigma-Aldrich) to select the transfected cells. We sorted cells with BD FACSCanto™ II Flow Cytometry System in order to choose the ones with high GFP expression levels.

6.3. STABLE TRANSDUCTION OF SHRNA IN THP-1 CELL LINE

Short hairpin or small hairpin RNA (shRNA) is a way to induce RNA interference-mediated posttranscriptional gene silencing for target genes. The shRNA consists of an RNA molecule with a hairpin-like structure that once inside the cell, the DICER enzyme converts the hairpin-like structure into a Small interfering RNA (siRNA) which is then engaged with RISC to scan and find a complementary messenger RNA (mRNA) to induce mRNA cleavage and then suppress gene expression.

THP-1 cells were seeded in 12-well plate 24 hours prior to viral infection. Next day, we mixed cRMPI with Polybrene (hexadimethrine bromide) at a final concentration of 5µg/ml. We changed the media from plate wells with 1 ml of this Polybrene/media mixture per well. Finally, we thawed the lentiviral particles at room temperature and infected the THP-1 cells by adding the 10uL of Unc18-2 shRNA Lentiviral Particles. At day 3 we splitted THP-1 cells in 1:3 and continued incubating for 48 hours in complete medium. At day 5 we selected the stable clones with Puromycin dihydrochloride selection (2 µg/ml). In order to prove the effect of UNC18-2 shRNA expression we used Western Blot analysis.

7. PROTEIN IMMUNOBLOTTING BY WESTERN BLOT

Western Blot is a widely used technique for the study of proteins. This method allows the detection of proteins contained within a biological sample. The specificity of Western Blot is achieved using an antibody that recognizes and binds to a unique epitope of the protein of interest.

To determine protein expression in both PMBCs and cultured cells were lysed for 30 min at 4°C using complete lysis buffer. Protein lysates were boiled 5 min at 95°C and loaded on 4-12% SDSPAGE gels. After being transferred onto PVDF (polyvinylidene fluoride) membranes and blocked with 5% skimmed milk in PBST for 1 h. Membranes were incubated overnight at 4°C with the corresponding primary antibody, washed three times 10 min in PBST, incubated 1h at RT with the corresponding secondary antibodies and washed again three times 10 min in PBST. Chemiluminescence signal was revealed using Odyssey® Fc Dual-Mode Imaging System.

8. IMMUNOPRECIPITATION

Immunoprecipitation (IP) is a technique that involves precipitating a protein in a solution using an antibody that specifically binds to that particular protein. This process can be used to isolate and concentrate a particular protein and therefore detect the binding partners. Immunoprecipitation requires that the antibody must be coupled to a solid substrate at some point in the procedure.

Cells were lysed for 30 min at 4°C using complete lysis buffer (LB). Usually, each confluent (10 cm diameter) plate of COS-7 or RBL 2H3 cells were lysed into 1 ml of complete LB. Cell lysates were clarified by centrifugation at 13.200 xg, for 15 min at 4°C. Once the crude lysate was obtained, 30 µl was saved at 4°C to be used as control and the rest was process. Prior to the IP itself, a pre-cleaning procedure of the whole lysate was required, in order to remove potentially reactive components able to bind to the IP

antibody or protein G beads in a non-specific way. The basic pre-cleaning procedure consisted in three rounds of incubation of the whole lysate with 30 μ l of protein G-Shepharose beads (Amersham Bioscences) plus isotopic control Ab (usually 1 μ g/ml of Mouse Ig), 30 min at 4°C, discarding the beads in every round. Afterwards, pre-cleaned lysate was incubated with 30 μ l of protein G-Shepharose plus 1 μ g/ml of specific Ab for 3h at 4°C. Then, the beads are cleaned x3 with incomplete LB in order to eliminate any compound retained between the agarose beads. The elution from the bead-antibody complex to recover the immunoprecipitated proteins was performed by adding 2x Protein Loading Buffer and boiling the samples for 5 min at 95°C. The protein lysate was then loaded into an SDS-Page gel to perform immunoblotting.

Table 6. *Antibodies used in Western Blot technique.*

Antibody/ies	Brand	Concentration
Primary		
STXBP2 Rabbit PolyAb	Proteintech Europe	1/1000
Ms pAb to STX11 (0.5 mg/mL)	Abcam	1/1000
α -actin (A5060)	Sigma-Aldrich	1/250
Munc13-4/UNC13D Antibody	Thermo-Scientific	1/1000
Secondary		
HRP-Rabbit Anti-Mouse IgG	ZYMED	1/1250
Goat anti-rabbit IgG-HRP	Santa Cruz Biotechnology	1/1250
HRP-Rabbit Anti-Goat IgG	Jackson ImmunoResearch	1/1250
α -HA biotin clone 12CA5	Roche	1/1250
Conjugated		
GFP (B-2) HRP	Santa Cruz Biotechnology	1/1000
OctA-Probe (H-5) HRP	Santa Cruz Biotechnology	1/1000

9. FLOW CYTOMETRY

Flow cytometry is a standard laboratory tool in the evaluation and identification of leukocyte populations and specific lymphocyte subpopulations. The analysis of the expression of cell surface markers (clusters of differentiation (CD) allows to determine the cell lineage and to examine the stage of differentiation and cell activation.

9.1. Extracellular and intracellular staining

For surface cell markers staining, cells were incubated in the dark for 20 minutes with the specific staining mix. After incubation, cells were washed once and taken up in PBS.

For intracellular staining of cytokines in THP-1 cells, a first step with PerFix-nc kit (Beckman Coulter, Fullerton, CA, USA) was necessary. THP-1 cells were fixed by adding 5 μ L of the Fixative Reagent and were incubated at room temperature in the dark for 15 minutes. Following, 200 μ L of the Permeabilizing Reagent and the corresponding staining mix. Incubation at room temperature in the dark for 30 minutes. Finally, it was added 1x Final Solution and resuspended in PBS. Surface markers and intracellular cytokines were measured by flow cytometry using a 10-color/3 lasers Navios™ flow cytometer (Beckman Coulter, Fullerton, CA, USA) (Table 7).

Table 7. *Antibodies used in Flow Cytometry.*

Antibodies	Dilution	Clone	Brand
CD14-APC-AF750	1:40	RMO52	Beckman Coulter
CD71-FITC	1:25	YDJ1.2.2	Beckman Coulter
CD103-APC	1:25	2G5	Beckman Coulter
IL1b- (APC) (1:250)	1:250	AF647	Immunostep
IL-8-PE	1:50	REA731	Miltenyi Biotec
IL-10-FITC	1:25	JES3-9D7	Miltenyi Biotec
INF γ -FITC	1:25	D9D10	Bio-Rad
CD56-PE	1:1	N901	Beckman Coulter
CD107a-APC	1:5	H4A3	Beckman Coulter

9.2. NK cell Cytotoxicity

PBMCs adjusted at 4×10^6 cells/ml were incubated overnight (O/N) at 37°C 5% CO₂ in fresh cRPMI media to eliminate mononuclear cells. Next day, PBMCs and K562 were mixed at different ratios (PBMC: K562) 100:1, 50:1, 25:1, 12:1, 6:1, 3:1 and 6ul of Propidium iodide (PI) was added. After 4 hours at 37°C 5% CO₂, cells were analyzed by flow cytometry using a 10-color/3 lasers Navios™ flow cytometer (Beckman Coulter, Fullerton, CA, USA).

9.3. NK cell Degranulation

PBMCs adjusted at 4×10^6 cells/ml were incubated overnight (O/N) at 37°C 5% CO₂ in cRPMI media with or without IL-2 [500UI/ml] in a 96 well-plate. Next day, cells were harvested and incubated with 100ul of PHA at 2ug/mL or with K562 at 1:1 ratio or with

cRPMI and with anti-CD107a (Table 7). After 2 (K562 activated cells) or 4 (PHA activated cells) hours at 37°C 5%CO₂, anti-CD56 (Table 7) antibody staining procedure was performed. Finally, cells were analyzed by flow cytometry using a 10-color/3 lasers Navios™ flow cytometer (Beckman Coulter, Fullerton, CA, USA).

10.B-HEXOSAMINIDASE RELEASE OF RBL-H3

Stable-transfected and non-transfected RBL cells were resuspended in Tyrodes' buffer (135 mM NaCl, 5 mM KCl, 1,8 mM CaCl₂, 1 mM MgCl₂, 5,6 mM glucose, 20 mM Hepes, 1 mg/mL BSA, pH: 7.4) and seeded at 0.1×10^6 cells/well in a 96-well-plate at final volume of 50 μ L overnight. Next day, cells were washed twice with Tyrodes' buffer and incubated 1 hour at 37 °C with Tyrodes' buffer as negative control, with PMA (Phorbol 12-myristate 13-acetate) (5ug/mL)/Ionomycin(1mM) or with lysis buffer (2% Triton X-100) as maximal degranulation value. Next, in another 96-well-plate, 50 μ L of substrate solution (1 mM P-nitrophenyl-N-acetyl- β -D-glucosamine in 0.05 M citrate buffer, pH = 4.5) was added to wells, and 20 μ L of supernatant containing exocytic granules were transferred to these wells. Mixture was incubated for 1 h at 37 °C to develop colorimetric reaction and then 150 μ L of stop solution (0.05 M sodium carbonate buffer, pH = 10.0) was added. Absorbance was read at 405 nm.

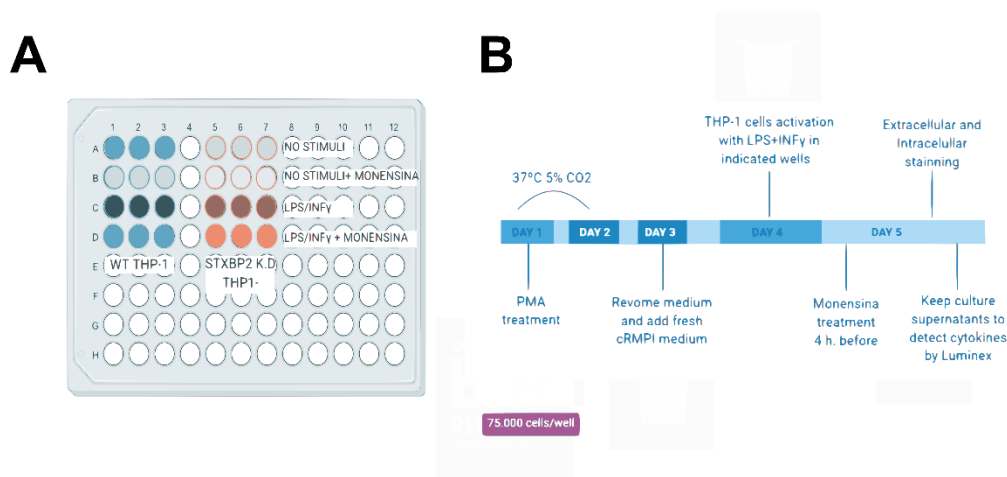
Table 8. Buffer Recipes for β -hexosaminidase release

Recipes	Concentration
Tyrodes (pH:7.4)	
NaCl	135mM
KCl	5mM
CaCl ₂	1,8mM
MgCl ₂	1mM
Glucosa	5,8mM
HEPES	20mM
BSA mg/ML	1mg/mL
Substrate (pH:4.4)	
1mM P-nitrophenyl N-acetyl-beta-D- glucosamine	1mM
Citrate	50mM
STOP (pH:10)	
Sodium carbonate	50mM
Sodium bicarbonate	50mM

11. THP-1 differentiation assay

To study the effect of STXBP2 silencing on the transport and secretion of cytokines by activated macrophages, the THP-1-line cells were differentiated into macrophages and stimulated with LPS and IFN γ to induce M1 polarization. For differentiation of the THP-1 cell line to a macrophage phenotype (cell adhesion), cells were resuspended in cRMI medium containing 5ng/ml PMA (Sigma-Aldrich, Saint Louis, MO, USA) at day 1. Briefly, cells were seeded into 96 flat-bottom plates (SPL Life Sciences Co., Ltd. Pocheon-si, Gyeonggi-do, Korea) using a yield of 75.000 cells/well (200 μ l/well). And incubated for 2 days at 37°C 5% CO $_2$. At day 3, cells were PBS-washed and incubated 24 hours with fresh cRMPI medium.

At day 4, half of the cells were activated with LPS (100ng/ml) and IFN γ (20 ng/ml) for 24 hours. Following activation, culture supernatants were aspirated, aliquoted (per triplicate) and stored at -80°C. For intracellular staining of cytokines, THP-1 cells were treated with monensin (Santa Cruz Biotechnology Inc., Dallas, Texas, USA) for 4 hours prior to staining. Finally, THP-1 cells were resuspended and incubated in blocking buffer containing 20 μ g/ml human IgG for 30 minutes at 4°C to avoid unspecific antibodies unions. After incubation, cells were washed with PBS for further staining protocols.



12. LUMINEX Cytokine detection

Cytokines IL-4, IL-6, IL-8, IL-10, IL-1 β and TNF α from supernatant were measured using the procartaplex high sensitivity immunoassay kit (Thermo Fisher Scientific, Waltham, MA, USA) following manufacturer's instructions. Results were obtained with MapixtmTM instrument (Luminex Corporation, Austin Texas, USA a).

V. RESULTS

CHAPTER 1: KINETICS OF PHYTOHEMAGGLUTININ (PHA) AND K562 INDUCED DEGRANULATION BASED ON CD107a EXPRESSION IN PEDIATRIC POPULATION

1.1.PHA DEGRANULATION SHOWED AND INCREASED % OF NK CELLS EXPRESSING CD107A

Freshly isolated PBMCs from pediatric and adult healthy donors were incubated with cell line K562 as target cells or with PHA. Following a 4-h incubation in the presence of CD107a antibody, NK cells were stained for CD56. It was observed that the upregulation of CD107a expression by stimulation with PHA was significantly higher than that with K562 cells either on resting or activated NK cells (Table 9).

Table 9. Significantly different CD107a upregulation

	Upregulation of CD107a	
	PHA (Mean \pm Std. Error)	K562 (Mean \pm Std. Error)
Resting NK (without IL-2)	37.9 \pm 3.1	18 \pm 1.1
Activated NK (with IL-2)	46.2 \pm 3.5	29 \pm 2.7

Representative data from one subject is shown in Figure 7A-B. Low CD107a surface expression was detected on NK cells (resting: 1.1%; activated: 1%) (Figure 7A-B). Following stimulation with K562, upregulation of CD107a was observed in 16.7% or 21.7% of CD56+ resting or activated NK cells, respectively (Figure 7A). Following PHA stimulation, upregulation of CD107a was observed in 44.9% or 52.6% of CD56+ resting or activated NK cells, respectively (Figure 7B). Overall results for CD107a expression of the 39 pediatric healthy controls are shown in Figure 7C.

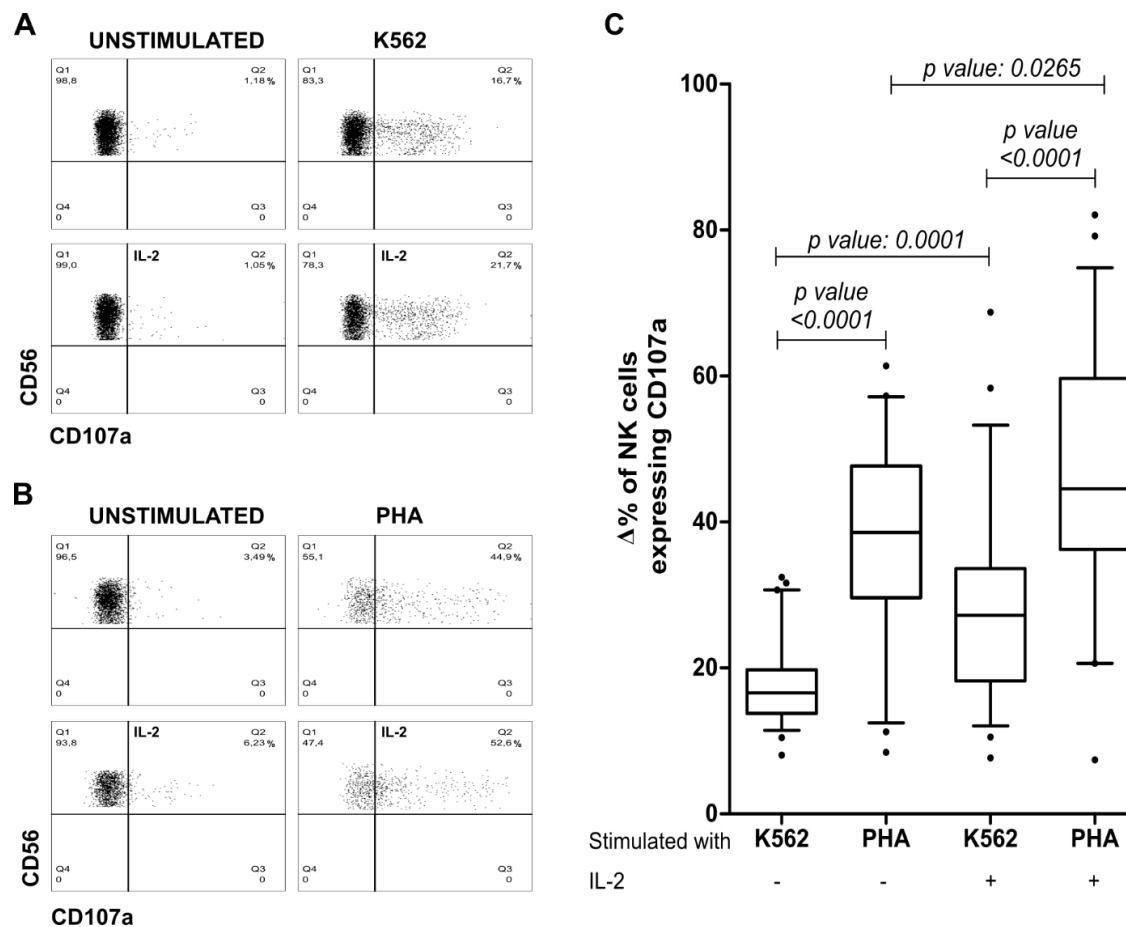


Figure 7. PHA and K562 NK cell degranulation in Pediatric healthy donors. (A-B) Representative data from one healthy subject and (C) summary of all the volunteer's healthy donors showing the upregulation of CD107a in NK cells after being stimulated with K562 or PHA with or without IL-2.

1.2. CYTOTOXIC FUNCTIONS OF ACTIVATED NK CELLS IN BOTH ADULTS AND CHILDREN DISPLAY INTER-INDIVIDUAL VARIATION

Several studies have reported an age-related variation in NK cells regarding the NK cell number and NK cell subpopulations ($CD56^{dim}$ and $CD56^{bright}$) (Shearer et al. 2014). Thus, we sought to establish low limit of normality for NK cell degranulation and cytotoxicity in healthy adults and children. The total number of healthy controls included in the analysis were 37 children subdivided into four-year age groupings (less than 1 year, 1 to 3-year-olds, 4 to 5-year-olds, 6 to 7-year-olds and 8 to 11-year-olds) and 59 adults >18 years.

When analyzing the cytotoxic activity across the four age groups and adults separately, it was observed that pediatric patients had a significantly lower cytotoxicity than adults with an upward trend. Specifically, the lowest expression was in the youngest age group

(<1 year) and adult values were reached at the age of 8 years (Figure 8A). The increment of the cytotoxic activity is concomitant with the increasing % of NK cells expressing CD56^{dim} (Figure 8A). Regarding the upregulation of CD107a expression on NK cells, differences between groups were significantly lower in activated NK cells in the two youngest age group (<1 and 1-3 years) and reaching the adult levels at 4 years and remained at that level thereafter (Figure 8B).

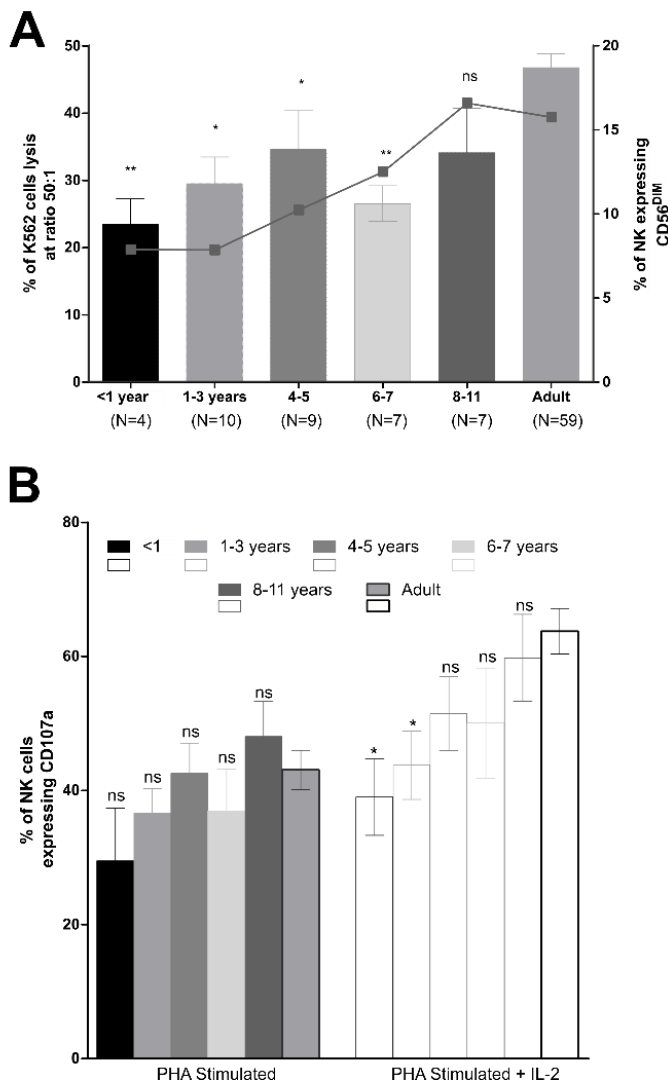


Figure 8. Significant variation of NK cell cytotoxicity and PHA-degranulation between age groups of healthy children and adults. (A) Graph bars showing the percentage of K562 cell lysis at 50:1 ratio effector:target cells at left Y axes. On right Y axes is shown the % of NK CD56^{dim} positives cells. (B) Graph bars showing the percentage of CD107a upregulation in NK cells. All data shown is mean \pm SEM * p <0.05, ** p <0.01 and ns. Not significant.

1.3.MEASUREMENT OF CD107A UPREGULATION IN ACTIVATED NK CELLS AFTER PHA STIMULATION HAS A HIGH DIAGNOSTIC ACCURACY FOR DETECTING HLH PATIENTS.

When assessing the diagnostic capability of degranulation of PHA-activated NK cells by using ROC analysis, the 17.8% cut showed the greatest ability to discriminate patients

with HLH from healthy controls with an area below the 0.92 AUC curve (Figure 9). At this optimal threshold the sensitivity of PHA degranulation to detect patients with impaired degranulation compared with healthy controls was 100%, and specificity was 72.7%. Moreover, the positive predictive value (PPV) and the negative predictive value (NPV) of laboratory-defined PHA-degranulation cut-off were 83.3% and 95.5%, respectively.

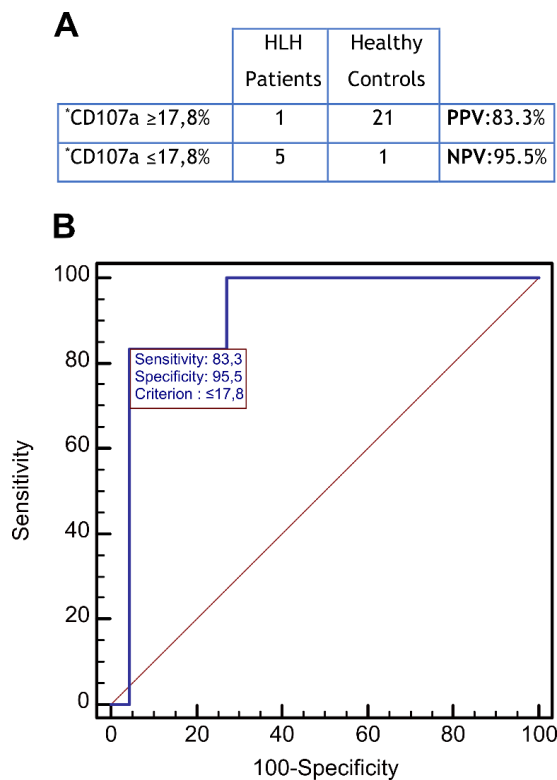


Figure 9. Diagnostic accuracy of CD107a upregulation. (A) Table with Sensitivity/specificity/PPV/NPV of the CD107a upregulation considering 17.8% as the low limit of normality. (B) ROC curve showing diagnostic accuracy of CD107a upregulation to detect HLH patients with impaired degranulation. Sensitivity and specificity of the set-up cut-off are shown inside the box.

1.4.APPLICATION IN CLINICAL PRACTICE

During the 2011 to 2015 period, 120 patients fulfilling the HLH diagnostic criteria were tested for cytotoxic function in the immunology laboratories in Hospital Universitari Vall d'Hebron, Barcelona. Twelve patients carried putatively relevant mutations and are listed in Table 10. Seven patients had mutations in HLH related genes (3 in PRF-1, 1 in UNC13D, 1 in STXBP2, 1 in RAB27a and 1 in LYST). Three patients presented with monoallelic variants in HLH related genes (STXP2 and UNC13D). Finally, 2 patients had mutations in other non-HLH-related genes.

Setting up and improving NK cell cytotoxicity and degranulation techniques in Hospital Universitari Vall d'Hebron (HUVH) allowed us to diagnose 12 patients who underwent to an HLH episode. These patients are listed in Table 10 and specifically they were: 7 FLH patients (3 with FLH2, 1 with FHL3, 1 with FHL5, 1 with GS2 and 1 with CH), 3 patients

with monoallelic variants in HLH related genes and 2 patients with mutations in non-HLH genes. All patient's except FHL2 patients (data not showed), showed low expression of $\Delta\%$ CD107a on NK cells compared to healthy controls ($p < 0.0001$) (Figure 10 **Error! No s'ha trobat l'origen de la referència.**).

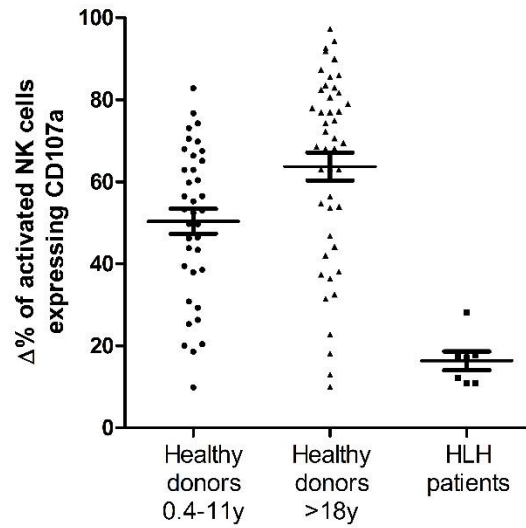


Figure 10. Distribution of CD107a expression among adults, pediatric healthy donors and patients with HLH

Table 10. Patients diagnose with HLH in Hospital Universitari Vall d'Hebron (HUVH).

	Gene	Mutation		Protein effect		Zygoty	Type
		Allele 1	Allele 2	Allele 1	Allele 2		
Mutations in HLH genes							
Patient 1	PRF1	c.1376C>T		p.pro459Leu.		Hom.	Missense
Patient 2	PRF1	c.1428delG		p.Gly476fsX2		Hom.	Deletion
Patient 5	PRF1	c.50delT	c.1122G>A	p.Leu17ArgfsX34	p.Trp374X	Compound Het.	Deletion / Nonsense
Patient 3	RAB27a	c.239+3A>G				Hom.	Splicing
Patient 4	LYST	c.8380insT		p.Tyr2794LeufsX8		Hom.	Insertion
Patient 6	UNC13D	c.753+1G>T	c.2448-11G>A	p.Asp252fs		Compound Het.	Splicing / Splicing
Patient 7	STXBP2	c.728T>G	c.1247-1G>C	p.Leu243Arg	p.Val417LeufsX126	Compound Het.	Missense / Nonsense
Patient 8	STXBP2	c.568C>T		p.Arg190Cys		Het.	Missense
Patient 9	UNC13D	c.3224G>A		p.Arg1075Gln		Het.	Missense
Patient 10	UNC13D	c.2782C>T c.811C>T		p.Arg928Cys p.Pro271Ser		Het.	Missense
Mutations in non-HLH genes							
Patient 11	MMACHC	c.271dupA				Hom.	Duplication
Patient 12	PEPD	c.977G>A				Hom.	

CHAPTER 2: ANALYSIS OF THE NOVEL MUTATION L243R FOUND IN A PATIENT WITH FHL5: FUNCTIONAL AND MOLECULAR CHARACTERIZATION

2.1. CLINICAL CASE PRESENTATION: EBV-INDUCED HLH.

Caucasian 2-year-old boy from non-consanguineous parents, who was admitted with EBV infection and persistent fever, and whose older brother died at the age of 3 years of EBV mononucleosis and HLH triggered by EBV (Figure 11). Neither of the patient's parents have presented clinical manifestations. Physical examination revealed a hepatosplenomegaly. Laboratory test found pancytopenia (hemoglobin, neutrophils and platelets), with increased lactate dehydrogenase (LDH) and serum ferritin. Subtle alterations in the percentage of CD8+ and B cells and in absolute number (Lymphocytes ($2.3 \times 10^9/L$)) were found in the lymphocyte subpopulations (CD3+ T cells (76%) (0-2 years: 52-77%), CD4+ T cells (34%) (0-2 years: 30-58%), CD8+ T cells (41%) (0-2 years: 12-27%), CD19+ B cells (9%) (0-2 years: 15-28%) and CD56+CD16+ (12%) (0-2 years: 3-24%). Hemophagocytosis was detected in bone marrow aspirate and in cervical node biopsy. PCR screening for EBV was positive in blood and lymph node. The diagnosis of EBV-induced HLH was established (fulfillment of five diagnostic criteria: persistent fever, hepatosplenomegaly, high triglyceride levels, pancytopenia and hemophagocytosis in bone marrow) and with the suspicion of FHL due to positive family history. The patient was treated according to HLH-2004 protocol plus Rituximab, with progressive improvement (fever subsided, lymph nodes and spleen size decreased) followed by a neutralization of the viral load. However, 4 months later the patient relapsed with a new episode of HLH concomitant with a rise of EBV copies. After diagnosis of primary HLH, the patient underwent a successful bone marrow transplant from a non-related donor (Table 11).

Table 11

	1st Episode	2nd Episode
Age (years)	2	3
Fever	Yes	No
Hepatosplenomegaly	Yes	No
Hb (g/L)	Low	12,4
Neutrophils (10^9 cells/L)	Low	2,9
Platelets (10^9 cells/L)	Low	272
Triglycerides (mg/dL)	High	86
Ferritin (g/L)	335	264,3
LDH (U/L)	956	616
Haemophagocytosis	Yes	ND
sCD25 (U/ml)	ND	1055
NK cell activity	ND	Absent
Degranulation ^a (with/out IL-2)	ND	51/30
EBV (Copies/ml)	10^4	32
Neurological manifestations	No	No
Treatment protocol	HLH-2004	HLH-2004
Outcome		Alive

^apathological: $\leq 30\%$ LU based on laboratory defined normal ranges at our center; ND, no data available.

2.2. NORMAL PERCENTAGE OF NK CELLS EXPRESSING CD107A BUT ABERRANT DEGRANULATION PATTERN.

NK cell-mediated lysis of K562 target cells was assessed using a standard 4-hour cytotoxicity assay by flow cytometry showing absent capability of NK cells to kill target K562 cells at different ratios (Figure 11B). Degranulation studies in NK cells and CD8 T cells stimulated with PHA alone or in combination with IL2 showed normal percentage of CD107 expression that increased with the addition of IL2. However, the pattern of expression of CD107a in both cell populations showed a decrease in fluorescence intensity, indicating a degranulation defect (Figure 11C and D).

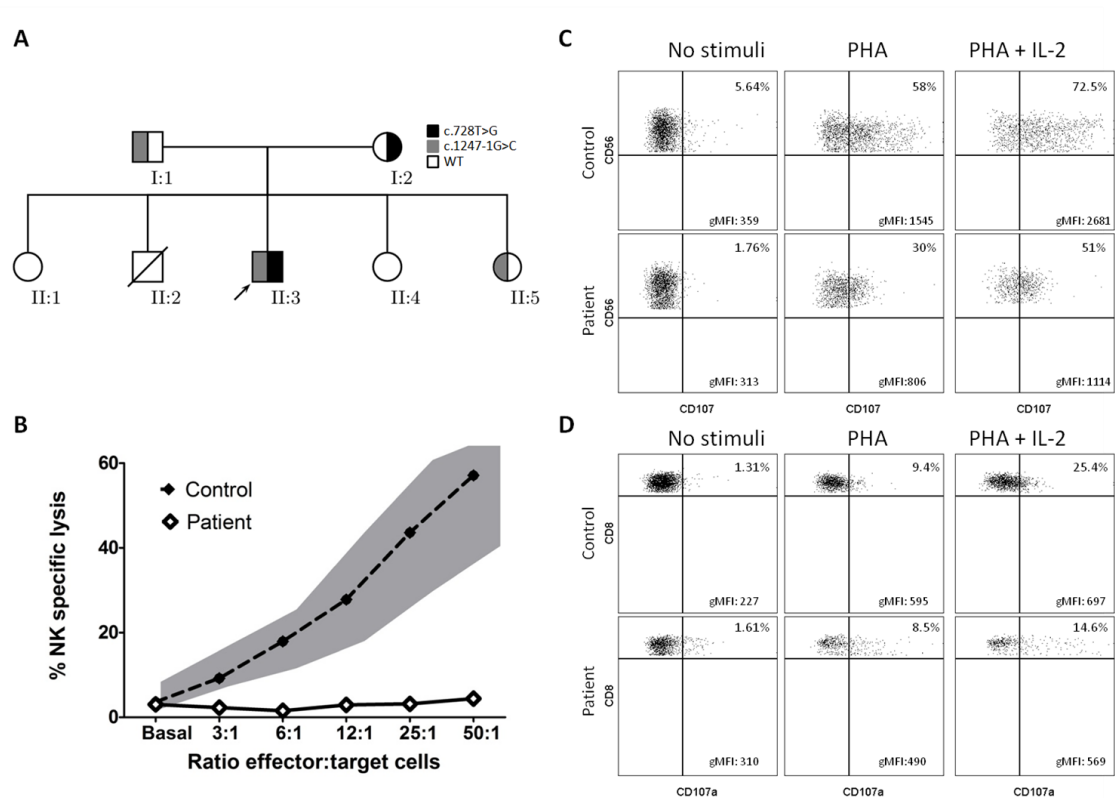


Figure 11. STXBP2L243R leads to absent cytotoxicity and decreased degranulation. (A) Family pedigree affected patient is indicated with an arrow. (B) Graphic showing specific lysis of K562 cells for different effector cell to target cell (E:T) ratios evaluated in a 4-h PI-staining. Shaded area indicates normal ranges of degranulation tested in healthy individuals. (C and D) Degranulation assay in NK and CD8 cells, respectively. PBMC were incubated overnight with or without IL-2 and stimulated either alone or with PHA for 4h at 37°C. Thereafter, cells were stained with fluorochrome-conjugated anti-CD56, CD8 and anti-CD107a mAbs. CD107a surface expression was gated on CD56 and CD8 cells and the percentage is expressed in the right high corner. The CD107a MFI is expressed in the right down corner.

2.3. STXBP2^{L243R} MISSENSE MUTATION RESULTS IN A LOST OF MUNC18-2 AND SYNTAXIN-11 EXPRESSION IN BOTH TRANSFECTED CELLS AND PATIENT'S PBMCS.

The patient's clinical presentation, together with basic laboratory results, cytotoxicity and degranulation studies, indicated the need of performing the genetic study on degranulation defects. The genetic analysis identified two compound heterozygous mutations in the STXBP2 gene. The first one was a previously reported splice-site mutation (c.1247-1G>C) mainly causing the deletion of exon 15, resulting in a frameshift and a premature stop codon (p.V417LfsX126) (zur Stadt, Rohr, Seifert, Koch, Grieve,

Pagel, Strauss, et al. 2009). This mutation was a splice mutation, but other minor spliced products were generated, which could retain some function, and a milder defect in CTL cytotoxicity was observed in a patient homozygous for this mutation. The second mutation was a novel missense mutation in exon 9 (c.728T>G) that generates a change in the amino acid 243 (p.L243R). Parents were both carriers of each mutation. At the time of the patient's diagnosis, his mother became pregnant and the preconception counseling study was performed and the fetus was found to be heterozygous (Figure 11A). In order to evaluate the impact of the L243R mutation in STXBP2 protein, the *in silico* scored predictive algorithms PolyPhen-2 and Sorting Tolerant from Intolerant (SIFT) were used and the data obtained indicated that the pathogenicity of L243R was “probably damaging”, with a score of 0.981 (sensitivity: 0.57, specificity: 0.94), and “damaging” with a score of 0, respectively (Sim et al. 2012). To understand the molecular repercussions of the L243R mutation on STXBP2 function, we analyzed its impact on the experimentally determined structure and predicted interactions of the protein. We found that the residue L243 is located within the core of domain 2 with a percentage of accessible surface area (ASA) of 0%. We determined the multiple sequence alignment (MSA) of the protein family, confirming that together with its spatial neighbors, this residue is evolutionarily highly conserved (Figure 12).

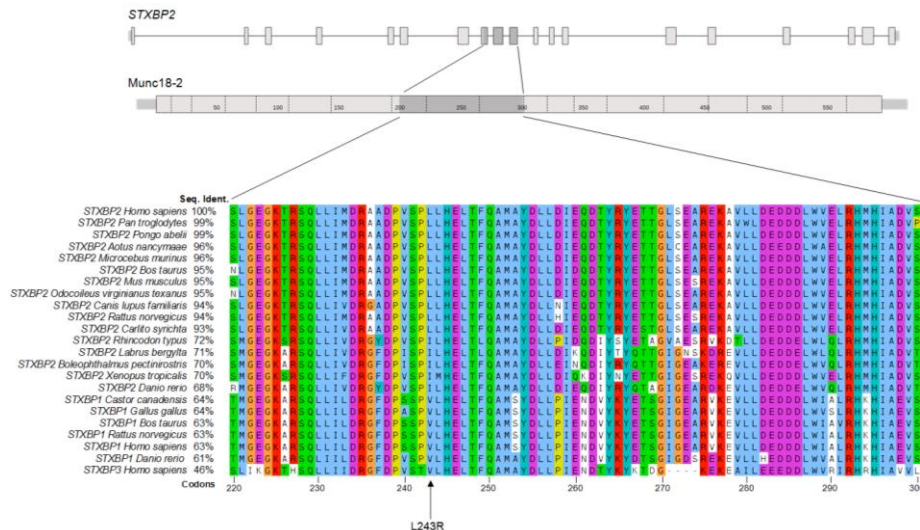


Figure 12. Multiple Sequence Alignment (MSA) from various species for STXBP2, STXBP1 and STXBP3. Conserved hydrophobic residues at position 243 are indicated with an arrow.

The residue L243 has a rich, mainly hydrophobic, interaction network that is important to stabilize domain 2 and 3, which is lost when doing *in silico* mutagenesis (Figure 13B and

C). Moreover, analysis of the expected impact of L243R mutation in protein stability using the FoldX tool predicts a destabilizing effect, with a value of 2.33 Kcal/mol (Schymkowitz et al. 2005).

In order to determine how the mutation L243R affects protein stability *in vivo*, the levels of expression of STXBP2 wild type (WT) and L243R mutant were analyzed by western blot in transfected COS-7 cells. Triplicate transfection experiments were performed using appropriate controls. As shown in Figure 13D, all three lanes corresponding to independently WT transfected construct show a high level of expression of protein, whilst the expression of the mutated form of STXBP2 is dramatically diminished. The densitometric quantification of wt and L243R STXBP2 bands shows that the mutated protein represents less than five per cent of the wt expressed protein (Figure 13C).

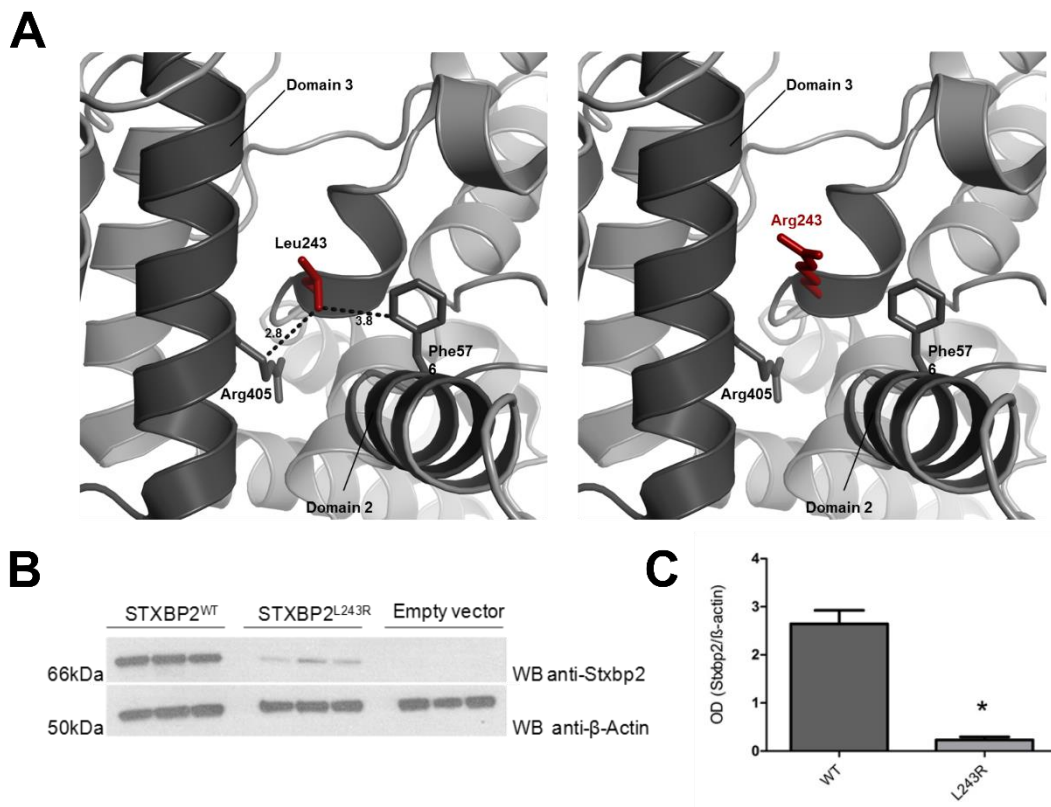


Figure 13. Structure, modelling and molecular analyses of the mutant STXBP2L243R. (A) Intraprotein contacts of residue L243 and mutant R243. (B) Representative western blot of three independent experiments of wild type (WT) and mutated (L243R) STXBP2 protein. COS-7 cells were transiently transfected independently by triplicate with an empty vector, wt and L243R HA-STXBP2 constructs. Blots were probed with a rabbit polyclonal anti STXBP2 and monoclonal anti β-actin antibody). (C) Densitometric evaluation of STXBP2 protein expression from western-blot;

diagram representing the mean optical density (OD) of STXBP2 protein normalized to that of β -actin. * $P < 0.05$ vs. control. Error bars represent standard deviation.

Finally, we analyzed the levels of expression of STXBP2 in patient's PBMC. As shown in Figure 14, the expression of STXBP2 was almost undetectable by western blot in PBMC's patient lysates compared to PBMC from two healthy donors. Moreover, we detected a decrease in the levels of expression of STX11, as described previously in patients with a diagnosis of FHL5 with no expression of STXBP2 (Côte et al. 2009).

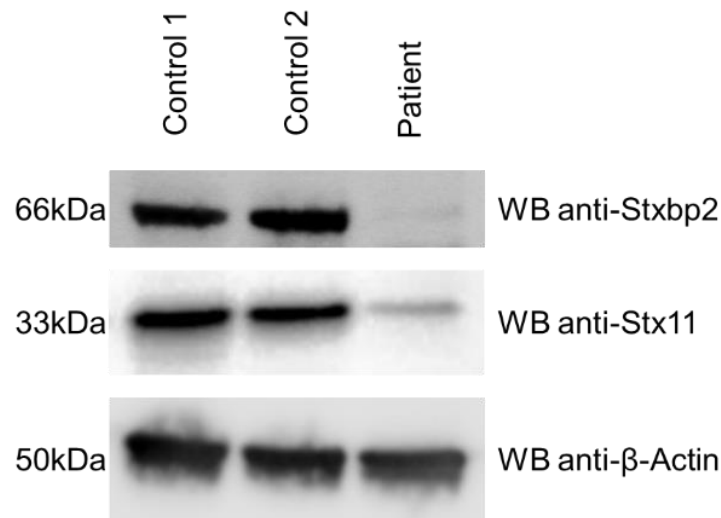


Figure 14. Western blotting comparing the levels of expression of STXBP2 and STX11 in PBMC from patient and two healthy donors. Blots were probed with previously described anti-STXBP2 and anti- β -actin antibody and anti-STX1.

CHAPTER 3: FUNCTIONAL AND MOLECULAR CHARACTERIZATION OF NOVEL AND REPORTED MUTATIONS FOUND IN PATIENTS DIAGNOSED WITH AN ATYPICAL FORM OF HLH.

In the study of patients suffering from a hemophagocytic syndrome, we report the sequential clinical presentation along with the lymphocyte degranulation and cytotoxicity functions in three unrelated patients (**Table 10**; P8, P9, 910) fulfilling HLH diagnostic criteria. At disease onset, a defective function was assessed. Following therapy for their first HLH flare, all patients showed remission of symptoms as well as normalization of laboratory parameters. In the long-term follow-up, three patients presented with HLH reactivations concomitant with impaired functional assays.

4.1. CASE REPORTS: UNSUAL HLH CLINICAL PRESENTATION

PATIENT 8: 8-years-old boy from non-consanguineous parents with 15 days fever evolution was referred to our institution to discard a lymphoproliferative disorder. Laboratory tests revealed progressive pancytopenia, splenomegaly, bone marrow hemophagocytosis, hyperferritinemia, absent NK cytotoxicity and impaired degranulation. Microbiology tests detected positive parvovirus B19 PCR. The diagnosis of HLH secondary to ParvB19 was made based on the fulfilling of more than 5 criteria of the guideline HLH- 2004 protocol.

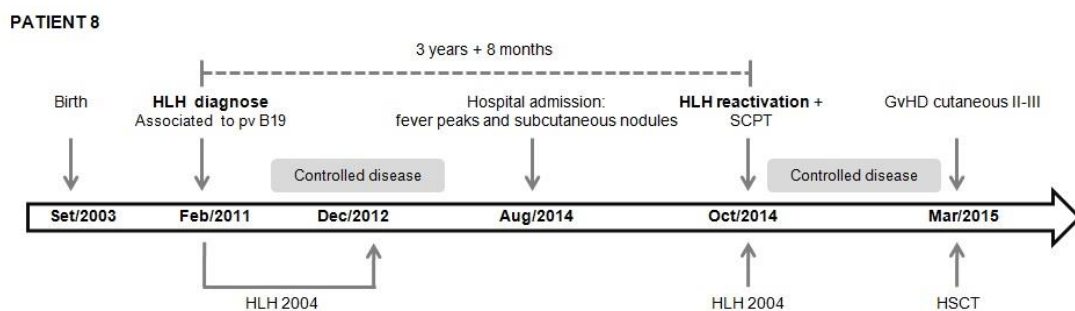


Figure 15. Timeline to illustrate the chronology of the HLH onset, HLH relapse as well as the treatment used in each situation from patient 8.

He was successfully treated according to HLH2004-protocol with a complete remission. Three years later the patient was admitted to our hospital with fever peaks and subcutaneous nodules. Histopathologic findings from skin biopsy revealed a mixed-

pattern of panniculitis and lipophage macrophages leading to the diagnosis of subcutaneous panniculitis T-cell lymphoma. Laboratory test were consistent with the development of a concomitant HLH reactivation with low cytotoxicity and impaired degranulation. Finally, the patient was treated with hematopoietic stem-cell transplantation.

PATIENT 9: 9-month-old boy, born from non-consanguineous parents with past medical history of cutaneous Langerhans cell histiocytosis (LCH) diagnosed at 2 months of age. He was admitted to our institution with an exacerbation of cutaneous lesions, fever, vomit hypoalbuminemia, diarrhea and generalized edema, hence an extended study of the disease confirming diagnose of systemic LCH was performed. Treatment was started with prednisone and vinblastina following the LCH-III international protocol and after 1 month of disease progression the patient started with Ara-C and cladribina (LCH-S 2005). After the third cycle of Ara-C and cladribina the patient presented with a complete hematological remission of LCH. However, high ferritin levels (2800mcg/L) with hipertriglicerids (280mg/dL) were detected. Due to the clinical suspicion of an HLH syndrome we performed the laboratory test. We found the presence of bone marrow hemophagocytosis, low NK cytotoxicity, impaired degranulation and elevated sCD25 levels. As the patient fulfilled 5 of 8 HLH diagnostic criteria, HLH treatment was included resulting in a control disease with a decrease in the CD25s levels, normalized ferritin levels, and NK cytotoxicity recover.

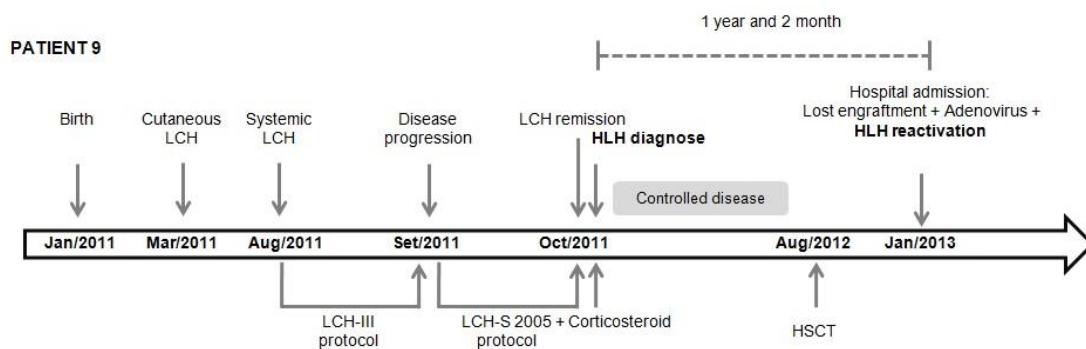


Figure 16. Timeline to illustrate the chronology of the HLH onset, HLH relapse as well as the treatment used in each situation from patient 9.

The patient went through a HSCT at 16 months of age from a non-related donor. Five months later he presented a failure of engraftment, that caused the reactivation of the

underlying disease and HLH relapsed. Adenovirus PCR was positive, and laboratory test revealed an absent NK cytotoxicity and impaired degranulation.

PATIENT 10: 13-years-old boy born from non-consanguineous parents with no past medical history was admitted to the hospital with a clinical suspicious of EBV-secondary HLH. On presentation, the patient referred to nine days prolonged fever without responding to antibiotics. On physical exam, there was a generalized jaundice, hepatosplenomegaly and pruritic morbilliform rash in lower limbs. Subsequently the laboratory test revealed pancytopenia, hepatomegaly, bone marrow hemophagocytosis, high ferritin levels, low NK cytotoxicity, impaired degranulation and positive detection of EBV. The patient was diagnosed with HLH syndrome fulfilling 6 of 8 HLH criteria. According to the HLH-2004 protocol the patient started the treatment with cyclosporin and dexamethasone leading to a good evolution of the clinical and analytical parameters. After one-year disease free, the patient was admitted again with prolonged fever and the laboratory test revealed absent NK cytotoxicity suggesting an HLH relapse. Dexamethasone treatment was started, and all the parameters were restored.

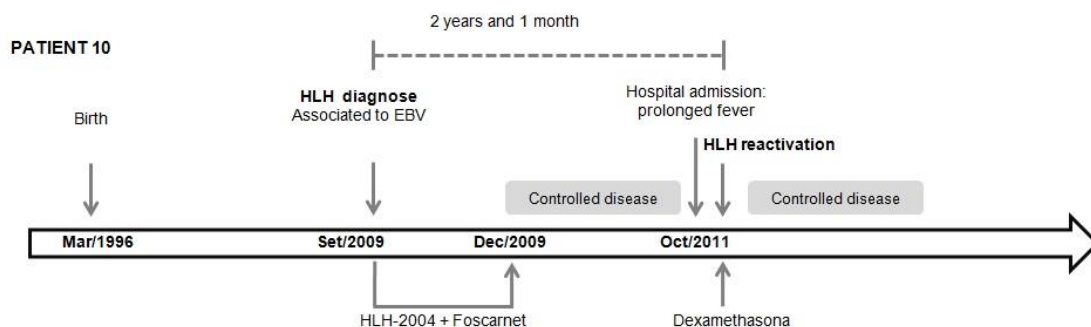


Figure 17. Timeline to illustrate the chronology of the HLH onset, HLH relapse as well as the treatment used in each situation from patient 10.

4.2. DEGRANULATION AND CYTOTOXICITY REACHED NORMAL LEVELS AFTER HLH ACUTE PHASE

We measured the percentage of NK cells expressing CD107a and the percentage of NK specific lysis of patients P8, P9 and P10. At HLH onset, P8 presented a 30% of NK cells positive for CD107a in the context of a pv B19 infection. After the HLH2004-protocol, the number of NK cells being able to degranulate increased up to 86,5% (Figure 18A). Unfortunately, during the second episode the technical control failed and the sample was not suitable for analysis. We were able to collect samples during the acute phase of first and second episode from P9, showing a decreased NK cell degranulation (21,4%

and 24% of NK cells expressing CD107a, respectively) compared to the follow-ups measured after HLH2004-protocol (39% and 52,1%) (Figure 18A-B). During the first episode of P10, functional techniques of NK cells were not yet set up. At HLH reactivation, P10 showed a 14,8% of positive CD107a NK cells that increased up to 46,8% after HLH2004-protocol (Figure 18B).

Regarding cytotoxicity, all patients were under the normal ranges of NK cells cytotoxicity as compared to healthy donors during the acute phase. However, after HLH2004-protocol NK cell specific lysis reached normal values (Figure 18A-B). These results agree with degranulation outcomes seen above.

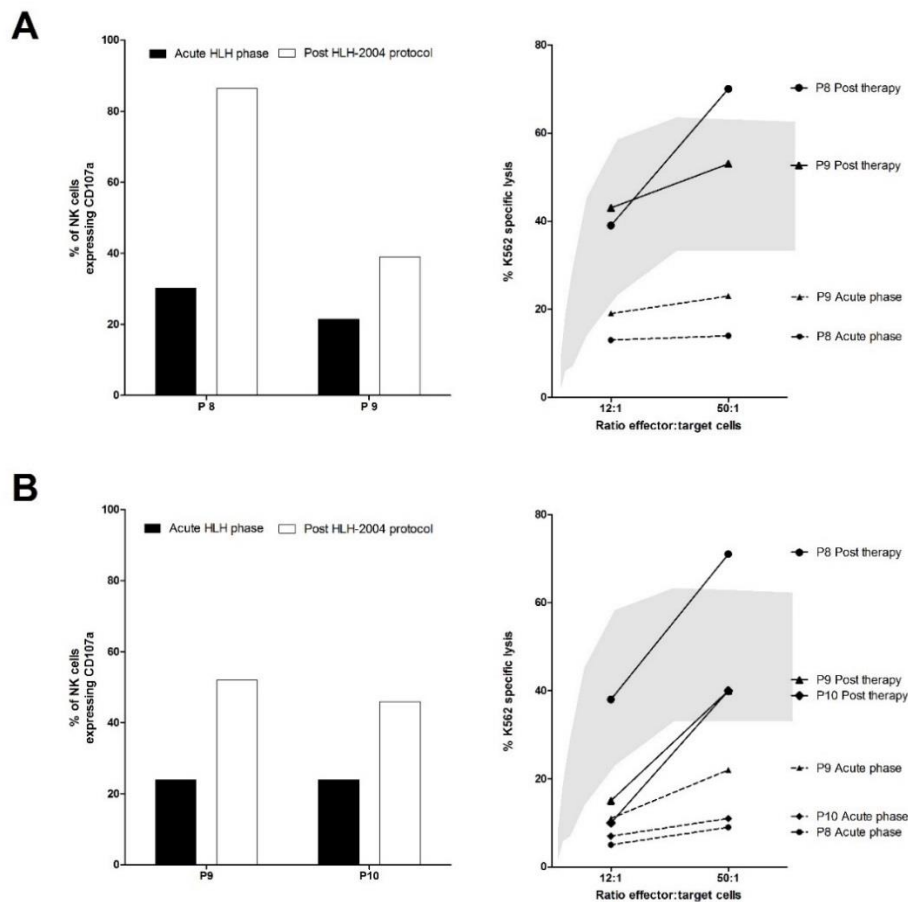


Figure 18. Normalization of degranulation and cytotoxic activity during the follow-up in patients with HLH. (A). Degranulation and Cytotoxic activity during the first HLH episode of patients 8 and 9. Degranulation was impaired during the acute HLH phase (black bars) and recovered after HLH-2004 protocol treatment (white bars). Cytotoxicity at ratios 12:1 and 50:1 was absent in these patients during acute HLH phase but reached normal levels after HLH 2004 treatment. (B). Degranulation and Cytotoxic activity in HLH reactivation of patients 8, 9 and 10. Shaded area represent levels from healthy subjects of NK cell specific lysis.

4.3. GENETIC ANALYSIS REVEALED MONOALLELIC VARIANTS IN HLH RELATED GENES

In last section, we described three unrelated patients who suffered clear HLH episodes with concomitant disease reactivation. Moreover, cytotoxicity and degranulation were impaired during the acute phase of HLH. Genetic analysis of 3 patients detected monoallelic variants in *STXBP2* and/or *UNC13D* genes. Specifically in P8, the genetic

analysis identified a new heterozygous mutation in *UNC13D* gene at exon 32 (c.3224G>A / p.Arg1075Gln) and a heterozygous missense SNP (rs144586070) located in *STXBP2* gene which leading an amino acid change at V205I with a MAF of A=0.006 and a 97% of homozygosis in the dbSNP analyzed samples. The father is carrier of the *UNC13D* mutation and the mother of the *STXBP2* SNP both without symptoms of disease. Both mutations were considered pathogenic by the protein prediction softwares SIFT and Polyphen. In P9 the genetic analysis identified a new heterozygous mutation in *STXBP2* gene at exon 7 (c. 568C>T / pArg190Cys) and two herezozygous SNP in *UNC13D* gene, rs17581728 located in intron 21 nerbay the donor site with MAF of T=0.165 and rs1135688 located in exon 27 causing and amonoacid change, K867E, with MAF of C=0.49. The new heterozygous mutation (c.568C>T; R190C) was predicted to be tolerated by SIFT but pathogenic in Polyphen. Finally, the genetic analysis in P10 identified two heterozygous variants in trans in *UNC13D* gene, c.2782C>T; p.R928C classified as being/tolerated and c.811C>T; p.P271S predicted as probably damaging (Table 13).

4.4.ANALYSIS OF MUTATIONS FOUND IN PATIENTS P8, P9 AND P10

Monoallelic mutations can confer a higher risk of suffering HLH by leading to a scenario with lower levels of protein, since only the wild type allele can produce normal protein. However, monoallelic variants can also behave as dominant negative and the mutated allele will interfere with the wild type copy.

Next, we wondered if the mutations found in *STXBP2* and *UNC13D genes* in patients presented previously could explain their phenotype. As the repertoire of monoallelic mutations in *STXBP2* gene is restricted to one case, we enriched the number of *STXBP2* monoallelic mutations by selecting 10 monoallelic mutations previously reported (Table 12) but not studied in patients diagnose with HLH.

Table 12. Selected monoallelic mutations from literature.

Variant gene	Variant protein	Reported in:
c.1298C>T	A433V	(Al Hawas et al. 2012a)
c.767T>C	L256P	(X. J. Xu et al. 2017)
c.184A>G	N62D	(Seo et al. 2016)
c.1204C > G	R402G	(Mukda et al. 2017)
c.575G>A	R192H	(X. J. Xu et al. 2017)
c.704G>T	R235G	(Genovese et al. 2016)
c.704G>C	R235P	(Tesi et al. 2015)
c.1586G>C	R529P	(K. Zhang et al. 2014a)
c.1663A>G	R555G	(Lyu et al. 2018)
c.1444G>A	Val482I	(Seo et al. 2016)

4.4.1. Monoallelic mutations in gene *STXBP2* are mainly distributed along structural domains 2 and 3.

We mapped monoallelic mutations from P8-P10 and from the literature onto the crystallized human Munc18-2 (PDB: 4cca, (Hackmann et al. 2013)) to study the distribution and molecular modeling-based predictions of monoallelic variants in Munc18-2 protein. All 11 monoallelic mutations are mainly distributed along structural domains 2 and 3 of the Munc18-2 protein (Figure 18A). We further investigated the accessible surface area (ASA) of all the mutated residues, except for residue R555 because of a gap in the PDB. We used ASA values to recognize buried or exposed residues. The buried residues usually form hydrophobic cores to maintain the structural integrity of proteins while the exposed residues are tightly related to protein functions (Gong et al. 2017). We found that 8 mutations lay in the core of Munc18-2 (Figure 18C) creating important interactions (Supplementary Figure 30) to maintain the 3D structural conformation of Munc18-2. In our mapping we also identified mutations A433 laying on the surface of the protein which may interact with other proteins.

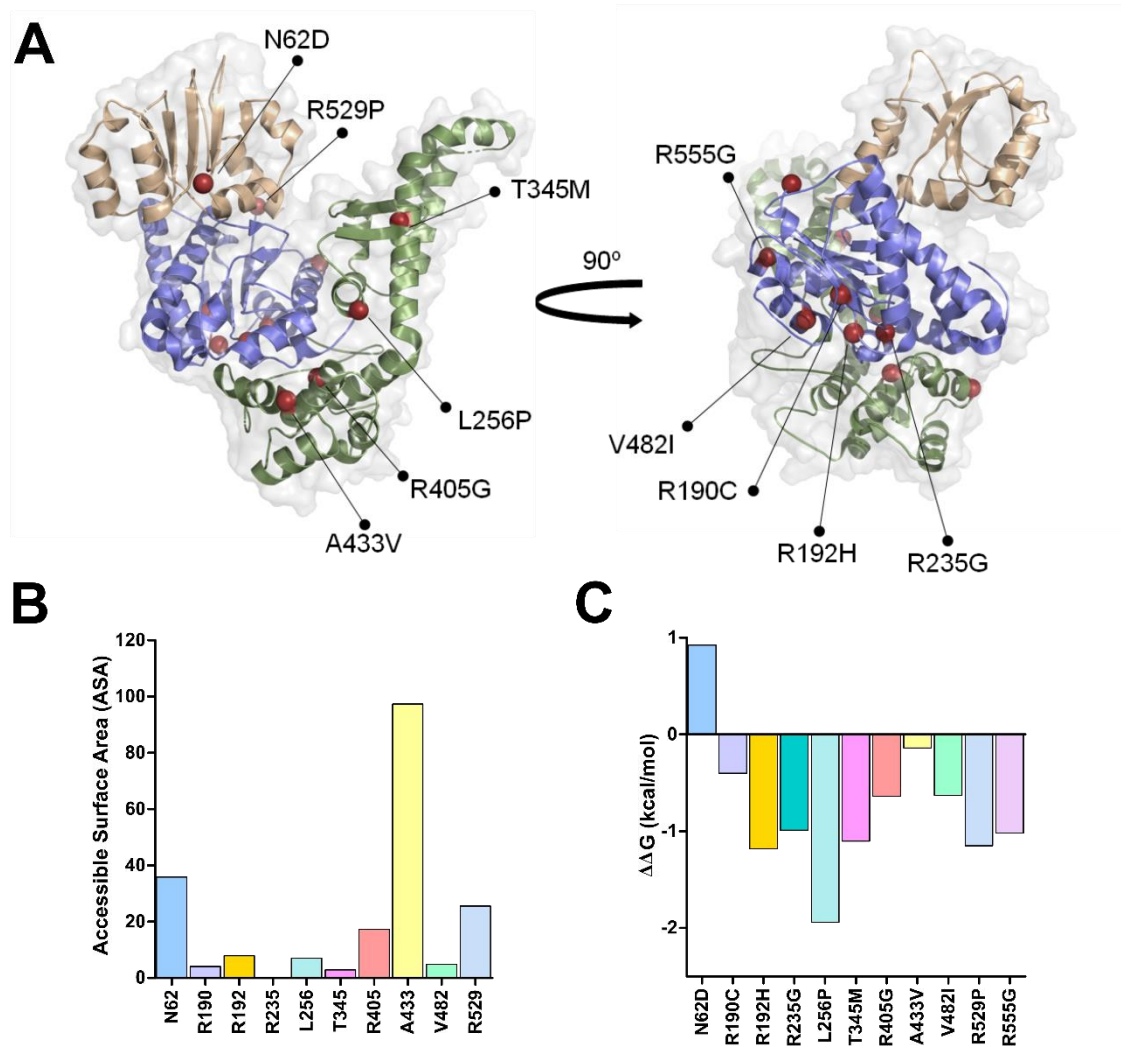


Figure 19. Distribution and Molecular modeling-based predictions of monoallelic variants in Muc18-2 protein. (A) Structure of the Muc18-2 protein (PDB ID: 4CCA), with the locations of amino acid residues mutated (N62D, R190C, R192H, R235G, L256P, T345M, R405G, A433V, V482I, R529P, R555G). Structural domains 1 (pale pink), 2 (blue) and 3 (green) are indicated as a cartoon. (B) Bar graph showing the stability predictions of the Muc18-2 protein containing the indicated monoallelic variants, obtained using I-Mutant 2.0 software. Negative values of energy change ($\Delta\Delta G$) indicates a decrease in the stability of the mutated protein. (C) Bar graph showing the accessible surface area (ASA) for each amino acid are presented with a monoallelic variant. Residue R555 was not possible to obtain ASA because of a gap in PDB structure.

We next tested whether these mutations affect the stability of Muc18-2 by calculating changes in free energy. We calculated protein stability changes ($\Delta\Delta G$) from the protein structure by using I-Mutant2.0 software. All mutations except N62D induced significant decreases in the stability of the protein (Figure 19C). Thus, the mutants are less stable than the wild-type protein.

Table 13. Clinical description and laboratory findings of patients P8, P9 and P10.

Clinical information	P8		P9		P10	
Ethnic Origen	Caucasian		Caucasian		Caucasian	
Consanguinity	No		No		No	
Sex	M		M		M	
Onset of disease	7 years		9 months		13 years	
Trigger	Parvovirus B19		LCH		EBV	
Fever	Yes		No		Yes	
Splenomegaly	Yes		No		Yes	
Laboratory tests						
Haemoglobin (9-12,2g/dL)	8.3		Normal		8.4	
Platelets (150-670x10 ⁹ /L)	136		Normal		70	
Neutrophils (1,4-6,5x10 ⁹ /L)	0.4		Normal		n.a	
Triglycerides (60-100mg/dL)	n.a		280		n.a	
Fibrinogen (2,38-4.98g/dL)	n.a		0.9		n.a	
Ferritin (25-400ng/mL)	800		2800		16286	
Direct Bilirubina (0.15-1.1 mg/dL)	0.11		n.a		n.a	
CRP (0.1-0.5mg/dL)	0.53		n.a		0.67	
PT (15-22.4s)	>80		n.a		n.a	
APTT (24-39s)	49.1		n.a		n.a	
AST (5-40U/L)	757		19		38	
ALT (5-40U/L)	342		41		85	
LDH (98-975U/L)	7260		n.a		n.a	
Bone Marrow Haemophagocytosis	Yes		Yes		Yes	
CD25s (<2400U/mL)	1135		6224		1712	
Perforin expression	Normal		Normal		Normal	
NK degranulation	Absent		Reduced		Reduced	
Cytotoxicity	Absent		Low		Absent	
Central Nervous System affection	No		No		No	
HLH flares/ time after the first episode	Yes/ 3 years		Yes/ 2 years		Yes/ 1 year	
Fulfilment of HLH diagnostic criteria	Yes (6/8)		Yes (5/8)		Yes (7/8)	
Disease recurrence	Yes		Yes		Yes	
Molecular study						
Affected gene/s	UNC13D STXBP2		UNC13D STXBP2		UNC13D	
Variant (Mutation/SNP)	Mutation rs144586070		rs17581728 rs1135688 rs370053399		rs35037984 rs139564938	
Nucleotide change	c.3224G>A c.604G>A		c.1992+5G>A c.2599A>G		c.2782C>T c.811C>T	
Aminoacid change	p.Arg1075Gln p.Val202Ile		n.a p.Lys867Glu p.Arg190Cys		p.Arg928Cys p.Pro271Ser	
Allele	Het Het		Het Het		Het Het	
MAF	n.a 0.0120		0.1575 0.4994		0.0002 0.0104	
1000 GENOMES (Iberian Population in Spain)	n.a G=1.0000 A=0.0000		G=0.7009 A=0.2991 A=0.5888 G=0.4112		C=1.0000 T=0.0000	
SIFT*	Damaging (0.03) Damaging (0)		n.a Tolerated (0,21) Tolerated (0,06)		Tolerated (0,1) Tolerated (0,56)	
PolyPhen-2 v2.2.2r398*	Probably damaging (0.998) Possibly damaging (0.809)		n.a Benign Probably damaging (1,00)		Benign Probably damaging (0,977)	

ALT, Alanine transaminase; APTT, activated partial thromboplastin time; AST, Aspartate transaminase; CD25s, soluble form of alpha subunit of interleukin-2 receptor; CRP, C-reactive protein; Het., Heterozygous; LCH, Langerhans cell histiocytosis; LDH, Lactate dehydrogenase; MAF, Minor allele frequency; N/A, not applicable; ND, not determinate; PT, Prothrombin Time; SNP, single nucleotide polymorphism.

*Only aminoacid change mutations have been tested.

4.4.2. Protein expression of monoallelic STXBP2 mutations

To determine molecular impact of the selected monoallelic variants in *STXBP2* found in patients with HLH and in the literature, we transfected COS-7 cell line with the 11 mutations and analyzed protein expression by Western Blot (Figure 20A). We used the mutation L243R previously studied in chapter 2 and P477L (reported in zur Stadt U R.J. 2009 as having no expression) as negative/cut-off control. The *STXBP2* quantification was normalized based on the β -actin expression, which is constitutively expressed. On one hand, eight of the 11 monoallelic mutations showed similar or even higher expression to wild type protein. On the other hand, 3 of the studied mutations (R235G, L256P and R405G) affected the levels of expression showing a significant reduced expression compared to wild type (Figure 20B).

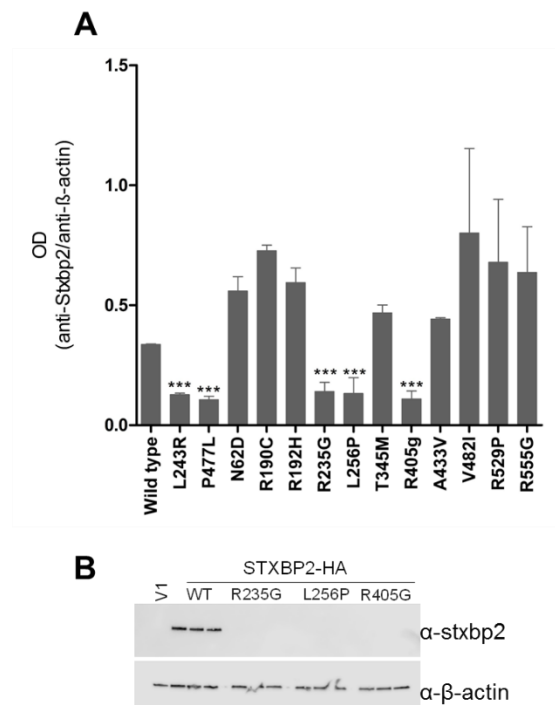


Figure 20. Western blotting analysis of cell lysates obtained from cells transfected with empty vector (V1), wild-type, negative controls (L243R and P477L) and the other 11 mutations. (A) Ratios of optical density of *STXBP2* expression to actin of each monoallelic variant. (B) Western blot image of the unexpressed variants performed it in triplicate. All data shown is mean \pm SEM, *** $p < 0.01$.

4.4.3. *Munc18-2^{R190C}* does not impair *STX11* protein binding.

Initially, we focused on the mutation R190C which did not alter Munc18-2 expression. This mutation was found in heterozygosity in P9, a 2 months old boy with degranulation/cytotoxic defects concomitant with EBV infection. In order to study the pathologic role of this mutation and specifically the ability to interact with STX11, COS-7 cell line was transiently co-transfected with the HA-STXBP2^{R190C} with GFP-STX11^{WT}. Forty-eight hours post-transfection, cells were lysed and subjected to anti-GFP immunoprecipitation (IP) and SDS-PAGE analysis. Empty vector (v1) was used as negative control and HA-STXBP2^{wt} encoding construct as positive control. The co-transfection of HA-STXBP2^{wt} with GFP-STX11^{wt} showed a band at 66kDa when using the anti-STXBP2 antibody, indicating a normal interaction between proteins. The co-transfection of HA-STXBP2^{R190C} with GFP-STX11^{wt} also showed a band at the same molecular weight but less intense. Of note, the input band of the same lane is also less intense indicating less amount of STXBP2 protein loaded or transfected. Even so, the assay confirmed the direct interaction of mutated STXBP2^{R190C} with STX11 (Figure 21).

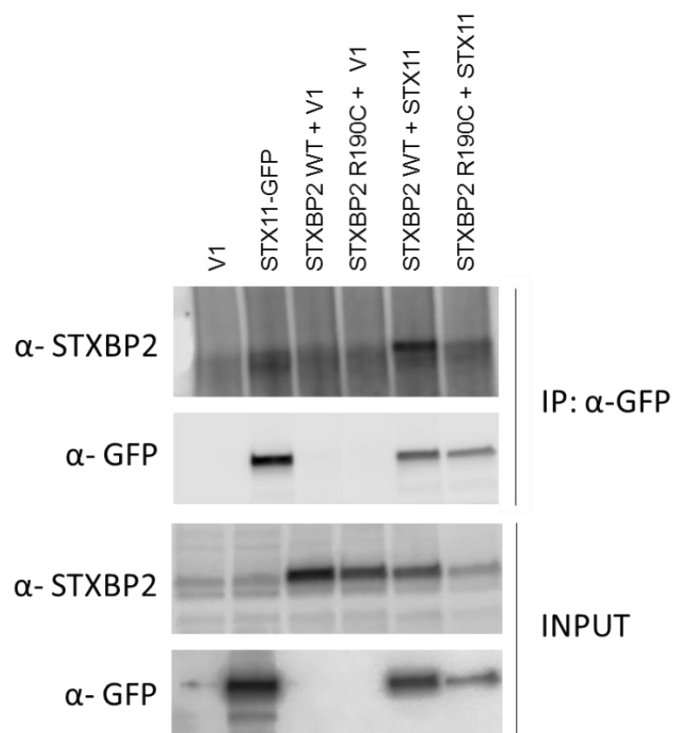


Figure 21. Detection of the mutated STXBP2^{R190C} interaction with stx11 by co-immunoprecipitation. COS-7 cells were co-transfected with plasmids as indicated in the figure, and immunoprecipitation was performed 24 hours later. STXBP2^{R190C} interacts with STX11.

4.4.4. *Munc18-2^{R190C}* and *Munc18-2^{R529P}* reduce degranulation in RBL-2H3 cells.

To examine whether this mutation had a functional effect on the protein, the experimental conditions were adjusted to study the functional capacity of degranulation of the RBL-H3 line transfected with mutant or wt constructions. Thus, human GFP-STXBP2^{R190C} and GFP-STXBP2^{wt} were transfected into cell line RBL-H3 using lipofectamine 3000. Later, transfected cells were sorted based on GFP expression (Figure 22B) to generate RBL-2H3 cells stably expressing GFP-STXBP2^{R190C} or GFP-STXBP2^{wt}. Subsequently, we measured the amount of β -hexosaminidase released after activation with PMA plus Ionomycin. RBL-2H3 cells stably expressing GFP-STXBP2^{R190C} showed a significant reduced degranulation activity compared to GFP-STXBP2^{wt} and non-transfected RBL-2H3 cells (Figure 22A). From the 11 mutations we reviewed from literature we could reproduce the same experiment with the mutant STXBP2^{R529P} resulting in a reduced degranulation as well. This mutation was found in patient n° P19 of K. Zhang et al. 2014 in which specific degranulation functional test was not reported. Despite the fact that we lacked background information we chose this mutation because of the molecular characteristics (Figure 19) and because of the in silico programs Polyphen and SIFT classify it as pathogenic.

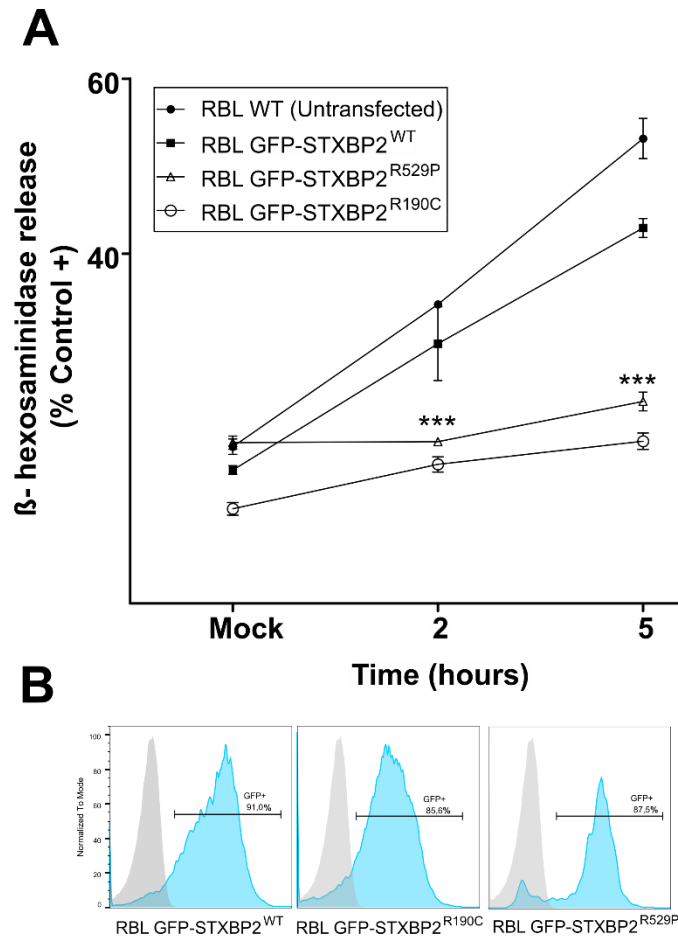


Figure 22. Degranulation test performed on the RBL-2H3 cell line stable transfected with mutants R190C and R529P. (A) RBL-2H3 cells were stably transfected with STXBP2^{WT}-GFP, STXBP2^{R190C}-GFP or STXBP2^{R529P}-GFP and were stimulated with PMA (5ug/mL) and Ionomycin 1mM for 2 and 5 hours. The data shown are the mean \pm SEM of two independent experiments each performed in triplicate. *** p <0.0. (B) Flow cytometry histogram confirming consistent GFP expression (blue lines) in RBL-2H3 cell line. Untransfected RBL (grey) were used to set the gates.

4.4.5. Monoallelic Variants UNC13D^{P271S}, UNC13D^{R928C} and UNC13DR^{1075Q} do not affect Munc13-4 protein expression.

Unfortunately, no crystal structure of the protein Munc13-4 has been described and we could not perform a bioinformatic analysis. We directly carried out the molecular analysis of the mutations UNC13D^{P271S}, UNC13D^{R928C} and UNC13D^{R1075Q} found in P9 and P10.

We transfected COS-7 with GFP-UNC13D^{P271S}, GFP-UNC13D^{R928C} and GFP-UNC13D^{R1075Q} mutations to analyze protein expression by Western Blot. In Figure 23B anti-GFP antibody was used to detect UNC13D protein. The three bands for each transfection correspond to the wild type and the three mutants revealing similar expression levels (Figure 23B). The UNC13D quantification was normalized based on the β -actin expression, which is constitutively expressed (Figure 23C)

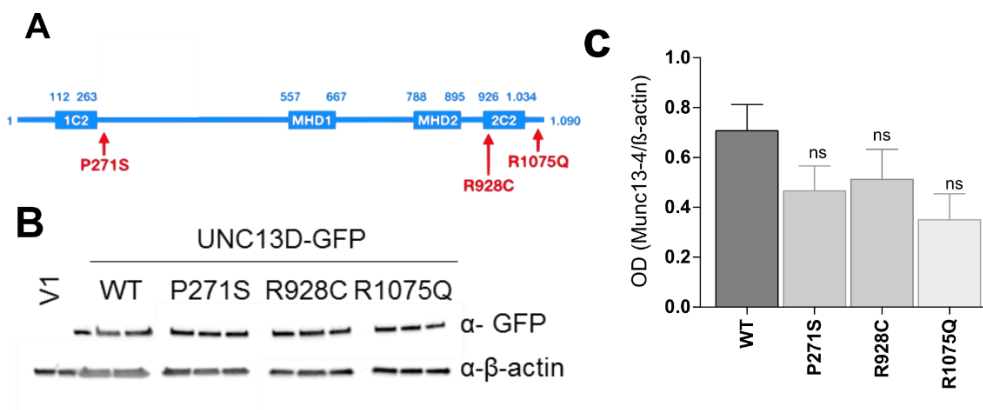


Figure 23. Protein expression of the *UNC13D* mutants analysis of transfected COS-7 lysates. (A) Schematic representation of the *UNC13D* mutant's localization. (B) Western blot image *UNC13D* variants performed in triplicate. (C) Ratios of optical density of *UNC13D* expression to actin of each monoallelic variant. All data shown is mean \pm SEM; ns: no significance ($p > 0.05$).

4.4.6. Monoallelic Variants *UNC13D*^{P271S}, *UNC13D*^{R928C} and *UNC13D*^{R1075Q} do not affect interaction of Munc13-4 with their partners.

In order to study the likely pathologic role of these mutations, we sought to discriminate whether these mutations could have an effect on their protein-protein interaction. For that, COS-7 cells were transiently co-transfected with FLAG/GFP-*UNC13D*^{mut} and with GFP-STX11 or FLAG-Rab27a. Interactions with STX11 and Rab27 were analyzed using anti-GFP IP. Empty vector (v1) was used as negative control and FLAG/GFP-*UNC13D*^{WT} encoding constructs as positive controls. Co-IP involving of FLAG-*UNC13D*^{wt/mutants} with GFP-STX11^{wt} showed a band around 120kDa with anti-FLAG(*UNC13D*) antibody in all lanes containing either the wild type or mutated proteins. Same results were observed in Co-IP involving GFP-*UNC13D*^{wt/mutants} with FLAG-RAB27a^{wt}. Thus, the assay confirmed

the direct interaction of mutants UNC13D^{P271S}, UNC13D^{R928C} and UNC13D^{R1075Q} with Rab27a and STX11 (Figure 24).

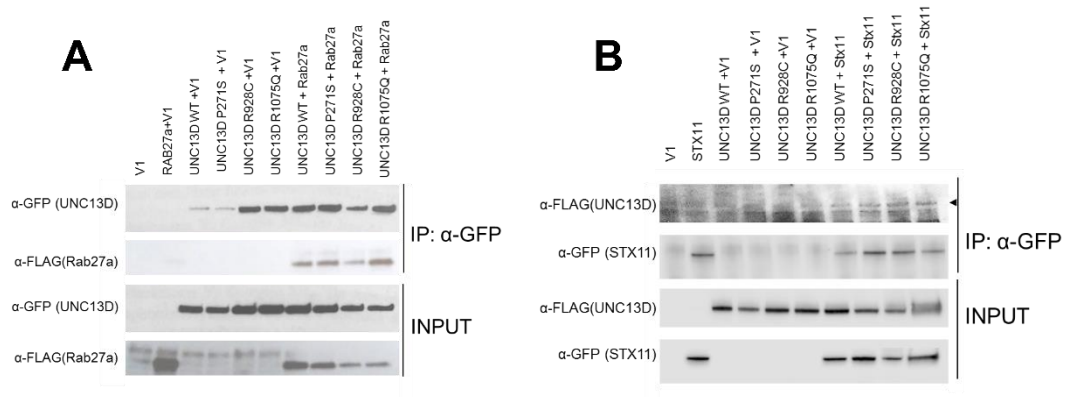


Figure 24. Detection of the mutated UNC13D interactions by co-immunoprecipitation assay. COS-7 cells were cotransfected with plasmids as indicated in the figure, and immunoprecipitation was performed 24 hours later. Proteins were detected by Western analysis. (A-B) All mutants UNC13DP271S, UNC13DR928C and UNC13DR1075Q interact with Rab27a and Stx11 respectively.

CHAPTER 4: GENERATE STABLE STXBP2 KNOCKDOWN CELL LINES TO STUDY THE ROLE OF STXBP2 IN CELL TRAFICKING.

To study the role of STXBP2 in cell trafficking, we transduced THP-1 macrophage-like and RAMOS cell lines with STXBP2 shRNA lentiviral particles to generate knock down (K.D) cells. The transduced cells were selected in the presence of puromycin (0.25 mg/ml) for 20 days. We confirmed by western blot that Muc18-2 expression exhibited a 75,22% of reduction in K.D THP-1 cells and 84.2% (Figure 25A) in K.D RAMOS compared to wild type (100%) cells. The quantification data of STXBP2 in both cells were normalized based on the expression of β -actin, which is expressed constitutively. The expression of β -actin in the two cell types was similar, indicating that in the knock down the protein synthesis was not affected by the transduction process (Figure 25B-C).

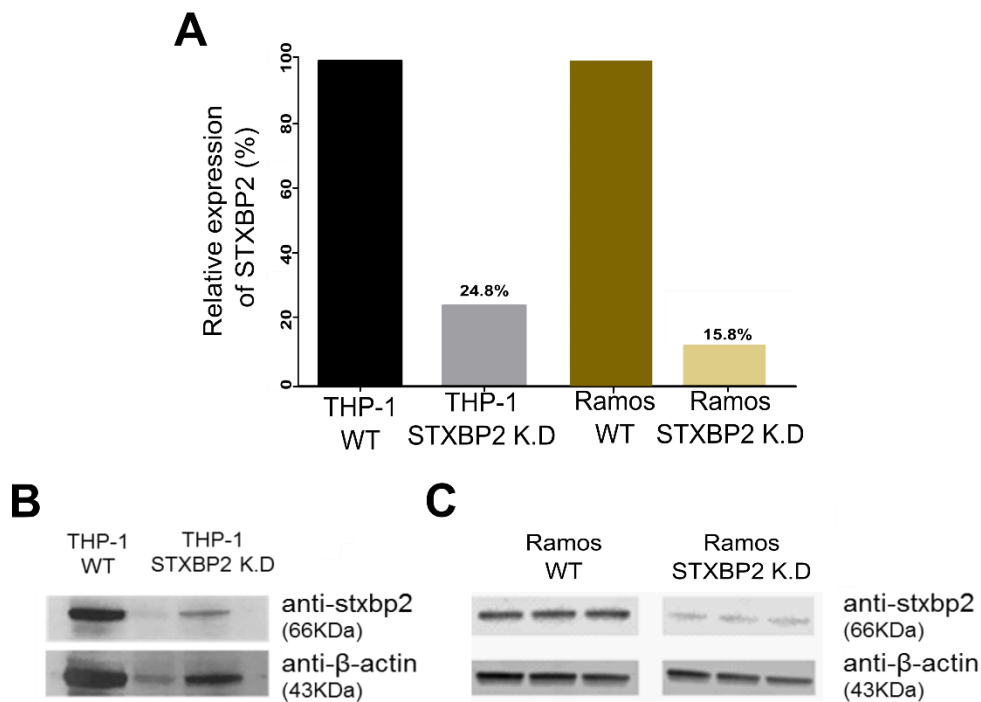


Figure 25. Assessment of STXBP2 expression in THP-1 cells by western blot. Cell lysates from THP-1 WT and STXBP2 K.D were compared using western blot analysis with anti-stxpb2 antibody. Actin staining of the same membrane was used to show equivalent protein loading and the quantification analysis

5.1. STXBP2 IS INVOLVED IN THE ENDOSOMAL TRAFFICKING

To assess the implication of STXBP2 in intracellular trafficking we analyze transferrin receptor (CD71) and the $\alpha\text{E}\beta 7$ integrin (CD103) as they are markers commonly used to identify recycling endosomes. STXBP2 WT and K.D THP-1 cells were pre-treated with PMA as previously described and then activated with LPS + $\text{IFN}\gamma$. On one hand, the expression of CD103 in STXBP2 K.D THP-1 cells were significantly higher than in WT THP-1 cells, both in unstimulated and LPS + $\text{IFN}\gamma$ treated cells (Figure 26A). On the other hand, the expression of CD71 showed no significant differences between THP-1 cell lines (Figure 26B).

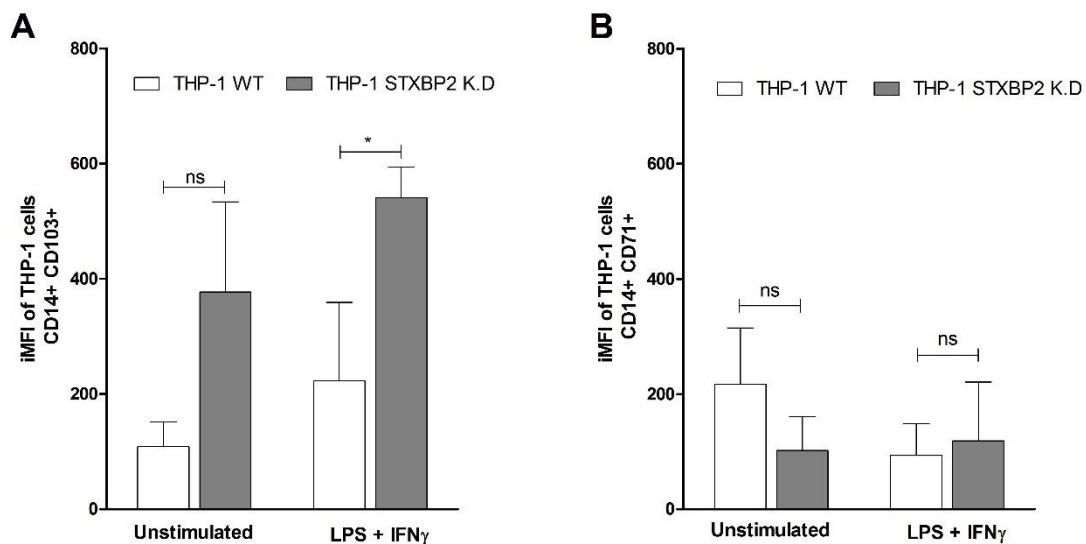


Figure 26. Representation of CD103 and CD71 expression in both THP-1 WT and STXBP2 KD cells. (A) iMFI of unstimulated and LPS + $\text{IFN}\gamma$ treated WT and STXBP2 K.D cells for CD103 and (B) CD71. The data shown are the mean \pm SEM of three independent experiments each performed in triplicate. * $p < 0,05$; iMFI: normalized MFI by percentage of cells expressing CD103 or CD71)

5.2. STXBP2-KD RAMOS CELLS EXPRESS LESS CD107A

Next, we analyzed how STXBP2 silencing affected degranulation in B Lymphocytes B. We performed degranulation assays on WT and STXBP2-KD Ramos cell lines. Ramos cells were activated by inducing crosslinking of the BCR with anti-IgM. To assess the activation capability of STXBP2-KD Ramos by CD69 expression on the cell surface. Stimulation with anti-IgM alone or in combination with IL-4 induced cell activation as shown by the increase in CD69 expression in both WT and KD Ramos cells (Figure 27A)

Degranulation was measured based on the presence of CD107a in the membrane. Stimulation with anti-IgM alone or with IL-4 or IL-21 was used to induce a T-independent activation, or IgM with sCD40L to induce a T-dependent activation. We analyzed the integrated mean fluorescence (iMFI) of the upregulation of CD107a. STXBP2-KD Ramos showed a significant decrease of CD107a iMFI compared to WT Ramos (Figure 27B).

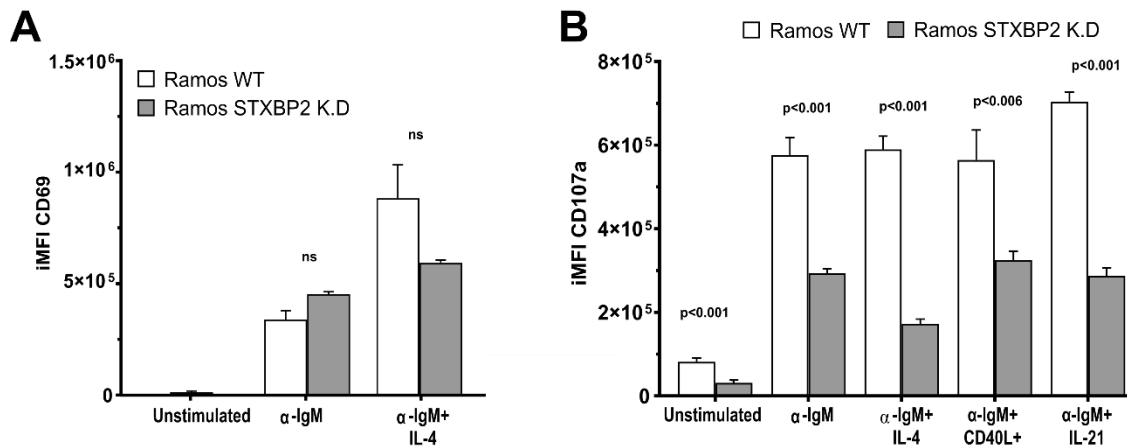


Figure 27. Activation and degranulation of Ramos WT and STXBP2 K.D cells. The average fluorescence intensity (iMFI) is represented according to the stimuli used. (A) Expression of CD69 after 4 hours activation with anti-IgM or with anti-IgM + IL-4. (B) Expression of CD107a after activation of 2 hours with the indicated stimuli (anti-IgM, anti-IgM + IL-4, anti-IgM + CD40L, anti-IgM + IL-21). The cells were incubated together with anti-CD107a-APC. The data shown are the mean \pm SEM of three independent experiments each performed in triplicate. * $p < 0,05$; iMFI: normalized MFI by percentage of cells expressing CD69 or CD107a.

CHAPTER 5. COMPREHENSIVE REPOSITORY OF HLH MUTATION DATA FOR MEDICAL RESEARCH AND GENETIC DIAGNOSIS OF HLH.

In recent years, the number of studies reporting new HLH mutations in related and non-related genes has increased, trying to shed light into the pathophysiology of the disease. These mutations have been published in original and case report articles as well as in universal databases as ClinVar, OMIM (Online Mendelian Inheritance in Man) or HGMD (The Human Gene Mutation Database). However, due to the large number of involved genes, these collections quickly became outdated since they are not interactive and do not allow searches according to different criteria. Thus, we have created a free access repository of HLH mutation data for medical research and HLH genetic diagnosis that collects detailed information of known genetic mutations underlying HLH.

6.1. There are 434 genetic variants involved in HLH

HLHdb presents all the variants published in literature for the four genes identified as causative of primary HLH (*PRF1*, *UNC13D*, *STXBP2*, *STX11*). It comprises 237 missense, 75 frameshift, 56 splicing, 49 nonsense, 10 intronic, 8 in-frame deletions and 5 large rearrangements distributed among the four genes (Figure 28). Moreover, we have collected the allelic status of the carriers. Importantly, a variant can be found as biallelic, monoallelic or both. In addition, we included whether a functional assay has been carried out in order to describe a functional consequence of the variant (Figure 28A). The information has been integrated with other relevant databases, like clinical evidence from ClinVar and UniProt, population allele frequency from ExAC and gnomAD and pathogenicity predictions from well-known tools (PolyPhen-2, CADD, PON-P2 and SIFT). We found that 88% of the variants had a pathogenic prediction by some *in silico* predictor and 95% had an allele frequency below 1% but only 0,5% can be found in ClinVar database.

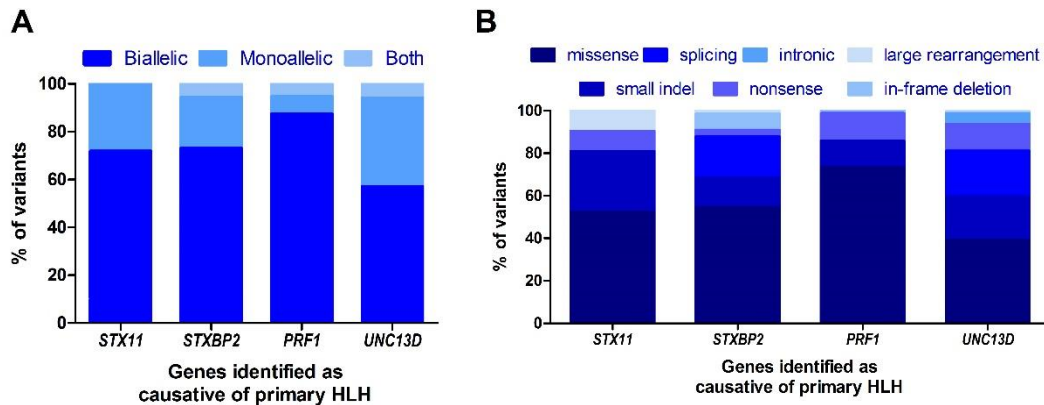


Figure 28. Distribution of protein variant types in STX11, STXBP2, PRF1 and UNC13D genes. (A) Allelic status of the variants among each gene. (B) Variant consequence in protein.

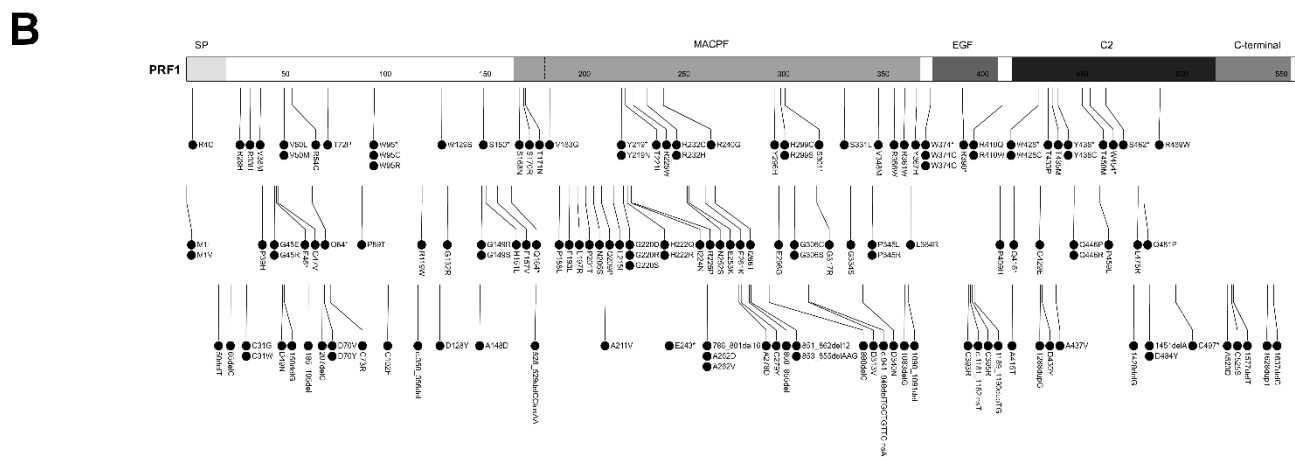
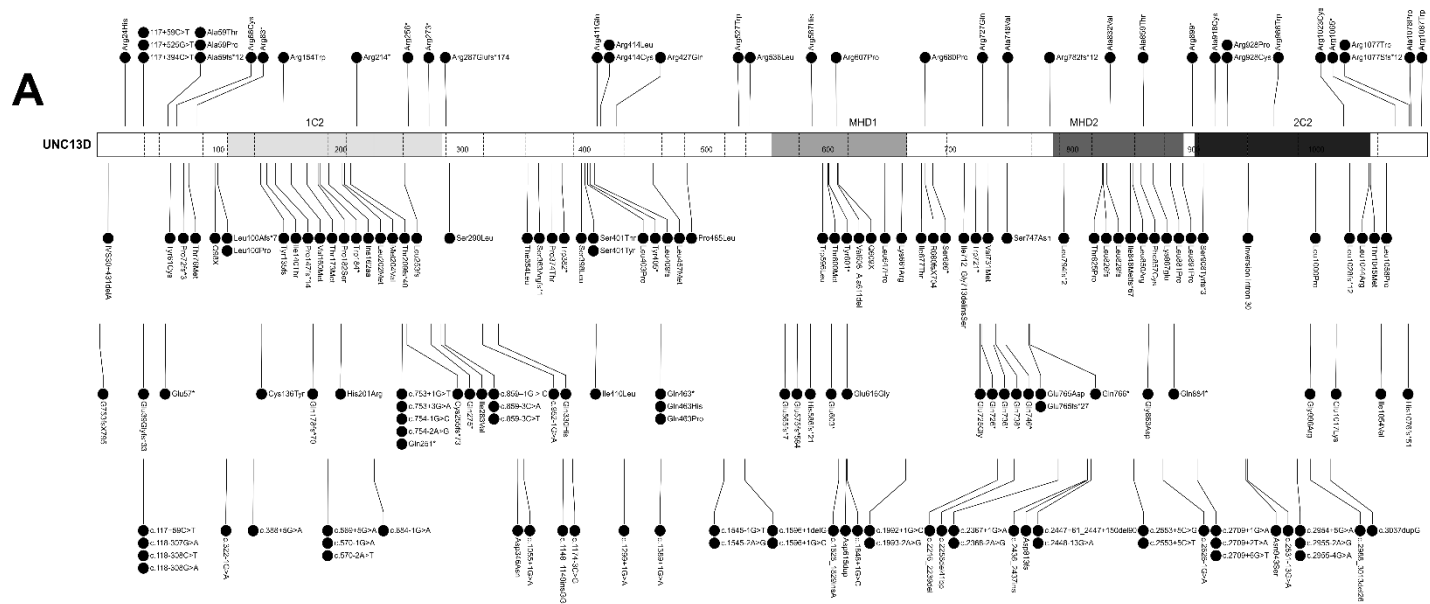
5.2. Mutation distribution along proteins is uniform

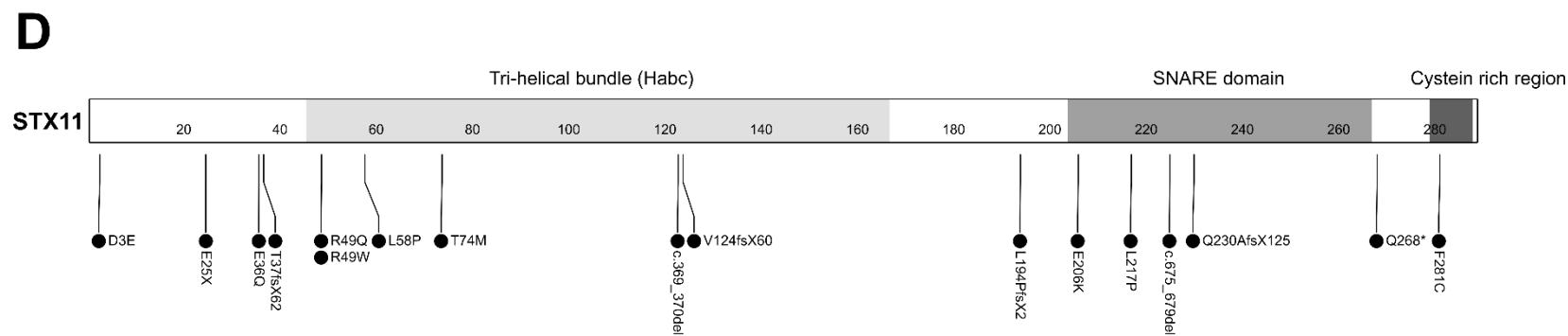
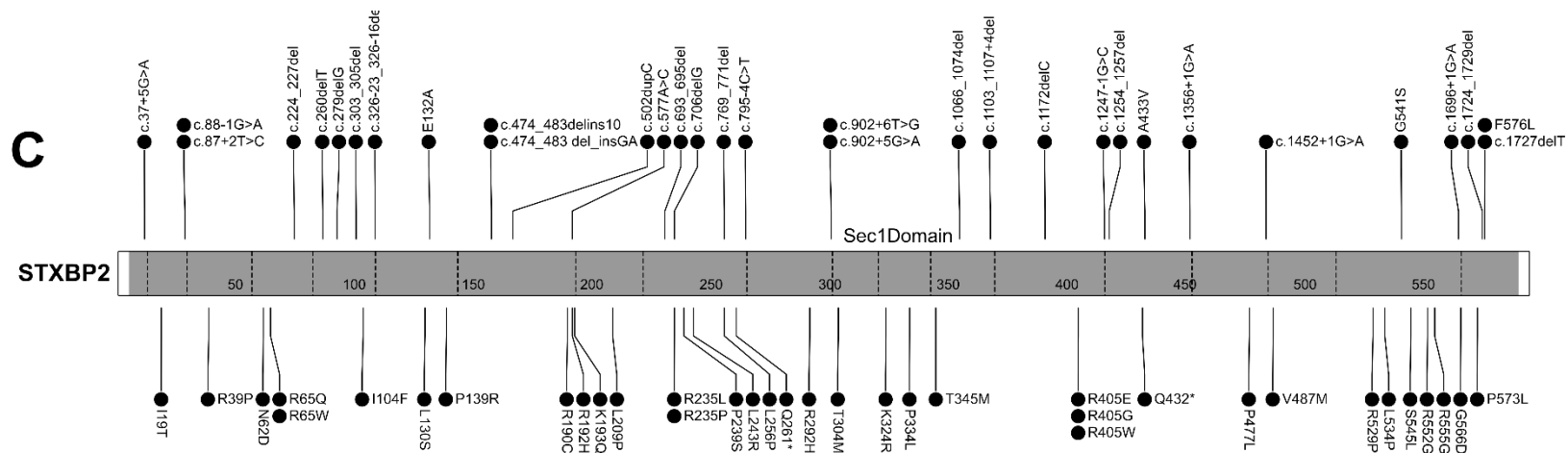
In general, the more base pairs a gene has, the more likely it is to be affected by a mutation. Therefore, UNC13D that has 1090 amino acids, is the protein with a higher number of mutated residues followed by Perforin, STXBP2 and STX11. Nevertheless, we calculated mutation density as the number of mutations found in the gene divided by the number of amino acids of that protein, revealing that perforin is more prone to mutation per number of amino acids (Table 14).

Table 14.

Gene	N ^o of AA	N ^o of mutations	Mutation density
STXBP2	590	69	12%
STX11	287	21	7%
UNC13D	1090	239	22%
PRF1	559	155	28%

We mapped all mutations found in the literature for each protein and we observed a uniform distribution of the mutated residues along studied proteins. Detailed distribution of the mutations in each protein are showed in Figure 31A-D.





5.3. HLHdb is a user-friendly website

All this information is collected at <http://hlhdb.biotoclin.org>. This website is structured in several parts. First, there is a welcome page where the database is presented. The user can find the genes responsible of the HLH disorder and a little description of each gene. There, the user can select a gene of their interest and is transferred to the gene view where all the variants of that gene are listed. In the gene view, there is summarized the main characteristics of all the variants of that gene. It is annotated whether a variant was found as biallelic and/or monoallelic in the literature, whether it was described in more than one patient and whether there is functional evidence supporting it. Moreover, additional information of *in silico* predictors and population allele frequencies of the variant are shown. At last, a link to a detailed view of the variant is linked (Figure 29A). In the variant view, all the information regarding that variant is shown. There is a section characterizing the variant, a reference to the first paper describing the variant, the annotation whether the variant has been described as biallelic and/or monoallelic, whether it has been found in more than one patient and whether a functional assay has been carried out. Then, there is a section about *in silico* predictors. There, the prediction of the variant for the CADD, PolyPhen-2, PON-P2 and SIFT predictors can be found. Afterwards, there is a section with the main databases of interest and their information about the variant. There are databases reporting clinical evidence of the variants causing the disease such as ClinVar, reporting residues of biological relevance such as UniProt, collecting variant information such as dbSNP or Ensembl, and calculating population allele frequency such as the ExAC and gnomAD. Furthermore, there is a section about general knowledge of the disease, gene and protein with links to the databases DECIPHER, OMIM, HPO, etc., (Figure 29B).

A PRF1

Genetic Variant*	Protein Variant**	Variant Type	Biallelic	Monoallelic	Described >1 patient	Functional evidence	Bibliography	PolyPhen-2	SIFT	ExAC	Details
c.1A>G	p.Met1Val	Missense	Yes		Yes	Yes		Possibly damaging			
c.3G>A	p.Met1Ile	Missense	Yes					Possibly damaging			
c.10C>T	p.Arg4Cys	Missense	Yes	Yes	Yes			Benign		1.4·10 ⁻⁰³	
c.50del	p.Leu17Rfs*34	Frameshift	Yes		Yes	Yes					
c.65del	p.Pro22Rfs*29	Frameshift	Yes		Yes						
c.83G>A	p.Arg28His	Missense		Yes	Yes			Possibly damaging			
c.91T>G	p.Cys31Gly	Missense	Yes			Yes		Probably damaging			
c.93C>G	p.Cys31Trp	Missense	Yes		Yes	Yes		Probably damaging			

B

PRF1: G149S

Bibliography:	
Biallelic:	Yes
Monoallelic:	-
Described >1 patient:	-
Functional Evidence:	Yes

What is predicted by other tools?

Predictor	Score	Label
CADD	27.8	Damaging
PolyPhen-2	1.3	Probably damaging
PON-P2	0.896	Pathogenic
SIFT	-	-

Disclaimer: This resource is publicly intended for research purposes. The authors are not responsible for neither its use nor misuse. The data provided are not intended as advice of any kind. The authors have worked with care in the development of this server, but assume no liability or responsibility for any error, weakness, incompleteness or temporariness of the resource and of the data provided.

Interpreting the variant

Learn more about the variant

	ClinVar	Pathogenic (letters provided, single submitted)
Clinical Evidence	UniProt	-
Biological Relevance	Functional residue	domain: M4CFE
Variant Information	dbSNP	rs147462227
	Ensembl	variant
Population Allele Frequency	ExAC	1.407e-04
	gnomAD	1.421e-04

Explore the biomedical information

Disease	Protein	Gene
DECIPHER	S198NG	Ensembl
HPD	UniProt	GenoCards
DisProt		NCBI
UniProt		NCBI
OMIM		OMIM
Orphanet		

Locate your variant in the protein

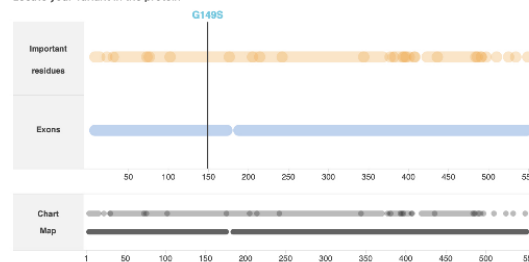


Figure 29. Gene view and detailed view of the variants. (A) Screenshot of the PRF1 gene view showing the main characteristics of some of the variants of that gene. It is possible to see whether a variant was found as biallelic and/or monoallelic, described in more than one patient, the functional evidence, in silico predictors and population allele frequencies. (B) Screenshot of the link to a detailed view of the variant G149S. In the variant view there is a summary of all the information regarding that variant, other in silico predictions (CADD, PolyPhen-2, PON-P2 and SIFT), databases reporting clinical evidence of the variants (ClinVar), reporting residues of biological relevance (UniProt), collecting variant information (dbSNP or Ensembl), and calculating

population allele frequency (ExAC and gnomAD). Finally, there is a section to locate the variant in the protein.

5.4. More than 10% of HLH variants were errantly reported

In order to obtain a harmonized, interchangeable and clear dataset, we followed the Human Genome Variation Society (HGVS) guidelines for variant nomenclature (<http://varnomen.hgvs.org>). We found that 15% of the variants did not follow the guidelines and they were renamed. In Table 15, are listed all the corrected variants. The first columns indicate de name of the gene in where the variant was corrected, the second and the third columns are listed the variants as were in the original manuscript. Finally, in the two last columns are listed the variants corrected and how we listed in the database.

Table 15. Corrected variant nomenclature of the literature

Gene	Original genetic variant	Original protein variant	Standard genetic variant	Standard protein variant	Comments
STX11	c.110delC	p.Thr37fs*62	c.110delC	p.Thr37Argfs*26	Protein variant corrected: new amino acid added and stop codon position corrected
STX11	c.675_679delCGAGC		c.675_679delCGAGC	p.Glu226Leufs*127	Protein variant calculated from genetic variant
STX11	c.369_370delAG	p.Val124fsX60	c.369_370delAG	p.Val124Glyfs*61	Protein variant corrected: new amino acid added and stop codon position corrected
STX11	c.581_584delTGCC	p.Leu194Profs*2	c.581_584delTGCC	p.Leu194Profs*3	Genetic variant corrected: deleted sequence corrected; Protein variant corrected: stop codon position corrected
STX11	c.867dupG	p.Gln230AlafsX125	c.687dupG	p.Gln230Alafs*125	Genetic variant corrected: position corrected
STX11	c.842T>C	p.Phe281Cys	c.842T>G	p.Phe281Cys	Genetic variant corrected: new nucleotide corrected according to protein variant
STXBP2	c.1204C > G	p.Arg402Gly	c.1213C>G	p.Arg405Gly	Genetic variant corrected: position corrected according to reference transcript; Protein variant corrected: position corrected according to reference isoform
STXBP2	c.1214G>A	p.Arg405Glu	c.1214G>A	p.Arg405Gln	Protein variant corrected: new amino acid corrected according to genetic variant
STXBP2	c.1654A > G	p.Arg552Gly	c.1663A>G	p.Arg555Gly	Genetic variant corrected: position corrected according to reference transcript; Protein variant corrected: position corrected according to reference isoform
STXBP2	c.1727delT	p.Phe576SerfsX4	c.1727delT	p.Phe576Serfs*5	Protein variant corrected: stop codon position corrected
STXBP2	c.1172delC	p.Pro391fs	c.1172delC	p.Pro391Argfs*27	Protein variant corrected: new amino acid added and stop codon position added
STXBP2	c.1243_1246delAGTG		c.1252_1255delAGTG	p.Ser418Argfs*7	Genetic variant corrected: position corrected according to reference transcript; Protein variant calculated from genetic variant
STXBP2	c.474_483delins10		c.474_483delinsGA	p.Cys158Trpfs*78	Protein variant calculated from genetic variant
STXBP2	c.292_294delGCG		c.301_303delGCG	p.Ala101del	Genetic variant corrected: position corrected according to reference transcript; Protein variant calculated from genetic variant
PRF1	c.1083delG		c.1083delG	p.Arg362Glyfs*3	Protein variant calculated from genetic variant
PRF1	c.1090_1091delCT	p.Leu364fs	c.1090_1091delCT	p.Leu364Glyfs*93	Protein variant corrected: new amino acid and stop codon position added
PRF1	c.1189_1190dupTG		c.1189_1190dupTG	p.His398Alafs*23	Protein variant calculated from genetic variant
PRF1	c.1451delA		c.1451delA	p.Asp484Valfs*25	Protein variant calculated from genetic variant
PRF1	c.1577delT	p.Leu526fs*87	c.1577delT	p.Leu526Cysfs*87	Protein variant corrected: new amino acid added
PRF1	c.1628dupT		c.1628dupT	p.Glu545Glyfs*41	Protein variant calculated from genetic variant
PRF1	c.1637delC		c.1637delC	p.Pro546Leufs*67	Protein variant calculated from genetic variant
PRF1	c.207delC	p.Pro69fs	c.207delC	p.Asp70Thrfs*37	Protein variant corrected: position corrected and new amino acid and stop codon position added
PRF1	23 bp nt 1146-1168		c.1146_1168del	p.Pro383Argfs*67	Genetic variant corrected; Protein variant calculated from genetic variant
PRF1	c.283T>C		c.283T>C	p.Trp95Arg	Protein variant calculated from genetic variant
PRF1	c.503G>A	p.Ser108Asn	c.503G>A	p.Ser168Asn	Protein variant corrected: position corrected
PRF1	c.50delT		c.50delT	p.Leu17Argfs*34	Protein variant calculated from genetic variant
PRF1	c.65delC		c.65delC	p.Pro22Argfs*29	Protein variant calculated from genetic variant
PRF1	c.786_801del16	p.Ala262fs*22	c.786_801del	p.Gln263Serfs*21	Protein variant corrected: position and stop position corrected
PRF1	c.851_862del12	cod284-287	c.851_862del	p.Lys284_Lys287del	Protein variant corrected
PRF1	c.853_855delAAG	DelK285	c.853_855delAAG	p.Lys285del	Protein variant corrected
PRF1	c.879delC	p.His283*	c.879delC	p.Gln294Lysfs*36	Protein variant corrected based on genetic variant
PRF1	c.150delG		c.150delG	p.Thr51Profs*56	Protein variant calculated from genetic variant
PRF1	c.941_948delTGCTGTTCCinsA		c.941_948delTGCTGTTCCinsA	p.Leu314Glnfs*14	Protein variant calculated from genetic variant
PRF1	c.350_356delTGGCCCGinsATGC		c.350_356delTGGCCCGinsATGC	p.Val117Aspfs*439	Protein variant calculated from genetic variant
PRF1	c.1181_1182insT	p.Gly394fs*	c.1181_1182insT	p.Gln394Hisfs*64	Protein variant calculated from genetic variant

VI. DISCUSSION

The main goal of this thesis was to investigate the genetic basis of HLH by studying novel and previously undescribed mutations at molecular and functional level. The diagnosis of HLH is currently a challenge for clinicians since some of the clinical manifestations can occur in other multisystemic diseases that, in turn, can also act as an HLH triggers. The clear identification of mutations causing HLH leads to an unequivocal diagnosis of the disease, but this occurs only in a small percentage of patients. For this reason, identifying new mutations and their role in HLH would allow a better classification of patients, establishment of a more accurate diagnosis and finally leading to a better treatment for those patients.

Establishing Reference Intervals in adult and pediatric population for the cytotoxicity activity and for the NK cell degranulation.

Since inter-individual biological variability occurs in different immunological parameters, it is necessary to have reference values in healthy individuals that allow the correct interpretation of the results when evaluating patients with a specific diagnostic suspicion (Kaczorowski et al. 2017). NK cytotoxicity and CD107a upregulation functional assays are commonly used in many laboratories as a tool for HLH diagnosis. For this purpose, the threshold or cut-off was determined for these tests and thus be able to differentiate, in a more robust way, HLH patients with impaired degranulation from those that do not.

To do this, we first compare the results using two different degranulation stimuli, K562 cell line or PHA. K562 cell line is MHC I devoid and hence it acts as target cells for NK cells (Shabrish, Gupta, and Madkaikar 2016). Whereas PHA binds to sugars on glycosylated surface proteins crosslinking them and leading to activation. Our results show a significantly higher CD107a upregulation in NKdim cells using PHA instead of K562. Thus, we suggest that the degranulation assay with PHA would allow a better identification of patients with impaired degranulation. (Yenan T Bryceson et al. 2012). Overnight incubation with IL-2 increased percentage of NK cells expressing CD107a in PHA or K562 activation conditions. According to the literature, resting NK cell degranulation is induced only by mutual costimulation of nonactivating receptors. In contrast, activated (IL-2)-NK cell degranulation is induced by a higher number of receptors suggesting a likely redundancy in the activation pathway, thus boosting the degranulation (Yenan T. Bryceson et al. 2006).

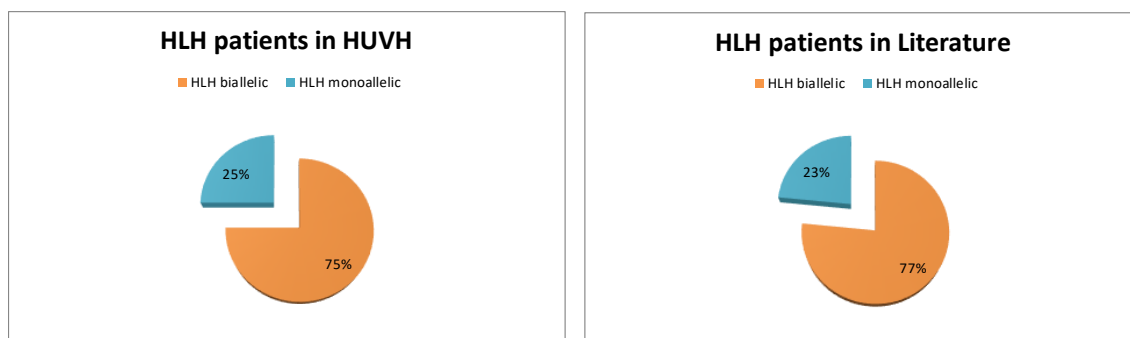
The optimization of functional assays that enable us to identify pathological NK cytotoxicity or degranulation is a basic aspect to diagnose HLH. For this reason, we use in our routine laboratory practice a healthy adult control sample to validate the functional

technique. Since HLH is a disease that has been observed in children with an onset peak age between one and six months but also in adults (Janka and Lehmsberg 2014), we sought to investigate if there were differences in cytotoxicity and degranulation within children and adults. Cytotoxicity was low in children under 8 years and then increases to adult levels (Figure 8B). These results are consistent with the observation that NK cells expressing CD56^{dim} increased with age (Figure 8A)(Gounder et al. 2018). As CD56^{dim} is a marker of maturity in NK cells (Luetke-Eversloh, Killig, and Romagnani 2013), the low cytotoxicity described in our cohort of healthy children may be due to the fact that their NK cells already had limited attack capacity, which will increase during life until adulthood levels. However, in the degranulation assay following PHA activation we only found significant differences when comparing activated NK cells in children under 3 years. Exposing NK cells to an interleukin-2 leads to increased expression of markers associated with activation (NKp30, NKp44, and NKp46)(Abraham et al. 2019). However, the effect of age on the expression of these markers is controversial (Hazeldine and Lord 2013). In this regard, our data suggest that under 3 years of age the NK cell phenotype is not able to respond properly to IL-2 and that is probably the reason why we see a decline in degranulation. In summary, the diversity of NK cell cytotoxicity and degranulation that we have demonstrated in healthy controls suggests that we may use a group of healthy control age match as comparators when analyzing the assays results, especially in cytotoxicity assay where the differences are more accused.

Even though cytotoxicity is included in HLH diagnosis criteria, this assay is not specific for primary HLH and recent reports (Jordan et al. 2019; Cetica et al. 2016) agreed with the fact that these criteria should change and include degranulation for reliable diagnosis of HLH. Based on these recommendations, we established a cut-off for degranulation in activated NK cells stimulated with PHA of 17.8% providing a 83,3% of sensitivity and 95,5% of specificity (Figure 9). The negative predictive value (NPV) was 95,5% which means that almost all screened patients with a CD107a upregulation above 17.8% will truly don't have the disease. Prior studies from Bryceson *et al.* showed that abnormal CD107a upregulation below 20% in activated NK cells could provide similar sensitivity (~80%) and specificity (~90%) for detecting mutations in degranulation genes(Yenan T Bryceson et al. 2012). Rubin *et al.* also measured a diagnostic threshold using the Mean channel of fluorescence (MCF) of the CD107a upregulation (CD107a MCF \leq 143) resulting in a 93.8% of sensitivity and 73% of specificity(Rubin et al. 2017). Of note, even following different protocols and choosing different cut-off units in Bryceson and Rubin *et al.* reports, they obtained similar results of sensitivity and specificity. In our experiments we used PHA as stimuli to calculate the cut-off value, however similar

results regarding sensitivity and specificity were obtained. This suggests that NK cell degranulation is a robust mechanism that allowed a rapid and reliable classification of patients and it would be very valuable to have it included in HLH diagnostic criteria.

Based on these laboratory techniques and clinical findings, we have diagnosed 12 patients with HLH in our center. In 10 patients we have found mutations in genes from the degranulation pathway. However, 2 patients presented homozygous mutations in non-HLH genes. These two patients together with patients with perforin defects were not discussed in this thesis. Of note, although the cohort of patients described here is small, the proportion of patients with homozygous/compound heterozygous and with heterozygous mutations is the same as seen in the literature (Cetica et al. 2016; X. J. Xu et al. 2017)



Finally, the reference ranges and the cut-off of cytotoxicity and degranulation tests identified here will hopefully aid in interpreting NK cells degranulation and cytotoxicity in pediatric and adult population with HLH.

Functional and molecular characterization of novel mutations found in patients diagnosed with FHL.

In the work presented in this thesis, we characterized the novel mutation p.L243R in *STXBP2* gene described in a patient diagnosed with FHL5. The patient was carrier of this mutation (p.L243R) in one allele and of the p.V417LfsX126 mutation previously reported in the other allele (zur Stadt, Rohr, Seifert, Koch, Grieve, Pagel, Strauß, et al. 2009). The functional effect of these mutations results in a lack of cytotoxicity and an altered degranulation assay (Figure 11B-C). The p.L243R mutation impairs *STXBP2* protein expression in transfected COS-7 cells (Figure 13B). Moreover, no expression of *STXBP2* could be detected by western blotting in patient's PBMC (Figure 14). The reduced expression of L243R respect to wild-type *STXBP2* could be caused both by mRNA and/or protein instability. As far as to a single DNA substitution within the traduced mRNA sequence would hardly induce mRNA degradation, the most probably explanation would be that the substitution of lysine 243 by an arginine produces a change in protein folding. Misfolded proteins would be then removed by the ubiquitin proteasome system (UPS) (Pilla, Schneider, and Bertolotti 2017). This data agrees with the results obtained from the molecular simulation that predicts that residue leucine 243 is fundamental for protein structure (Figure 13A). *In silico* analysis of the structural properties of L243 residue showed that it is located in a buried site of the protein that provides anchoring between domains 2 and 3 and has contacts with previously reported mutated residues (Hackmann et al. 2013). Its effect is predicted to disrupt the stability of the protein and lead to degradation of *STXBP2*, as demonstrated by the absence of protein expression. Taken together, our data suggest that L243R mutation produces a change in the three-dimensional structure of *STXBP2*. This change causes an incorrect folding of the protein, resulting in an unstable protein that is degraded via proteasome. Furthermore, the data obtained with COS-7 cells demonstrate a significant decrease in the expression of the mutant (>95%). p.V417LfsX126 is the most commonly reported mutation in FHL5 patients and has been described in both homozygosity and compound heterozygosity together along with other missense mutations (Pagel, Beutel, Lehmborg, Koch, Maul-Pavicic, Rohlf, Al-Jefri, Beier, Bomme Ousager, et al. 2012). In homozygosis, a variable reduced protein expression with a lower molecular weight has been detected, while in compound heterozygosity, as in this case, a total absence of the protein has been observed, probably due to the instability of the combination with the product of the other mutated allele (Zhao et al. 2013; Rohr et al. 2010; Esmailzadeh et al. 2015). Accordingly, the combination of the mutations p.V417LfsX126 and p.L243R result in almost total absence of *STXBP2* protein expression in our patient. In previous

reports of patients with a diagnosis of FHL5 in which the decreased expression of STXBP2 was shown, a reduction in STX11 expression levels has been also demonstrated (Côte et al. 2009).

One possible explanation for the residual degranulation observed in the patient could be the redundant function of STXBP2 family proteins, such as Munc18-1 (Lopez et al. 2018; Hackmann et al. 2013). In any case, there is a discrepancy between the total lack of cytotoxic activity compared with the partial degranulation measured by the expression of CD107a on the cell surface. In addition to lytic granules, CD107a is found in endosomes and cytokine containing granules. It is conceivable that the residual degranulation measured via CD107a would be STXBP2 independent. In fact, although we detect NK CD107a positive cells in the patient after PHA degranulation (30% of the NK cells), was very low compared to MFI obtained in healthy control cells. This data suggests that in patient's NK cells only a small percentage of vesicles containing CD107a are fused to the membrane after PHA activation. It might be that those vesicles are STXBP2-independent endosomes and cytokine containing granules. If that was the case, the specific activation of STXBP2 dependent trafficking via K562 cell line interaction with NK cells would result in a total lack of cytotoxic activity as detected in the patient. Taken together, our data shown that the combination of mutations p.V417LfsX126 and p.L243R produces the impairment of STXBP2 expression, causing familial hemophagocytic lymphohistiocytosis type 5 in the studied patient.

Functional and molecular characterization of novel and reported mutations found in patients diagnosed with an atypical form of HLH.

Monoallelic mutations are those found in heterozygosis directly affecting one allele of the gene. When a monoallelic mutation does not decrease the levels of protein expression, we must wonder how can it cause pathogenesis. In the case of these two proteins (Munc18-2 and Munc13-4) that have several binding domains to other proteins, the monoallelic mutation could be affecting this binding. However, not only can cause the break of the joint, but it can create permanent interactions acting as if it were a negative dominant mutation. This would reduce the amount of wt free protein able to do the corresponding function.

During the period 2011-2019, 12 patients who met diagnostic HLH criteria were tested for cytotoxic and degranulation and three of them carried monoallelic mutations in HLH-related genes *UNC13D* and *STXBP2* (Table 13). These patients presented HLH symptoms fulfilling HLH-2004 diagnostic criteria. They were Caucasian and no consanguinity or HLH familial history was reported in any of them. NK cell cytotoxic and degranulation assays were impaired during the acute phase of disease but clearly recovered after the episode (Figure 18A). Moreover, all had a recurrence of HLH symptoms where functional defects were detected again (Figure 18B). The presenting clinical picture of these patients is very heterogeneous. However, there are some features that are remarkable. First, the reversion of degranulation and cytotoxicity assays until normalization in the follow-up after the acute HLH phase. In general, patients with homozygous or biallelic defects in HLH-related genes do not show a recovery in functional assays, therefore these results suggested patients with a sporadic or secondary HLH (Faitelson and Grunebaum 2014). Second, all patients presented disease reactivation with fulfillment of HLH-2004 diagnostic criteria and laboratory evidence of functional defects. Disease reactivation after initial remission of symptoms has been regarded as supporting the diagnosis of a primary HLH (Cetica et al. 2016). Finally, the presence of several heterozygous genetic variants in familial HLH-related genes (*UNC13D* and *STXBP2*) was shown in all the patients. In silico analyses of the structural effects of the variants indicate that most of them are probably pathogenic with a very low prevalence in the healthy population. Zang et al (K. Zhang et al. 2011) have already reported the presence of hypomorphic mutations in one or two HLH-related genes with a later onset of clinical symptoms and more indolent course of the disease. These findings are also consistent with the latest publications indicating a potential digenic or polygenic model of HLH both in mice and human (K. Zhang et al. 2014b; Cetica et al. 2016; F. E. Sepulveda et al. 2016). The evaluation of these patients opens

the question of how to assess cases with monoallelic mutations in HLH-related genes and whether we should consider these patients as an HLH high-risk group.

To address this question, we analyzed in depth the monoallelic variants in *STXBP2* and *UNC13D* genes found in patients P8, P9 and 10. Moreover, we selected and studied as well, 11 monoallelic variants in *STXBP2* gene already reported in literature.

Therefore, we started by molecularly mapping all *STXBP2* monoallelic variants in the crystal structure (PDB:4cca). Residue Alanine 433 was mapped on the cell surface and the mutation A433V was described in a patient with FHL5 with a partial secretion defect (Al Hawas et al. 2012b). From studies made in STXBP1 protein, which is crucial for the exocytosis of neurotransmitters (Ma et al. 2015) and has a high homology with STXBP2, residue A433 could be involved in important interactions with v-SNARE proteins needed for degranulation. The other 10 studied residues were located within the core of the protein Munc18-2 (**Error! No s'ha trobat l'origen de la referència.A-B**) and the mutations found on them, were predicted to disrupt the stability (**Error! No s'ha trobat l'origen de la referència.C**). This was confirmed in 3 variants (R235G, L256P and R405G) by their loss of protein expression in COS-7 lysates (Figure 20B). We suggest that these mutations cause a partial loss of *STXBP2* protein leading to the HLH phenotype seen in patients who carry *STXBP2*^{L256P} (X.-J. Xu et al. 2017) and *STXBP2*^{R405G} (Mukda et al. 2017). Patient carrying R235G (Genovese et al. 2016) was described in a patient schizophrenia and they do not report HLH phenotype.

The rest of the variants showed normal protein expression and therefore they were the most obvious candidates to cause a negative dominant effect. We analyze in depth the mutation R190C since it was described in our hospital in a 2-month-old boy with degranulation and cytotoxic defects concomitant with EBV infection. First, we asked whether Stx11 and Munc18-2 were able to bind each other and we found that *STXBP2*^{R190C} did not affect the STX11 interaction capacity. Next, based on a publication describing that *STXBP2* participates in the process of degranulation via IgE receptor (Martin-Verdeaux et al. 2003) and the fact that the homology between human and rat protein is greater than 98%, we obtained RBL-2H3 stable lines that express *STXBP2* wt-EGFP and *STXBP2* R190C-EGFP constructs.

Using this cellular model, we show that the stable RBL-H3 ***STXBP2*^{R190C} had a decreased degranulation** compared to stable RBL-H3 transfected with *STXBP2* wt-EGFP (Figure 22). The development of HLH has been described as a threshold disease which depends on the trigger and the residual cytotoxic capacity of NK and CTLs (Birthe Jessen et al. 2013). Therefore, one explanation for the normalization of the functional

activities of the patient P9, could be that the mutation **R190C in heterozygosis confers a residual NK degranulation which is enough to maintain balance in normal conditions**. However, under EBV infection, this residual activity was not able to cope with it and thus the patient developed HLH picture. Like STXBP^{R190C}, we analyzed the mutation STXBP2^{R529P} and we obtained similar results in the degranulation pattern of the stable RBL-H3 transfected with STXBP2^{R529P} in which we observed a decreased degranulation. Overall, these data strongly suggest that STXBP2^{R190C} and STXBP2^{R529P} mutations encode for a Munc18-2 protein that acts in a dominant-negative fashion by interfering with the STXBP2^{wt}.

When assessing the pathogenicity of UNC13D mutants; UNC13D^{P271S}, UNC13D^{R928C} and UNC13D^{R1075Q} found in patients P8 and P10 (*Table 10*) was carried out following a similar sequential analysis protocol than the performed for stxbp2 mutants.

There is not a crystal structure of Munc13-4 to map the mutations found in P8 and P10. Nevertheless, we located the mutants along the protein sequence (Figure 23A) revealing that mutant P271S is located at the N-terminal region and mutants R928C and R1075Q at the C-terminal region of Munc13-4 which are the binding sites for Rab27a/ Rab11 and for STX11, Vamp-8 and STX7, respectively (Brose, Rosenmund, and Rettig 2000). When analyzing the expression of the mutants (Figure 23B-C) we did not find any alteration of UNC13D levels compared to wt. Co-IP assays were also performed to assess the interaction of UNC13D mutants with partners Rab27a and STX11. Results showed that none of the mutated UNC13D proteins affected the binding with RAB27a (Figure 24A) and syntaxin 11 (Figure 24B).

Studies made in platelets from Unc13d heterozygous mice showing a reduced degranulation and therefore they demonstrated that Munc13-4 is a limiting factor at controlling the secretory pathway (Ren et al. 2010). Extrapolating this to patients P8 and P10, one likely explanation for impaired degranulation could be that the mutants block the Munc13-4 wt protein leading to a decline of free functional wt protein for degranulation.

Given that we have not test all the functional partners of Munc13-4, another explanation could be that these mutants affected the binding with other SNAREs.

Generate stable stxbpd2 knockdown cell lines to study the role of stxbp2 in cell trafficking.

HLH can be initiated by alterations in the cytolytic pathway of NK cells and CD8 lymphocytes and / or by hyperactivation of macrophages, and the involvement of one can lead to alterations in the other. In chapter number 4, we identified the involvement in intracellular trafficking of STXBP2 protein in monocytes and B lymphocytes. Defects in STXBP2 cause FLH-5, leading to an impairment of vesicle docking and fusion with the cell membrane (Spessott et al. 2017). We knockdown STXBP2 protein in THP-1 and Ramos cell lines to further comparison with WT cells.

First, we sought to elucidate whether STXBP2 has a role in monocytes intracellular trafficking by studying the marker CD103, α subunit of the $\alpha\text{E}\beta 7$ integrin. In general, integrins undergo an exocytic–endocytic cycle to control diverse cellular processes (Bridgewater, Norman, and Caswell 2012) being useful to study these pathways. Thus, using THP-1 STXBP2 knockdown cells as a model, we found a higher expression of CD103 on the cell surface in the cell line with lower expression of STXBP2 compared to WT THP-1 cells. Expression of CD103 is upregulated when monocytes undergo differentiation to macrophages and also widely expressed in the endosomal compartments of human dendritic cells as a set of dynamic bonds that recirculate through the cell membrane indicating CD103 recycling (Swain et al. 2018). However, functional role of CD103 in macrophages has been poorly investigated. According to our results, it can be thought that STXBP2 is involved in the recycling pathway of CD103, so when STXBP2 is silenced, a blocking of the recycling pathway of CD103 occurs accumulating it in the cell surface.

One of the most well-known aspects of this is that $\beta 7$ integrins are responsible for efficient trafficking and retention of lymphocytes in the intestinal immune response and during intestinal inflammation, these integrins contribute to lymphocytes recruitment and disease pathogenesis (Gorfu, Rivera-Nieves, and Ley 2009). As clinical data of FHL5 suggested a higher associated with gastrointestinal symptoms (Marie Meeths et al. 2010) we speculated that one possible contribution could be due to the accumulation of the integrin CD103 in the cell surface resulting in more infiltration into the tissues leading to the pathology but further research is needed to confirm this hypothesis.

Another marker used to study the cell membrane trafficking is the transferring receptor 1 (CD71). Generally, CD71 binds to the ferrotransferrin inducing a receptor-mediated endocytosis. Any differences were observed when CD71 was analyzed, discarding the involvement of STXBP2 in this pathway. Pathways in the intracellular membrane traffic

is interdependent and many of the compartments and protein machines are common to both(Watson 2005). However, intracellular trafficking has vesicle protein-specific to control intracellular traffic.

Second, we studied the STXBP2 silencing in B lymphocytes. We studied the upregulation of CD107a and CD69 on WT and STXBP2 K.D Ramos cells. Expression of CD69 after BCR activation showed no differences between Ramos cell lines indicating similar pattern of early activation. When analyzing the expression of CD107a in STXBP2 K.D Ramos cells upregulated less amount of CD107a after BCR activation compared to WT Ramos. During immunological synapses B cells extract and process immobilized antigens of APC cells in order to present them through MHC class II molecules. This is required for B cells to primed CD4+ T cells and, form germinal centers and to produce high-affinity antibodies(Yuseff et al. 2013). This extraction process is carried out by a physical, mechanical or chemical mechanism. In the latter case, the activated B cell polarizes granules CD107⁺ containing proteases and other components that acidify the inter-synaptic space towards the synapse facilitating proteolytic extraction of the antigen(Yuseff et al. 2011) According to our results, defect in the degranulation that we observed in the STXBP2-KD line might affect the capture and antigenic processing in B lymphocytes leading to an ineffective clearing of the antigen and less activation of B lymphocytes leading to less production of antibodies which is a characteristic feature of FHL-5 patients. However, it would be interesting to verify whether this effect on degranulation is reproduced in B lymphocytes of FHL5 patients and to reproduce the research of Yusseff et al in the Ramos cell line to confirm whether STXBP2 is important in proteolytic extraction of the B-cell antigen.

To build a free access comprehensive repository of HLH mutation data for medical research and genetic diagnosis of HLH.

To our knowledge, this database is the first one for the HLH syndrome. The HLHdb covers a broad range of data about the reported mutations in the four genes associated to primary HLH. Moreover, HLHdb shows the pathogenic prediction by bioinformatics programs (SIFT, PolyPhen-2...) and shows the published functional pathogenic evidences leading to a user interpretation of the pathogenesis of each mutation. In order to build the HLHdb, we have focused on the genes involved in the cytotoxic granule formation and release. Several mutations that cause congenital immunodeficiency syndromes and are also associated with HLH are not reported yet in this database.

The development and maintenance of HLHdb will continue periodically in order to provide up-to-date mutation information. We will add new information only when a published manuscript will support it. This free access and easy-to-use resource will facilitate the molecular testing of HLH patients and emphasizes the need of this type of disease-specific database for those professionals dealing with PIDs.

The incoming use of NGS is expanding the number of genetic mutations found in patients very quickly. Regarding the primary HLH syndrome, the implementation of the HLHdb it is hoped to help in the search of the variants/mutations in the literature and to allow the genotype-phenotype correlation.

VII. CONCLUSIONS

Conclusions to this work have been grouped according to the objectives proposed

Objective 1: Establish reference ranges and thresholds for the cytotoxicity activity and for the NK cell degranulation assays in adult and pediatric population.

- In Adults, the lower limit of normality in NK lymphocyte degranulation using K562 is 5.57% and with PHA it is 12.15%.
- In Pediatric, the lower limit of normality in NK lymphocyte degranulation using K562 is 18% and with PHA it is 37.9%.
- We established a cut-off point of 17.8% with sensitivity of 83%, and specificity of 95%.

Objective 2: Evaluation of HLH patients using functional techniques of cytotoxicity and degranulation

- During the 2011 to 2015 period, 120 patients fulfilling the HLH diagnostic criteria were tested for cytotoxic function in our immunology department. Twelve patients carried relevant mutations. Seven patients had mutations in HLH related genes (3 in PRF-1, 1 in UNC13D, 1 in STXBP2, 1 in RAB27a and 1 in LYST). Three patients presented with monoallelic variants in HLH related genes (STXP2 and UNC13D). Finally, 2 patients had mutations in other non-HLH-related genes.

Objective 3: To perform functional and molecular characterization of novel mutations found in patients diagnosed with FHL.

- We have reported the novel mutation p.L243R in *STXBP2* gene described in a patient diagnosed with FHL5.
- *In silico* analysis of the structural properties of L243 residue showed that it is in a buried site of the protein that provides anchoring between domains 2 and 3 and has contacts with previously reported mutated residues.
- The p.L243R mutation impairs *STXBP2* protein expression in transfected COS-7 cells neither in western blot from patient's PBMC.
- The residual degranulation measured via CD107a would be *STXBP2* independent triggered by PHA stimulation

Objective 4: Conduct functional and molecular characterization of novel and reported mutations found in patients diagnosed with an atypical form of HLH.

- We have reported three patients who met diagnostic HLH criteria with monoallelic mutations in HLH-related genes. A novel mutation in STXBP2 gene at exon 7 (c.568C>T / pArg190Cys). Three mutations in UNC13D, c.3224G>A /p.Arg1075Gln, c.2782C>T; p.R928C and c.811C>T; p.P271S
- All patients had a recurrence of HLH symptoms in where functional defects were detected again.
- NK cell cytotoxic and degranulation assays were impaired during the acute phase of disease but clearly recovered after the episode.
- The evaluation of these patients opens the question of how to assess cases with monoallelic mutations in HLH-related genes and whether we should consider these patients as an HLH high-risk group.
- Monoallelic variants studied here are less stable than the wild-type protein.
- Eight of the 11 STXBP2 monoallelic mutations showed similar expression to wild type protein. The 3 variants R235G, L256P and R405G showed a loss of protein expression and we suggest that these mutations cause a partial loss of *STXBP2* protein contributing in the HLH phenotype in the patients harboring these variants.
- STXBP2^{R190C} does not impaired STX11 protein binding.
- We generated RBL-2H3 stable lines that express STXBP2^{wt-EGFP} or STXBP2^{R190C-EGFP} or STXBP2^{R529P-EGFP} constructs. Using this cellular model, we have shown that the stable RBL-H3 STXBP2^{R190C} and STXBP2^{R529P} had a decreased degranulation compared to stable RBL-H3 transfected with STXBP2 wt-EGFP or un-transfected RBL-H3
- The three monoallelic mutations in UNC13D (UNC13D^{P271S}, UNC13D^{R928C} and UNC13D^{R1075Q}) showed normal protein expression level.
- UNC13D^{P271S}, UNC13D^{R928C} and UNC13D^{R1075Q} do not not impaired STX11 and Rab27a protein binding.

Objective 5: To assess functional impact of the STXBP2 silencing in macrophages and B lymphocytes cell lines.

- We reduced the STXBP2 protein expression in THP-1 and Ramos cell lines in almost 80%.

- In THP-1 STXBP2 knockdown cells we found a higher expression of CD103 which can suggest that STXBP2 is involved in the recycling pathway of CD103.
- In Ramos STXBP2 knockdown cells we found similar expression than in Ramos wild type cells of CD69 after BCR activation with anti-IgM. However, the expression of CD107a in STXBP2 K.D Ramos cells was decreased compared to Ramos wt cells.

Objective 6: To build a free access comprehensive repository of HLH mutation data for medical research and genetic diagnosis of HLH.

We have created the first database for the HLH syndrome (HLHdb: <http://hlhdb.biotoclin.org>) focusing on the genes involved in the cytotoxic granule formation and release (*PRF-1*, *UNC13D*, *STXBP2* and *STX11*)

HLHdb covers a broad range of data about the reported mutations in the four genes associated to primary HLH. Moreover, HLHdb shows the pathogenic prediction by bioinformatics programs and the published functional pathogenic evidences.

leading to a user interpretation of the pathogenesis of each mutation. In order to build the HLHdb, we have focused on the genes involved in the cytotoxic granule formation and release. Several mutations that cause congenital immunodeficiency syndromes and are also associated with HLH are not reported yet in this database.

HLHdb is a a free access and easy-to-use resource that will facilitate the molecular testing of HLH patients and emphasizes the need of this type of disease-specific database for those professionals dealing with PIDs.

VIII. BIBLIOGRAPHY

BIBLIOGRAPHY

- Abbas, L V P.a.A. K. 1998. "Homeostasis and Self-Tolerance in the Immune System: Turning Lymphocytes Off." *Science* 280: 243–48.
- Abraham, Allistair A., Haili Lang, Emily Riehm Meier, Robert S. Nickel, Marcus Dean, Nurah Lawal, Barbara Speller-Brown, Yunfei Wang, Leslie Kean, and Catherine M. Bollard. 2019. "Characterization of Natural Killer Cells Expressing Markers Associated with Maturity and Cytotoxicity in Children and Young Adults with Sickle Cell Disease." *Pediatric Blood & Cancer* 66 (5): e27601.
<https://doi.org/10.1002/pbc.27601>.
- Allen, M, C De Fusco, F Legrand, R Clementi, V Conter, C Danesino, G Janka, and M Aricò. 2001. "Familial Hemophagocytic Lymphohistiocytosis: How Late Can the Onset Be?" *Haematologica* 86 (5): 499–503.
<http://www.ncbi.nlm.nih.gov/pubmed/11410413>.
- Andersson, L C, and Gahmberg C G N. K. 1979. "K562: A Human Erythroleukemic Cell Line." *International Journal of Cancer* 23: 143–47.
- Aruffo, Alejandro. 2002. "Transient Expression of Proteins Using COS Cells." In *Current Protocols in Molecular Biology*, Chapter 16:Unit 16.12. Hoboken, NJ, USA: John Wiley & Sons, Inc. <https://doi.org/10.1002/0471142727.mb1612s60>.
- Atteritano, M, A David, G Bagnato, C Beninati, A Frisina, C Iaria, G Bagnato, and A Cascio. 2012. "Haemophagocytic Syndrome in Rheumatic Patients. A Systematic Review." *European Review for Medical and Pharmacological Sciences* 16 (10): 1414–24. <http://www.ncbi.nlm.nih.gov/pubmed/23104659>.
- Beal, A M.e.a. 2008. "Protein Kinase C Regulates Stability of the Peripheral Adhesion Ring Junction and Contributes to the Sensitivity of Target Cell Lysis by CTL." *Journal of Immunology* 18: 4815.
- Bendelac, A, Park Sh R. M., and Roark JH. 1997. "Mouse CD1-Specific NK1 T Cells: Development, Specificity, and Function." *Annual Review of Immunology* 15: 535–62.
- Bode, Sebastian FN, Kai Lehmborg, Andrea Maul-Pavicic, Thomas Vraetz, Gritta Janka, Udo zur Stadt, and Stephan Ehl. 2012. "Recent Advances in the Diagnosis and Treatment of Hemophagocytic Lymphohistiocytosis." *Arthritis Research & Therapy* 14 (3): 213. <https://doi.org/10.1186/AR3843>.

- Bonilla, Francisco A., and Hans C. Oettgen. 2010. "Adaptive Immunity." *Journal of Allergy and Clinical Immunology* 125 (2): S33–40.
<https://doi.org/10.1016/j.jaci.2009.09.017>.
- Bots, Michael, and Jan Paul Medema. 2006. "Granzymes at a Glance." *Journal of Cell Science* 119 (Pt 24): 5011–14. <https://doi.org/10.1242/jcs.03239>.
- Bridgewater, Rebecca E., Jim C. Norman, and Patrick T. Caswell. 2012. "Integrin Trafficking at a Glance." *Journal of Cell Science* 125 (16): 3695.
<https://doi.org/10.1242/JCS.095810>.
- Brisse, Ellen, Carine H Wouters, and Patrick Matthys. 2016. "Advances in the Pathogenesis of Primary and Secondary Haemophagocytic Lymphohistiocytosis: Differences and Similarities." <https://doi.org/10.1111/bjh.14147>.
- Brose, N, C Rosenmund, and J Rettig. 2000. "Regulation of Transmitter Release by Unc-13 and Its Homologues." *Current Opinion in Neurobiology* 10 (3): 303–11.
<http://www.ncbi.nlm.nih.gov/pubmed/10851170>.
- Bryceson, Y. T., E. Rudd, C. Zheng, J. Edner, D. Ma, S. M. Wood, A. G. Bechensteen, et al. 2007. "Defective Cytotoxic Lymphocyte Degranulation in Syntaxin-11-Deficient Familial Hemophagocytic Lymphohistiocytosis 4 (FHL4) Patients." *Blood* 110 (6): 1906–15. <https://doi.org/10.1182/blood-2007-02-074468>.
- Bryceson, Yenan T. 2012. "Lymphocyte Cytotoxicity: Tug-of-War on Microtubules." *BLOOD* 119: 3873–75.
- Bryceson, Yenan T., Michael E. March, Hans-Gustaf Ljunggren, and Eric O. Long. 2006. "Synergy among Receptors on Resting NK Cells for the Activation of Natural Cytotoxicity and Cytokine Secretion." *Blood* 107 (1): 159–66.
<https://doi.org/10.1182/blood-2005-04-1351>.
- Bryceson, Yenan T, Daniela Pende, Andrea Maul-Pavicic, Kimberly C Gilmour, Heike Ufheil, Thomas Vraetz, Samuel C Chiang, et al. 2012. "A Prospective Evaluation of Degranulation Assays in the Rapid Diagnosis of Familial Hemophagocytic Syndromes." *Blood* 119 (12): 2754–63. <https://doi.org/10.1182/blood-2011-08-374199>.
- Canna, Scott W, Adriana A de Jesus, Sushanth Gouni, Stephen R Brooks, Bernadette Marrero, Yin Liu, Michael A DiMattia, et al. 2014. "An Activating NLR4 Inflammasome Mutation Causes Autoinflammation with Recurrent Macrophage

- Activation Syndrome.” *Nature Genetics* 46 (10): 1140–46.
<https://doi.org/10.1038/ng.3089>.
- Cetica, Valentina, Elena Sieni, Daniela Pende, Cesare Danesino, Carmen De Fusco, Franco Locatelli, Concetta Micalizzi, et al. 2016. “Genetic Predisposition to Hemophagocytic Lymphohistiocytosis: Report on 500 Patients from the Italian Registry.” *The Journal of Allergy and Clinical Immunology* 137 (1): 188–96.
<https://doi.org/10.1016/j.jaci.2015.06.048>.
- Chiang, Samuel Cern Cher, Jack J. Bleesing, and Rebecca A. Marsh. 2019. “Current Flow Cytometric Assays for the Screening and Diagnosis of Primary HLH.” *Frontiers in Immunology* 10 (July): 1740.
<https://doi.org/10.3389/fimmu.2019.01740>.
- Côte, Marjorie, Mickaël M Ménager, Agathe Burgess, Nizar Mahlaoui, Capucine Picard, Catherine Schaffner, Fahad Al-Manjomi, et al. 2009. “Munc18-2 Deficiency Causes Familial Hemophagocytic Lymphohistiocytosis Type 5 and Impairs Cytotoxic Granule Exocytosis in Patient NK Cells.” *The Journal of Clinical Investigation* 119 (12): 3765–73. <https://doi.org/10.1172/JCI40732>.
- Dotta, Laura, Silvia Parolini, Alberto Prandini, Giovanna Tabellini, Maddalena Antolini, Stephen F Kingsmore, and Raffaele Badolato. 2013. “Clinical, Laboratory and Molecular Signs of Immunodeficiency in Patients with Partial Oculo-Cutaneous Albinism.” *Orphanet Journal of Rare Diseases* 8 (1): 168.
<https://doi.org/10.1186/1750-1172-8-168>.
- Enders, Anselm, Klaus Schwarz B. Z., Ayami Yoshimi, Carsten Speckmann, Eva-Maria Knoepfle, Udo Kontny, Christoph Müller, et al. 2006. “Lethal Hemophagocytic Lymphohistiocytosis in Hermansky-Pudlak Syndrome Type II.” *BLOOD* 108: 81–87.
- Eskelinen, E.-L. 2006. “Roles of LAMP-1 and LAMP-2 in Lysosome Biogenesis and Autophagy.” *Molecular Aspects of Medicine* 27: 465–502.
- Esmaeilzadeh, Hossein, Mohammad Hasan Bemanian, Mohammad Nabavi, Saba Arshi, Morteza Fallahpour, Ilka Fuchs, Udo zur Stadt, et al. 2015. “Novel Patient with Late-Onset Familial Hemophagocytic Lymphohistiocytosis with STXP2 Mutations Presenting with Autoimmune Hepatitis, Neurological Manifestations and Infections Associated with Hypogammaglobulinemia.” *Journal of Clinical Immunology*. <https://doi.org/10.1007/s10875-014-0119-z>.

- Faitelson, Yoram, and Eyal Grunebaum. 2014. "Hemophagocytic Lymphohistiocytosis and Primary Immune Deficiency Disorders." *Clinical Immunology* 155 (1): 118–25. <https://doi.org/10.1016/j.clim.2014.09.008>.
- Farquhar, J w, and A e Claireaux. 1952. "Familial Haemophagocytic Reticulosis." *Archives of Disease in Childhood* 27 (136): 519–25. <http://www.ncbi.nlm.nih.gov/pubmed/13008468>.
- Feldmann, J et al. 2005. "Severe and Progressive Encephalitis as a Presenting Manifestation of a Novel Missense Perforin Mutation and Impaired Cytolytic Activity." *BLOOD* 1 (105): 7.
- Feldmann, Jérôme, Isabelle Callebaut, Graça Raposo, Stéphanie Certain, Delphine Bacq, Cécile Dumont, Nathalie Lambert, et al. 2003. "Munc13-4 Is Essential for Cytolytic Granules Fusion and Is Mutated in a Form of Familial Hemophagocytic Lymphohistiocytosis (FHL3)." *Cell* 115 (4): 461–73. <http://www.ncbi.nlm.nih.gov/pubmed/14622600>.
- Gao, Lili, Lijun Zhu, Liang Huang, and Jianfeng Zhou. 2015. "Synergistic Defects of UNC13D and AP3B1 Leading to Adult Hemophagocytic Lymphohistiocytosis." *International Journal of Hematology* 102 (4): 488–92. <https://doi.org/10.1007/s12185-015-1807-z>.
- Genovese, Giulio, Menachem Fromer, Eli A Stahl, Douglas M Ruderfer, Kimberly Chambert, Mikael Landén, Jennifer L Moran, et al. 2016. "Increased Burden of Ultra-Rare Protein-Altering Variants among 4,877 Individuals with Schizophrenia." *Nature Neuroscience* 19 (11): 1433–41. <https://doi.org/10.1038/nn.4402>.
- George, Melissa R. 2014a. "Hemophagocytic Lymphohistiocytosis: Review of Etiologies and Management." *Journal of Blood Medicine* 5: 69–86. <https://doi.org/10.2147/JBM.S46255>.
- . 2014b. "Hemophagocytic Lymphohistiocytosis: Review of Etiologies and Management." *Journal of Blood Medicine* 5: 69–86. <https://doi.org/10.2147/JBM.S46255>.
- Gong, Hai'e, Haicang Zhang, Jianwei Zhu, Chao Wang, Shiwei Sun, Wei-Mou Zheng, and Dongbo Bu. 2017. "Improving Prediction of Burial State of Residues by Exploiting Correlation among Residues." *BMC Bioinformatics* 18 (Suppl 3): 70. <https://doi.org/10.1186/s12859-017-1475-5>.

- Göransdotter Ericson, Kim, Bengt Fadeel, Sofie Nilsson-Ardnor, Cilla Söderhäll, AnnaCarin Samuelsson, Gritta Janka, Marion Schneider, et al. 2001. "Spectrum of Perforin Gene Mutations in Familial Hemophagocytic Lymphohistiocytosis." *The American Journal of Human Genetics* 68 (3): 590–97. <https://doi.org/10.1086/318796>.
- Gorfu, G, J Rivera-Nieves, and K Ley. 2009. "Role of Beta7 Integrins in Intestinal Lymphocyte Homing and Retention." *Current Molecular Medicine* 9 (7): 836–50. <http://www.ncbi.nlm.nih.gov/pubmed/19860663>.
- Gounder, Sellamuthu Subbanna, Basri Johan Jeet Abdullah, Nur Ezzati Izyan Binti Mohd Radzuanb, Farah Dalila Binti Mohd Zain, Nurhidayah Bt Mohamad Sait, Corine Chua, and Baskar Subramani. 2018. "Effect of Aging on NK Cell Population and Their Proliferation at Ex Vivo Culture Condition." *Analytical Cellular Pathology (Amsterdam)* 2018: 7871814. <https://doi.org/10.1155/2018/7871814>.
- Hackmann, Y., S. C. Graham, S. Ehl, S. Honing, K. Lehmborg, M. Arico, D. J. Owen, and G. M. Griffiths. 2013. "Syntaxin Binding Mechanism and Disease-Causing Mutations in Munc18-2." *Proceedings of the National Academy of Sciences* 110 (47): E4482–91. <https://doi.org/10.1073/pnas.1313474110>.
- Hawas, Rania Al, Qiansheng Ren, Shaojing Ye, Zubair A. Karim, Alexandra H. Filipovich, and Sidney W. Whiteheart. 2012a. "Munc18b/STXBP2 Is Required for Platelet Secretion." *Blood* 120 (12): 2493–2500. <https://doi.org/10.1182/blood-2012-05-430629>.
- Hawas, Rania Al, Qiansheng Ren, Shaojing Ye, Zubair A Karim, Alexandra H Filipovich, and Sidney W Whiteheart. 2012b. "Munc18b/STXBP2 Is Required for Platelet Secretion." *Blood* 120 (12): 2493–2500. <https://doi.org/10.1182/blood-2012-05-430629>.
- Hazeldine, Jon, and Janet M Lord. 2013. "The Impact of Ageing on Natural Killer Cell Function and Potential Consequences for Health in Older Adults." *Ageing Research Reviews* 12 (4): 1069–78. <https://doi.org/10.1016/j.arr.2013.04.003>.
- Henter, J I, M Aricò, G Elinder, S Imashuku, and G Janka. 1998. "Familial Hemophagocytic Lymphohistiocytosis. Primary Hemophagocytic Lymphohistiocytosis." *Hematology/Oncology Clinics of North America* 12 (2): 417–33. <http://www.ncbi.nlm.nih.gov/pubmed/9561910>.
- Henter, J I, A Ehrnst, J Andersson, and G Elinder. 1993. "Familial Hemophagocytic

- Lymphohistiocytosis and Viral Infections.” *Acta Paediatrica (Oslo, Norway: 1992)* 82 (4): 369–72. <http://www.ncbi.nlm.nih.gov/pubmed/8391350>.
- Henter, J I, G Elinder, O Söder, and A Ost. 1991. “Incidence in Sweden and Clinical Features of Familial Hemophagocytic Lymphohistiocytosis.” *Acta Paediatrica Scandinavica* 80 (4): 428–35. <http://www.ncbi.nlm.nih.gov/pubmed/2058392>.
- Henter, Jan-Inge, Annacarin Horne, Maurizio Aricó, R Maarten Egeler, Alexandra H Filipovich, Shinsaku Imashuku, Stephan Ladisch, et al. 2007. “HLH-2004: Diagnostic and Therapeutic Guidelines for Hemophagocytic Lymphohistiocytosis.” *Pediatric Blood & Cancer* 48 (2): 124–31. <https://doi.org/10.1002/pbc.21039>.
- Hines, Melissa R, and Kim E Nichols. 2017. “Go with the Flow: Perforin and CD107a in HLH.” *Blood* 129 (22): 2954–55. <https://doi.org/10.1182/blood-2017-04-773192>.
- Hong, W. 2005. “Cytotoxic T Lymphocyte Exocytosis: Bring on the SNAREs!” *Trends in Cell Biology* 15: 644–50.
- Horne, AnnaCarin, Kim Göransdotter Ramme, Eva Rudd, Chengyun Zheng, Yasser Wali, Zakia al-Lamki, Aytemiz Gürgey, Nevin Yalman, Magnus Nordenskjöld, and Jan-Inge Henter. 2008. “Characterization of *PRF1*, *STX11* and *UNC13D* Genotype-Phenotype Correlations in Familial Hemophagocytic Lymphohistiocytosis.” *British Journal of Haematology* 143 (1): 75–83. <https://doi.org/10.1111/j.1365-2141.2008.07315.x>.
- Hotchkiss, R S, Knudson Cm S. P., K C Chang, J P Cobb, D F Osborne, K M Zollner, T G Buchman, S J Korsmeyer, and Karl IE. 1999. “Overexpression of Bcl-2 in Transgenic Mice Decreases Apoptosis and Improves Survival in Sepsis.” *Journal of Immunology* 162 (7): 4148–56.
- Huang, Lufen, Jiang Pi, Jianlin Wu, Hua Zhou, Jiye Cai, Ting Li, and Liang Liu. 2016. “A Rapid and Sensitive Assay Based on Particle Analysis for Cell Degranulation Detection in Basophils and Mast Cells.” *Pharmacological Research* 111 (September): 374–83. <https://doi.org/10.1016/J.PHRS.2016.05.033>.
- Huck, Kirsten, Oliver Feyen, Tim Niehues, Franz Rüschemdorf, Norbert Hübner, Hans-Jürgen Laws, Tanja Telleps, et al. 2009. “Girls Homozygous for an IL-2-Inducible T Cell Kinase Mutation That Leads to Protein Deficiency Develop Fatal EBV-Associated Lymphoproliferation.” *Journal of Clinical Investigation* 119 (5): 1350–58. <https://doi.org/10.1172/JCI37901>.

- Ishii, Eiichi. 2016. "Hemophagocytic Lymphohistiocytosis in Children: Pathogenesis and Treatment." *Frontiers in Pediatrics* 4 (May): 47.
<https://doi.org/10.3389/fped.2016.00047>.
- Janka, Gritta E, and Kai Lehmsberg. 2014. "Hemophagocytic Syndromes — An Update." *YBLRE* 28: 135–42. <https://doi.org/10.1016/j.blre.2014.03.002>.
- Jessen, B., S. F. N. Bode, S. Ammann, S. Chakravorty, G. Davies, J. Diestelhorst, M. Frei-Jones, et al. 2013. "The Risk of Hemophagocytic Lymphohistiocytosis in Hermansky-Pudlak Syndrome Type 2." *Blood* 121 (15): 2943–51.
<https://doi.org/10.1182/blood-2012-10-463166>.
- Jessen, Birthe, Tamara Kögl, Fernando E. Sepulveda, Genevieve de Saint Basile, Peter Aichele, and Stephan Ehl. 2013. "Graded Defects in Cytotoxicity Determine Severity of Hemophagocytic Lymphohistiocytosis in Humans and Mice." *Frontiers in Immunology* 4: 448. <https://doi.org/10.3389/fimmu.2013.00448>.
- Johnson, Theodore S., Joyce Villanueva, Alexandra H. Filipovich, Rebecca A. Marsh, and Jack J. Bleesing. 2011. "Contemporary Diagnostic Methods for Hemophagocytic Lymphohistiocytic Disorders." *Journal of Immunological Methods* 364 (1–2): 1–13. <https://doi.org/10.1016/j.jim.2010.11.006>.
- Jordan, Michael B., Carl E. Allen, Jay Greenberg, Michael Henry, Michelle L. Hermiston, Ashish Kumar, Melissa Hines, et al. 2019. "Challenges in the Diagnosis of Hemophagocytic Lymphohistiocytosis: Recommendations from the North American Consortium for Histiocytosis (NACHO)." *Pediatric Blood & Cancer*, no. June: 1–12. <https://doi.org/10.1002/pbc.27929>.
- Jordan, Michael B, Carl E Allen, Sheila Weitzman, Alexandra H Filipovich, and Kenneth L McClain. 2011. "How I Treat Hemophagocytic Lymphohistiocytosis." *Blood* 118 (15): 4041–52. <https://doi.org/10.1182/blood-2011-03-278127>.
- Jourdan, M, Mechti N D. V. J., and B Klein. 2000. "Regulation of Bcl-2-Family Proteins in Myeloma Cells by Three Myeloma Survival Factors: Interleukin-6, Interferon-Alpha and Insulin-like Growth Factor 1." *Cell Death and Deifferentiation* 7 (12): 1244–52.
- Kaczorowski, Kevin J, Karthik Shekhar, Dieudonné Nkulikiyimfura, Cornelia L Dekker, Holden Maecker, Mark M Davis, Arup K Chakraborty, and Petter Brodin. 2017. "Continuous Immunotypes Describe Human Immune Variation and Predict Diverse Responses." *Proceedings of the National Academy of Sciences of the*

- United States of America* 114 (30): E6097–6106.
<https://doi.org/10.1073/pnas.1705065114>.
- Kägi, David, Bernhard Odermatt, and Tak W. Mak. 1999. “Homeostatic Regulation of CD8+ T Cells by Perforin.” *European Journal of Immunology* 29 (10): 3262–72.
[https://doi.org/10.1002/\(SICI\)1521-4141\(199910\)29:10<3262::AID-IMMU3262>3.0.CO;2-A](https://doi.org/10.1002/(SICI)1521-4141(199910)29:10<3262::AID-IMMU3262>3.0.CO;2-A).
- Koch, Henriette, Kay Hofmann, and Nils Brose. 2000. “Definition of Munc13-Homology-Domains and Characterization of a Novel Ubiquitously Expressed Munc13 Isoform.” *Biochemical Journal* 349 (1): 247. <https://doi.org/10.1042/0264-6021:3490247>.
- Law, Ruby H P, Natalya Lukoyanova, Iliia Voskoboinik, Tom T Caradoc-davies, Katherine Baran, Sandra Verschoor, Kylie A Browne, et al. 2010. “The Structural Basis for Membrane Binding and Pore Formation by Lymphocyte Perforin,” no. V: 4–10. <https://doi.org/10.1038/nature09518>.
- Lehmberg, Kai, Kim E Nichols, Jan-Inge Henter, Michael Girschikofsky, Tatiana Greenwood, Michael Jordan, Ashish Kumar, et al. 2015. “Consensus Recommendations for the Diagnosis and Management of Hemophagocytic Lymphohistiocytosis Associated with Malignancies.” *Haematologica* 100 (8): 997–1004. <https://doi.org/10.3324/haematol.2015.123562>.
- Liu, Chau-ching, Craig M Walsh, and John Ding-e Young. 1995. “Perforin : Structure and Function.”
- Loo, L S, Ong Ym H. L., H S Tay, C C Wang, and W Hong. 2009. “A Role for Endobrevin/VAMP8 in CTL Lytic Granule Exocytosis.” *European Journal of Immunology* 39 (12): 3520–28.
- Lopez, Jamie A., Tahereh Noori, Adrian Minson, Lu Li Jovanoska, Kevin Thia, Michael S. Hildebrand, Hedieh Akhlaghi, et al. 2018. “Bi-Allelic Mutations in STXBP2 Reveal a Complementary Role for STXBP1 in Cytotoxic Lymphocyte Killing.” *Frontiers in Immunology* 9 (MAR). <https://doi.org/10.3389/fimmu.2018.00529>.
- Lozano, Maria L, Jose Rivera, Isabel Sánchez-Guiu, and Vicente Vicente. 2014. “Towards the Targeted Management of Chediak-Higashi Syndrome.” *Orphanet Journal of Rare Diseases* 9. <https://doi.org/10.1186/S13023-014-0132-6>.
- Luetke-Eversloh, Merlin, Monica Killig, and Chiara Romagnani. 2013. “Signatures of

- Human NK Cell Development and Terminal Differentiation.” *Frontiers in Immunology* 4 (December): 499. <https://doi.org/10.3389/fimmu.2013.00499>.
- Luzio, J. Paul, Yvonne Hackmann, Nele M.G. Dieckmann, and Gillian M. Griffiths. 2014. “The Biogenesis of Lysosomes and Lysosome-Related Organelles.” *Cold Spring Harbor Perspectives in Biology* 6 (9). <https://doi.org/10.1101/CSHPERSPECT.A016840>.
- Lyu, Xiaodong, Zhen Guo, Yangwei Li, Ruihua Fan, and Yongping Song. 2018. “Identification of a Novel Nonsense Mutation in SH2D1A in a Patient with X-Linked Lymphoproliferative Syndrome Type 1: A Case Report.” *BMC Medical Genetics* 19 (1): 1–5. <https://doi.org/10.1186/s12881-018-0576-y>.
- Ma, Lu, Aleksander A Rebane, Guangcan Yang, Zhiqun Xi, Yuhao Kang, Ying Gao, and Yongli Zhang. 2015. “Munc18-1-Regulated Stage-Wise SNARE Assembly Underlying Synaptic Exocytosis.” *ELife* 4 (December). <https://doi.org/10.7554/eLife.09580>.
- Machaczka, Maciej. 2013. “Hemophagocytic Lymphohistiocytosis in Adults.” *Upsala Journal of Medical Sciences* 118 (3): 201–3. <https://doi.org/10.3109/03009734.2013.795634>.
- Madkaikar, Manisha, Snehal Shabrish, and Mukesh Desai. 2016. “Current Updates on Classification, Diagnosis and Treatment of Hemophagocytic Lymphohistiocytosis (HLH).” *The Indian Journal of Pediatrics* 83 (5): 434–43. <https://doi.org/10.1007/s12098-016-2037-y>.
- Marcenaro, S., Federico Gallo, Stefania Martini, Alessandra Santoro, Gillian M Griffiths, Maurizio Aricó, Lorenzo Moretta, and Daniela Pende. 2006. “Analysis of Natural Killer-Cell Function in Familial Hemophagocytic Lymphohistiocytosis (FHL): Defective CD107a Surface Expression Heralds Munc13-4 Defect and Discriminates between Genetic Subtypes of the Disease.” *Blood* 108 (7): 2316–23. <https://doi.org/10.1182/blood-2006-04-015693>.
- Marsh, R. A., L. Madden, B. J. Kitchen, R. Mody, B. McClimon, M. B. Jordan, J. J. Bleesing, K. Zhang, and A. H. Filipovich. 2010. “XIAP Deficiency: A Unique Primary Immunodeficiency Best Classified as X-Linked Familial Hemophagocytic Lymphohistiocytosis and Not as X-Linked Lymphoproliferative Disease.” *Blood* 116 (7): 1079–82. <https://doi.org/10.1182/blood-2010-01-256099>.
- Marshall, Jean S., Richard Warrington, Wade Watson, and Harold L. Kim. 2018. “An

- Introduction to Immunology and Immunopathology.” *Allergy, Asthma & Clinical Immunology* 14 (S2): 49. <https://doi.org/10.1186/s13223-018-0278-1>.
- Martin-Verdeaux, S., Isabel Pombo, Bruno Iannascoli, Michèle Roa, Nadine Varin-Blank, Juan Rivera, and Ulrich Blank. 2003. “Evidence of a Role for Munc18-2 and Microtubules in Mast Cell Granule Exocytosis.” *Journal of Cell Science* 116 (2): 325–34. <https://doi.org/10.1242/jcs.00216>.
- Mathieu Kurowska N.G., Nadine T Nehme Magali Court Jérôme Garin Alain Fischer Geneviève de Saint Basile, and Gaël Ménasché. 2012. “Terminal Transport of Lytic Granules to the Immune Synapse Is Mediated by the Kinesin-1/Slp3/Rab27a Complex.” *BLOOD* 119: 3879–89.
- McCusker, Christine, Julia Upton, and Richard Warrington. 2018. “Primary Immunodeficiency.” *Allergy, Asthma, and Clinical Immunology: Official Journal of the Canadian Society of Allergy and Clinical Immunology* 14 (Suppl 2): 61. <https://doi.org/10.1186/s13223-018-0290-5>.
- Meeths, M, Rudd E B. Y., C Zheng, S M Wood, K Ramme, K Beutel, H Hasle, et al. 2010. “Clinical Presentation of Griscelli Syndrome Type 2 and Spectrum of RAB27A Mutations.” *Pediatric Blood and Cancer* 54 (4): 563–72.
- Meeths, Marie, Miriam Entesarian, Waleed Al-Herz, Samuel C.C. Chiang, Stephanie M. Wood, Wafa Al-Ateeqi, Francisco Almazan, et al. 2010. “Spectrum of Clinical Presentations in Familial Hemophagocytic Lymphohistiocytosis Type 5 Patients with Mutations in STXBP2.” *Blood* 116 (15): 2635–43. <https://doi.org/10.1182/blood-2010-05-282541>.
- Ménager, Mickaël M, Gaël Ménasché, Maryse Romao, Perrine Knapnougel, Chen-Hsuan Ho, Mériem Garfa, Graça Raposo, Jérôme Feldmann, Alain Fischer, and Geneviève de Saint Basile. 2007. “Secretory Cytotoxic Granule Maturation and Exocytosis Require the Effector Protein HMunc13-4.” *Nature Immunology* 8 (3): 257–67. <https://doi.org/10.1038/ni1431>.
- Ménasché, Gaël, Elodie Pastural, Jérôme Feldmann, Stéphanie Certain, Fügen Ersoy, Sophie Dupuis, Nico Wulffraat, et al. 2000. “Mutations in RAB27A Cause Griscelli Syndrome Associated with Haemophagocytic Syndrome.” *Nature Genetics* 25 (2): 173–76. <https://doi.org/10.1038/76024>.
- Morimoto, Akira, Yozo Nakazawa, and Eiichi Ishii. 2016. “Hemophagocytic Lymphohistiocytosis: Pathogenesis, Diagnosis, and Management.” *Pediatrics*

- International* 58 (9): 817–25. <https://doi.org/10.1111/ped.13064>.
- Mukda, Ekchol, Objoon Trachoo, Ekawat Pasomsub, Rawiphorn Tiyasirichokchai, Nareenart Iemwimangsa, Darintr Sosothikul, Wasun Chantratita, and Samart Pakakasama. 2017. “Exome Sequencing for Simultaneous Mutation Screening in Children with Hemophagocytic Lymphohistiocytosis.” *International Journal of Hematology* 106 (2): 282–90. <https://doi.org/10.1007/s12185-017-2223-3>.
- Nagai, Kozo, Fumihiko Ochi, Kiminori Terui, Miho Maeda, Shouichi Ohga, Hirokazu Kanegane, Toshiyuki Kitoh, et al. 2013. “Clinical Characteristics and Outcomes of Chédiak-Higashi Syndrome: A Nationwide Survey of Japan.” *Pediatric Blood & Cancer* 60 (10): 1582–86. <https://doi.org/10.1002/psc.24637>.
- Nagle, Deborah L., Mohammad A. Karim, Elizabeth A. Woolf, Lisa Holmgren, Peer Bork, Donald J. Misumi, Sonja H. McGrail, et al. 1996. “Identification and Mutation Analysis of the Complete Gene for Chediak–Higashi Syndrome.” *Nature Genetics* 14 (3): 307–11. <https://doi.org/10.1038/ng1196-307>.
- Nicholson, Lindsay B. 2016. “The Immune System.” *Essays in Biochemistry* 60 (3): 275. <https://doi.org/10.1042/EBC20160017>.
- Niece, J Allyson, Zora R Rogers, Naveed Ahmad, Anne-Marie Langevin, and Kenneth L McClain. 2010. “Hemophagocytic Lymphohistiocytosis in Texas: Observations on Ethnicity and Race.” *Pediatric Blood & Cancer* 54 (3): 424–28. <https://doi.org/10.1002/psc.22359>.
- Ohadi, M, M R Lalloz, P Sham, J Zhao, A M Dearlove, C Shiach, S Kinsey, M Rhodes, and D M Layton. 1999. “Localization of a Gene for Familial Hemophagocytic Lymphohistiocytosis at Chromosome 9q21.3-22 by Homozygosity Mapping.” *American Journal of Human Genetics*. <https://doi.org/10.1086/302187>.
- Orange, J S. 2008. “Formation and Function of the Lytic NK-Cell Immunological Synapse.” *Nature Reviews Immunology* 8: 713–25.
- Pagel, Julia, Karin Beutel, Kai Lehmborg, Florian Koch, Andrea Maul-Pavicic, Anna-Katharina Rohlf, Abdullah Al-Jefri, Rita Beier, Lilian Bomme Ousager, et al. 2012. “Distinct Mutations in STXBP2 Are Associated with Variable Clinical Presentations in Patients with Familial Hemophagocytic Lymphohistiocytosis Type 5 (FHL5).” *Blood* 119 (25): 6016–24. <https://doi.org/10.1182/blood-2011-12-398958>.
- Pagel, Julia, Karin Beutel, Kai Lehmborg, Florian Koch, Andrea Maul-Pavicic, Anna

- Katharina Rohlf, Abdullah Al-Jefri, Rita Beier, Lilian Bomme Ousager, et al. 2012. "Distinct Mutations in STXBP2 Are Associated with Variable Clinical Presentations in Patients with Familial Hemophagocytic Lymphohistiocytosis Type 5 (FHL5)." *Blood* 119 (25): 6016–24. <https://doi.org/10.1182/blood-2011-12-398958>.
- Payne, Susan, and Susan Payne. 2017. "Immunity and Resistance to Viruses." *Viruses*, January, 61–71. <https://doi.org/10.1016/B978-0-12-803109-4.00006-4>.
- Perera, Suneth S, and Nitin K Saksena. 2012. "Innate, Adaptive and Intrinsic Immunity in Human Immunodeficiency Virus Infection." *American Journal of Infectious Diseases* 8 (3): 132–48. <https://doi.org/10.3844/ajidsp.2012.132.148>.
- Picard, Capucine, Waleed Al-Herz, Aziz Bousfiha, Jean-Laurent Casanova, Talal Chatila, Mary Ellen Conley, Charlotte Cunningham-Rundles, et al. 2015. "Primary Immunodeficiency Diseases: An Update on the Classification from the International Union of Immunological Societies Expert Committee for Primary Immunodeficiency 2015." *Journal of Clinical Immunology* 35 (8): 696–726. <https://doi.org/10.1007/s10875-015-0201-1>.
- Pilla, Esther, Kim Schneider, and Anne Bertolotti. 2017. "Coping with Protein Quality Control Failure." *Annual Review of Cell and Developmental Biology*. <https://doi.org/10.1146/annurev-cellbio-111315-125334>.
- Qian, Yaping, Judith A. Johnson, Jessica A. Connor, C. Alexander Valencia, Nathaniel Barasa, Jeffery Schubert, Ammar Husami, et al. 2014. "The 253-Kb Inversion and Deep Intronic Mutations in *UNC13D* Are Present in North American Patients with Familial Hemophagocytic Lymphohistiocytosis 3." *Pediatric Blood & Cancer* 61 (6): 1034–40. <https://doi.org/10.1002/pbc.24955>.
- Ramos-Casals, Manuel, Pilar Brito-Zerón, Armando López-Guillermo, Munther A Khamashta, and Xavier Bosch. 2014. "Adult Haemophagocytic Syndrome." *Lancet (London, England)* 383 (9927): 1503–16. [https://doi.org/10.1016/S0140-6736\(13\)61048-X](https://doi.org/10.1016/S0140-6736(13)61048-X).
- Ren, Qiansheng, Christian Wimmer, Michael C Chicka, Shaojing Ye, Yi Ren, Frederick M Hughson, and Sidney W Whiteheart. 2010. "Munc13-4 Is a Limiting Factor in the Pathway Required for Platelet Granule Release and Hemostasis." *Blood* 116 (6): 869–77. <https://doi.org/10.1182/blood-2010-02-270934>.
- Rigaud, Stéphanie, Nathalie Lambert M.-C. F., Benoit Pasquier, Véronique Mateo,

- Pauline Soulas, Lionel Galicier, Françoise Le Deist, Frédéric Rieux-Laucat, Patrick Revy, and Geneviève de Saint Basile & Sylvain Latour Alain Fischer. 2006. "XIAP Deficiency in Humans Causes an X-Linked Lymphoproliferative Syndrome." *Nature* 444:(7115): 110–14.
- Rohr, Jan, Karin Beutel, Andrea Maul-Pavicic, Thomas Vraetz, Jens Thiel, Klaus Warnatz, Ilka Bondzio, et al. 2010. "Atypical Familial Hemophagocytic Lymphohistiocytosis Due to Mutations in UNC13D and STXBP2 Overlaps with Primary Immunodeficiency Diseases." *Haematologica*.
<https://doi.org/10.3324/haematol.2010.029389>.
- Romberg, Neil, Khatoun Al Moussawi, Carol Nelson-Williams, Amy L Stiegler, Erin Loring, Murim Choi, John Overton, et al. 2014. "Mutation of NLRC4 Causes a Syndrome of Enterocolitis and Autoinflammation." *Nature Genetics* 46 (10): 1135–39. <https://doi.org/10.1038/ng.3066>.
- Rubin, Tamar S, Kejian Zhang, Carrie Gifford, Adam Lane, Sharon Choo, Jack J Bleesing, and Rebecca A Marsh. 2017. "Perforin and CD107a Testing Is Superior to NK Cell Function Testing for Screening Patients for Genetic HLH." *Blood* 129 (22): 2993–99. <https://doi.org/10.1182/blood-2016-12-753830>.
- Saint Basile, Geneviève de, and G. M.a.A. F. 2010. "Molecular Mechanisms of Biogenesis and Exocytosis of Cytotoxic Granules." *Nature Reviews Immunology* 11: 568–79.
- Saint Basile, Geneviève de, Gaël Ménasché, and Alain Fischer. 2010. "Molecular Mechanisms of Biogenesis and Exocytosis of Cytotoxic Granules." *Nature Reviews Immunology* 10 (8): 568–79. <https://doi.org/10.1038/nri2803>.
- Saint Basile, Geneviève de, Fernando E. Sepulveda, Sophia Maschalidi, and Alain Fischer. 2015a. "Cytotoxic Granule Secretion by Lymphocytes and Its Link to Immune Homeostasis." *F1000Research* 4 (F1000 Faculty Rev): 930.
<https://doi.org/10.12688/f1000research.6754.1>.
- Saint Basile, Geneviève de, Fernando E Sepulveda, Sophia Maschalidi, and Alain Fischer. 2015b. "Cytotoxic Granule Secretion by Lymphocytes and Its Link to Immune Homeostasis." *F1000Research* 4 (F1000 Faculty Rev): 930.
<https://doi.org/10.12688/f1000research.6754.1>.
- Saltzman, R.W., L. Monaco-Shawver, K.E. Sullivan, and J.S. Orange. 2011. "Novel

- Mutation in Syntaxin-Binding Protein 2 (STXBP2) in Familial Hemophagocytic Lymphohistiocytosis Type 5 (FHL-5) Prevents IL-2-Induced Natural Killer Cell Cytotoxicity and Degranulation.” *Journal of Allergy and Clinical Immunology* 127 (2): AB89–AB89. <https://doi.org/10.1016/j.jaci.2010.12.359>.
- Schymkowitz, Joost, Jesper Borg, Francois Stricher, Robby Nys, Frederic Rousseau, and Luis Serrano. 2005. “The FoldX Web Server: An Online Force Field.” *Nucleic Acids Research* 33 (SUPPL. 2). <https://doi.org/10.1093/nar/gki387>.
- Scott R, Robb-Smith A. 1939. “Histiocytic Medullary Reticulosis.” *Lancet* 1939; 2:194-198.
- Seo, J Y, K-O Lee, K-H Yoo, K-W Sung, H H Koo, S-H Kim, H J Kang, et al. 2016. “Prevalence of Type 5 Familial Hemophagocytic Lymphohistiocytosis in Korea and Novel Mutations in STXBP2.” *Clinical Genetics* 89 (2): 222–27. <https://doi.org/10.1111/cge.12682>.
- Sepulveda, F. E., A. Garrigue, S. Maschalidi, M. Garfa-Traore, G. Menasche, A. Fischer, and G. de Saint Basile. 2016. “Polygenic Mutations in the Cytotoxicity Pathway Increase Susceptibility to Develop HLH Immunopathology in Mice.” *Blood* 127 (17): 2113–21. <https://doi.org/10.1182/blood-2015-12-688960>.
- Sepulveda, Fernando E., Agathe Burgess, Xavier Heiligenstein, Nicolas Goudin, Mickaël M. Ménager, Maryse Romao, Marjorie Côte, et al. 2015. “LYST Controls the Biogenesis of the Endosomal Compartment Required for Secretory Lysosome Function.” *Traffic* 16 (2): 191–203. <https://doi.org/10.1111/tra.12244>.
- Sepulveda, Fernando E, Alexandrine Garrigue, Sophia Maschalidi, Meriem Garfa-Traore, Gaël Ménasché, Alain Fischer, and Geneviève de Saint Basile. 2016. “Polygenic Mutations in the Cytotoxicity Pathway Increase Susceptibility to Develop HLH Immunopathology in Mice.” *Blood* 127 (17): 2113–21. <https://doi.org/10.1182/blood-2015-12-688960>.
- Shabrish, Snehal, Maya Gupta, and Manisha Madkaikar. 2016. “A Modified NK Cell Degranulation Assay Applicable for Routine Evaluation of NK Cell Function.” *Journal of Immunology Research* 2016: 3769590. <https://doi.org/10.1155/2016/3769590>.
- Shearer, William T, Elizabeth Dunn, Luigi D Notarangelo, Christopher C Dvorak, Jennifer M Puck, Brent R Logan, Linda M Griffith, et al. 2014. “Establishing Diagnostic Criteria for Severe Combined Immunodeficiency Disease (SCID),

- Leaky SCID, and Omenn Syndrome: The Primary Immune Deficiency Treatment Consortium Experience." *The Journal of Allergy and Clinical Immunology* 133 (4): 1092–98. <https://doi.org/10.1016/j.jaci.2013.09.044>.
- Siegel, R M, Chun HJ C. F., and Lenardo MJ. 2000. "The Multifaceted Role of Fas Signaling in Immune Cell Homeostasis and Autoimmunity." *Nature Immunology* 1 (6): 469–74.
- Sim, Ngak-Leng, Prateek Kumar, Jing Hu, Steven Henikoff, Georg Schneider, and Pauline C. Ng. 2012. "SIFT Web Server: Predicting Effects of Amino Acid Substitutions on Proteins." *Nucleic Acids Research* 40 (W1): W452–57. <https://doi.org/10.1093/nar/gks539>.
- Smyth, Mark J., Janice M. Kelly, Vivien R. Sutton, Joanne E. Davis, Kylie A. Browne, Thomas J. Sayers, and Joseph A. Trapani. 2001. "Unlocking the Secrets of Cytotoxic Granule Proteins." *Journal of Leukocyte Biology* 70 (1): 18–29. <https://doi.org/10.1189/JLB.70.1.18>.
- Spessott, Waldo A., Maria L. Sanmillan, Margaret E. McCormick, Vineet V. Kulkarni, and Claudio G. Giraudo. 2017. "SM Protein Munc18-2 Facilitates Transition of Syntaxin 11-Mediated Lipid Mixing to Complete Fusion for T-Lymphocyte Cytotoxicity." *Proceedings of the National Academy of Sciences of the United States of America* 114 (11): E2176. <https://doi.org/10.1073/PNAS.1617981114>.
- Spessott, Waldo A, Maria L Sanmillan, Margaret E McCormick, Nishant Patel, Joyce Villanueva, Kejian Zhang, Kim E Nichols, and Claudio G Giraudo. 2015. "Hemophagocytic Lymphohistiocytosis Caused by Dominant-Negative Mutations in STXBP2 That Inhibit SNARE-Mediated Membrane Fusion." *Blood*.
- Stadt U R.J., Seifert W Koch F Grieve S Pagel J Strauss J Kasper B Nürnberg G Becker C Maul-Pavicic A Beutel K Janka G Griffiths G Ehl S Hennies H C zur. 2009. "Familial Hemophagocytic Lymphohistiocytosis Type 5 (FHL-5) Is Caused by Mutations in Munc18-2 and Impaired Binding to Syntaxin 11." *American Journal of Human Genetics* 85(4): 482-92.
- Stadt, Udo Zur, Karin Beutel, Susanne Kolberg, Reinhard Schneppenheim, Hartmut Kabisch, Gritta Janka, and Hans Christian Hennies. 2006. "Mutation Spectrum in Children with Primary Hemophagocytic Lymphohistiocytosis: Molecular and Functional Analyses OfPRF1, UNC13D, STX11, AndRAB27A." *Human Mutation* 27 (1): 62–68. <https://doi.org/10.1002/humu.20274>.

- Stadt, Udo zur, Jan Rohr, Wenke Seifert, Florian Koch, Samantha Grieve, Julia Pagel, Julia Strauss, et al. 2009. "Familial Hemophagocytic Lymphohistiocytosis Type 5 (FHL-5) Is Caused by Mutations in Munc18-2 and Impaired Binding to Syntaxin 11." *American Journal of Human Genetics* 85 (4): 482–92.
<https://doi.org/10.1016/j.ajhg.2009.09.005>.
- Stadt, Udo zur, Jan Rohr, Wenke Seifert, Florian Koch, Samantha Grieve, Julia Pagel, Julia Strauß, et al. 2009. "Familial Hemophagocytic Lymphohistiocytosis Type 5 (FHL-5) Is Caused by Mutations in Munc18-2 and Impaired Binding to Syntaxin 11." *American Journal of Human Genetics*.
<https://doi.org/10.1016/j.ajhg.2009.09.005>.
- Stepp, S E et al. 1999. "Perforin Gene Defects in Familial Hemophagocytic Lymphohistiocytosis." *Science (New York, N.Y.)* 286 (5446): 1957–59.
<http://www.ncbi.nlm.nih.gov/pubmed/10583959>.
- Strippoli, Raffaele, Ivan Caiello, and Fabrizio De Benedetti. 2013. "Reaching the Threshold: A Multilayer Pathogenesis of Macrophage Activation Syndrome." *The Journal of Rheumatology* 40 (6): 761–67. <https://doi.org/10.3899/jrheum.121233>.
- Sugita, Masahiko, Xiaochun Cao, Gerald F.M. Watts, Rick A. Rogers, Juan S. Bonifacino, and Michael B. Brenner. 2002. "Failure of Trafficking and Antigen Presentation by CD1 in AP-3-Deficient Cells." *Immunity* 16 (5): 697–706.
[https://doi.org/10.1016/S1074-7613\(02\)00311-4](https://doi.org/10.1016/S1074-7613(02)00311-4).
- Sun, Honghong, Shunyou Gong, Ruaidhri J. Carmody, Anja Hilliard, Li Li, Jing Sun, Li Kong, et al. 2008. "TIPE2, a Novel Negative Regulator of Innate and Adaptive Immunity That Maintains Immune Homeostasis." *Cell* 133 (3): 415.
<https://doi.org/10.1016/J.CELL.2008.03.026>.
- Tesi, Bianca, Kristina Lagerstedt-Robinson, Samuel C C Chiang, Eya Ben Bdira, Miguel Abboud, Burcu Belen, Omer Devecioglu, et al. 2015. "Targeted High-Throughput Sequencing for Genetic Diagnostics of Hemophagocytic Lymphohistiocytosis." *Genome Medicine* 7 (1): 130.
<https://doi.org/10.1186/s13073-015-0244-1>.
- Trottestam, Helena, Annacarin Horne, Maurizio Aricò, R Maarten Egeler, Alexandra H Filipovich, Helmut Gadner, Shinsaku Imashuku, et al. 2011. "Chemoimmunotherapy for Hemophagocytic Lymphohistiocytosis: Long-Term Results of the HLH-94 Treatment Protocol." *Blood* 118 (17): 4577–84.

<https://doi.org/10.1182/blood-2011-06-356261>.

Tsuchiya, Shigeru, Michiko Yamabe, Yoshiko Yamaguchi, Yasuko Kobayashi, Tasuke Konno, and Keiya Tada. 1980. "Establishment and Characterization of a Human Acute Monocytic Leukemia Cell Line (THP-1)." *International Journal of Cancer* 26 (2): 171–76. <https://doi.org/10.1002/ijc.2910260208>.

Usmani, G. Naheed, Bruce A. Woda, and Peter E. Newburger. 2013. "Advances in Understanding the Pathogenesis of HLH." *British Journal of Haematology* 161 (5): 609–22. <https://doi.org/10.1111/bjh.12293>.

Valdez, A C, Brown Mj C. J., and P A Roche. 1999. "Syntaxin 11 Is Associated with SNAP-23 on Late Endosomes and the Trans-Golgi Network." *Journal of Cell Science* 112: 845–54.

Veis, D J, Shutter Jr S. C., and Korsmeyer SJ. 1993. "Bcl-2-Deficient Mice Demonstrate Fulminant Lymphoid Apoptosis, Polycystic Kidneys, and Hypopigmented Hair." *Cell* 75 (2): 229–40.

Voskoboinik, Iliia, Mark J. Smyth, and Joseph A. Trapani. 2006. "Perforin-Mediated Target-Cell Death and Immune Homeostasis." *Nature Reviews Immunology* 6 (12): 940–52. <https://doi.org/10.1038/nri1983>.

Wang, Yini, Zhao Wang, Jia Zhang, Qing Wei, Ran Tang, Junyuan Qi, Lihong Li, Liping Ye, Jijun Wang, and Ling Ye. 2014. "Genetic Features of Late Onset Primary Hemophagocytic Lymphohistiocytosis in Adolescence or Adulthood." *PloS One* 9 (9): e107386. <https://doi.org/10.1371/journal.pone.0107386>.

WATSON, P. 2005. "Intracellular Trafficking Pathways and Drug Delivery: Fluorescence Imaging of Living and Fixed Cells." *Advanced Drug Delivery Reviews* 57 (1): 43–61. <https://doi.org/10.1016/j.addr.2004.05.003>.

Xu, Xiao-Jun, Yong-Min Tang, Hua Song, Shi-Long Yang, Wei-Qun Xu, Ning Zhao, Shu-Wen Shi, et al. 2012. "Diagnostic Accuracy of a Specific Cytokine Pattern in Hemophagocytic Lymphohistiocytosis in Children." *The Journal of Pediatrics* 160 (6): 984-990.e1. <https://doi.org/10.1016/J.JPEDS.2011.11.046>.

Xu, Xiao-Jun, Hong-Sheng Wang, Xiu-Li Ju, Pei-Fang Xiao, Yan Xiao, Hong-Man Xue, Hong-Yu Shi, et al. 2017. "Clinical Presentation and Outcome of Pediatric Patients with Hemophagocytic Lymphohistiocytosis in China: A Retrospective Multicenter Study." *Pediatric Blood & Cancer* 64 (4): e26264.

<https://doi.org/10.1002/psc.26264>.

Xu, Xiao Jun, Hong Sheng Wang, Xiu Li Ju, Pei Fang Xiao, Yan Xiao, Hong Man Xue, Hong Yu Shi, et al. 2017. "Clinical Presentation and Outcome of Pediatric Patients with Hemophagocytic Lymphohistiocytosis in China: A Retrospective Multicenter Study." *Pediatric Blood and Cancer* 64 (4): 1–6. <https://doi.org/10.1002/psc.26264>.

Yan, Nan, and Zhijian J. Chen. 2012. "Intrinsic Antiviral Immunity." *Nature Immunology* 13 (3): 214. <https://doi.org/10.1038/NI.2229>.

Yuseff, Maria-Isabel, Paolo Pierobon, Anne Reversat, and Ana-Maria Lennon-Duménil. 2013. "How B Cells Capture, Process and Present Antigens: A Crucial Role for Cell Polarity." *Nature Reviews Immunology* 13 (7): 475–86. <https://doi.org/10.1038/nri3469>.

Yuseff, Maria-Isabel, Anne Reversat, Danielle Lankar, Jheimmy Diaz, Isabelle Fanget, Paolo Pierobon, Violaine Randrian, et al. 2011. "Polarized Secretion of Lysosomes at the B Cell Synapse Couples Antigen Extraction to Processing and Presentation." *Immunity* 35 (3): 361–74. <https://doi.org/10.1016/j.immuni.2011.07.008>.

Zhang, Kejian, Shanmuganathan Chandrakasan, Heather Chapman, C. Alexander Valencia, Ammar Husami, Diane Kissell, Judith A. Johnson, and Alexandra H. Filipovich. 2014a. "Synergistic Defects of Different Molecules in the Cytotoxic Pathway Lead to Clinical Familial Hemophagocytic Lymphohistiocytosis." *Blood* 124 (8): 1331–34. <https://doi.org/10.1182/blood-2014-05-573105>.

Zhang, Kejian, Shanmuganathan Chandrakasan, Heather Chapman, C Alexander Valencia, Ammar Husami, Diane Kissell, Judith A Johnson, and Alexandra H Filipovich. 2014b. "Synergistic Defects of Different Molecules in the Cytotoxic Pathway Lead to Clinical Familial Hemophagocytic Lymphohistiocytosis." *Blood* 124 (8): 1331–34. <https://doi.org/10.1182/blood-2014-05-573105>.

Zhang, Kejian, Michael B Jordan, Rebecca A Marsh, Judith A Johnson, Diane Kissell, Jarek Meller, Joyce Villanueva, et al. 2011. "Hypomorphic Mutations in PRF1, MUNC13-4, and STXBP2 Are Associated with Adult-Onset Familial Hemophagocytic Lymphohistiocytosis." *Blood* 118 (22): 5794–99. <https://doi.org/10.1182/blood-2011-07-370148>.

Zhang, Mingce, Claudia Bracaglia, Giusi Prencipe, Christina J Bemrich-Stolz, Timothy Beukelman, Reed A Dimmitt, W Winn Chatham, et al. 2016. "A Heterozygous

RAB27A Mutation Associated with Delayed Cytolytic Granule Polarization and Hemophagocytic Lymphohistiocytosis.” *Journal of Immunology (Baltimore, Md. : 1950)* 196 (6): 2492–2503. <https://doi.org/10.4049/jimmunol.1501284>.

Zhao, Xi Wen, Roel P. Gazendam, Agata Drewniak, Michel Van Houdt, Anton T J Tool, John L. Van Hamme, Iwan Kustiawan, et al. 2013. “Defects in Neutrophil Granule Mobilization and Bactericidal Activity in Familial Hemophagocytic Lymphohistiocytosis Type 5 (FHL-5) Syndrome Caused by STXBP2/Munc18-2 Mutations.” *Blood*. <https://doi.org/10.1182/blood-2013-03-494039>.

Zheng, Fang, Juan Li, Hui Zha, Jue Zhang, Zhiquan Zhang, and Fangjun Cheng. 2016. “ITK Gene Mutation: Effect on Survival of Children with Severe Hemophagocytic Lymphohistiocytosis.” *The Indian Journal of Pediatrics* 83 (11): 1349–52. <https://doi.org/10.1007/s12098-016-2079-1>.

IX. ANNEX

ANNEX

Mutated residue	Residue Name	Residue Number	Minimum distance (Å)	N° of Contacts	Mutated residue	Residue Name	Residue Number	Minimum distance (Å)	N° of Contacts	Mutated residue	Residue Name	Residue Number	Minimum distance (Å)	N° of Contacts
N62	LYS	63	1.329	58	R235	ASP	234	1.329	47	R529	ALA	530	1.330	41
	ILE	61	1.330	57		ALA	236	1.332	37		GLY	559	2.377	14
	ASP	60	2.502	39		ASP	238	2.066	47		PRO	532	2.493	33
	HIS	35	3.499	23		GLU	546	2.164	23		GLY	531	2.528	56
	MET	33	3.873	4		GLY ⁴	541	2.241	22		LYS	560	2.613	16
	ASP	34	3.952	8		MET	539	2.391	30		ARG	533	2.878	47
	ARG	64	4.155	2		GLY	540	2.805	33		GLU	552	3.111	48
LYS	82	4.641	1	ALA	237	3.067	12	TRP	561	3.236	20			
R555	ALA	550	4.465	1	PHE ⁵	576	3.200	17	LYS	225	3.265	5		
	TYR	551	2.480	9	LEU	444	3.352	17	GLN ³	432	1.329	43		
	GLU ⁷	552	3.164	15	PRO	242	3.395	30	HIS	434	1.330	57		
	VAL	553	3.009	13	ALA	543	3.476	7	VAL	431	2.976	13		
	THR	554	1.329	37	LEU	571	3.497	7	SER	435	3.446	7		
	ALA	556	1.329	26	PRO ⁶	239	3.504	18	SER	436	4.687	3		
	THR	557	3.258	10	VAL	538	3.612	20	ASP	481	1.329	48		
GLU	558	3.263	16	VAL	542	3.668	11	MET	483	1.330	43			
GLY	559	4.908	1	MET	233	4.155	4	VAL	478	2.585	24			
T345	HIS	346	1.328	77	SER	241	4.376	4	ILE	479	2.610	50		
	SER	344	1.329	45	TYR	157	4.573	1	LEU	231	2.761	14		
	ASN	341	2.174	18	LEU ³	257	1.328	47	TRP	496	2.848	49		
	LYS	342	2.550	34	ASP	255	1.329	71	ALA	486	2.988	8		
	TYR	266	2.572	22	MET	252	2.240	46	LYS	480	3.055	17		
	TYR	343	2.765	21	HIS ²	356	3.056	44	LEU	491	3.168	22		
	LEU	349	3.158	6	HIS	245	3.143	13	GLU	484	3.427	9		
LYS	277	3.194	10	CYS	353	3.351	14	ASP	485	3.487	19			
VAL	279	3.350	15	ALA	253	3.381	15	MET	233	3.764	4			
LEU	347	3.365	10	PHE	357	3.387	15	LEU	460	4.700	2			
HIS	348	3.501	15	VAL	361	3.435	17	SER	458	1.331	32			
ASP	285	4.204	3	TYR	254	3.613	9	TYR	191	1.332	54			
TYR	264	4.619	3	ASP	258	4.308	2	LEU	460	1.907	26			
LEU	340	4.927	1	ALA	251	4.613	1	LYS ⁸	193	1.946	73			
R190	ILE	189	1.329	56	ILE	404	1.327	51	GLY	194	2.076	9		
	TYR	191	1.329	45	VAL	406	1.328	36	ALA	237	2.237	27		
	LEU	230	1.996	27	LEU ⁹	243	2.128	55	PRO	195	2.250	32		
	TRP	496	2.111	51	TYR	401	2.340	31	ILE	232	2.444	14		
	GLN	229	2.163	32	ASP	255	2.358	24	THR	198	2.446	21		
	LEU	491	2.198	44	HIS	245	2.767	60	TRP	496	2.604	61		
	PRO	497	2.498	30	ASP	402	2.861	46	LEU	495	2.742	17		
	PHE	498	2.865	92	LEU	244	2.897	17	ARG	469	2.771	5		
	LEU	231	2.877	33	LEU	409	3.015	15	ASP	234	2.801	37		
	ILE	232	2.911	14	LYS	403	3.199	14	ALA	236	2.801	7		
	ALA	188	3.298	17	LEU	407	3.303	10	MET	233	3.401	17		
	ASP	492	3.416	11	LEU	577	3.340	14	ARG ⁹	190	3.540	3		
	ARG	493	3.532	17	PRO ²	573	3.373	32	PRO	497	4.629	1		
	VAL	499	4.114	6	LEU	408	3.440	19	ALA	199	4.715	1		
ALA	202	4.636	2	GLU	368	3.758	12							
ARG ⁷	192	4.736	1	ALA	400	4.457	1							
ALA	486	4.965	1	THR	574	4.536	5							

SupplementaryFigure 30. Detailed inter-residue contact list of each residue found mutated in patients with HLH. Residues in red are those in which a reported mutation in at least one HLH patient has been described. Two residues were considered to be in contact when at least two of their atoms were located at a distance of 5 Å or less.

1. Mukda, E. et al. Exome sequencing for simultaneous mutation screening in children with hemophagocytic lymphohistiocytosis. *Int. J. Hematol.* 106, 282–290 (2017).
2. Hackmann, Y. et al. Syntaxin binding mechanism and disease-causing mutations in Munc18-2. *Proc. Natl. Acad. Sci. U. S. A.* 110, E4482-91 (2013).
3. Meeths, M. et al. Spectrum of clinical presentations in familial hemophagocytic lymphohistiocytosis type 5 patients with mutations in STXBP2. *Blood* 116, 2635–43 (2010).
4. Al Hawas, R. et al. Munc18b/STXBP2 is required for platelet secretion. *Blood* 120, 2493–500 (2012).
5. Tong, C.-R. et al. [The study of gene mutations in unknown refractory viral infection and primary hemophagocytic lymphohistiocytosis]. *Zhonghua nei ke za zhi* 50, 280–3 (2011).
6. Zhang, K. et al. Synergistic defects of different molecules in the cytotoxic pathway lead to clinical familial hemophagocytic lymphohistiocytosis. *Blood* 124, 1331–4 (2014).

7. Xu, X.-J. et al. Clinical presentation and outcome of pediatric patients with hemophagocytic lymphohistiocytosis in China: A retrospective multicenter study. *Pediatr. Blood Cancer* 64, e26264 (2017).
8. Seo, J. Y. et al. Prevalence of type 5 familial hemophagocytic lymphohistiocytosis in Korea and novel mutations in STXBP2. *Clin. Genet.* 89, 222–7 (2016).
9. This Thesis

